Universidad Autónoma de Madrid (UAM)
Faculty of Science
Department of Molecular Biology

Role of DisA and c-di-AMP in the DNA damage response of exponentially growing *Bacillus subtilis* cells

PhD Thesis

Carolina Gándara

Madrid 2015

Thesis presented by Carolina Gándara to obtain the degree of Doctor of Philosophy in Science at the Universidad Autónoma de Madrid (UAM), Madrid, Spain.

This work has been performed at the Spanish National Biotechnology Centre (CNB-CSIC) under the supervision of Dr. Juan Carlos Alonso.

Aos meus queridos pais

Abstract

Cells are constantly subjected to DNA lesions, which can result in replication fork stalling or collapse. A variety of DNA repair pathways have evolved to respond to the different types of exogenous and endogenous DNA damaging agents. A complex regulation exists to coordinate these processes, which are called DNA damage response (DDRs). DisA was initially described as a DNA damage checkpoint protein that ensures the genome integrity of *Bacillus subtilis* spores. However, basal levels of DisA were detected in vegetative cell extracts and highly dynamic foci were observed in vegetative cells expressing DisA-YFP under its native promoter. Since DisA is also present in non-spore forming bacteria, a more general role for DisA, that is not restricted to sporulation, was proposed.

In this work, it was demonstrated that c-di-AMP and the diadenilate cyclases (DAC), DisA and CdaA, contribute to elicit repair of stalled and collapsed forks, in exponentially growing *B. subtilis* cells. Absence of DisA or decreased intracellular levels of c-di-AMP impaired survival to alkylation DNA damage induced by methyl methanesulfonate (MMS). On the other hand, CdaA is involved in oxidative damage repair. The *radA* and *disA* functions were epistatic for MMS and showed also epistasis with functions involved in Holliday junction (HJ) processing. Both *radA* and *disA* were epistatic with *recG* and *recU*, while non-epistatic with *ruvAB*. *In vivo*, DisA-YFP foci lost its dynamics in the presence of unresolved HJs (Δ*recU* context).

Purified DisA showed DAC activity with preference for ATP over dATP to produce c-di-AMP. DisA could bind different DNA structures without specificity, although only highly stacked HJs could modulate DisA c-di-AMP synthesis. For the first time it was demonstrated that RadA/Sms could bind DNA, in the absence or presence of ATP, and with more affinity for single-stranded (ss) DNA and HJs. *In vitro* assays showed that DisA strongly inhibits RecG and RuvAB helicase activities. DisA also negatively affects RecU resolvase activity and RecA-mediated strand exchange reactions. Altogether, these results indicate that, in stalled forks induced by the presence of alkyl adducts, DisA modulates the DDR by binding branched DNA and reducing the synthesis of c-di-AMP. More precisely, DisA modulates recombinational DNA repair by protecting branched recombination intermediates, and therefore preventing fork reversal, HJ resolution and strand exchange. It is likely that DisA stimulate other specific DNA repair pathways, such as BER, and favours TLS since slightly lower mutation frequencies were detected in the absence of DisA.

Abbreviations

AS	Ammonium sulphate
ATP	Adenosine triphosphate
BER	Base excision repair
BSA	Bovine serum albumin
c-di-AMP	Cyclic diadenosine monophosphate
CFU	Colony-forming unit
CNB	Centro Nacional de Biotecnología
DAC	Diadenylate cyclase
DAPI	4', 6-diamidin-2-phenylindole
dATP	deoxyadenosine triphosphate
DDR	DNA damage response
DDT	DNA damage tolerance
DMSO	Dimethyl sulfoxide
DNA	Deoxyribonucleic acid
DNaseI	Deoxyribonuclease I
DSB	Double-strand break
dsDNA	Double-stranded DNA
DSS	Disuccinimidyl suberate, Suberic acid
DTT	Dithiothreitol
EDTA	Ethylenediaminetetraacetic acid
EMSA	Electrophoretic mobility shift assay
H_2O_2	Hydrogen peroxide
HJ	Holliday Junction
HhH	Helix-hairpin-Helix
HR	Homologous recombination
IPTG	Isopropil-β-D-1-tiogalactopiranósido
kDa	Kilo-dalton
K_{Dapp}	Apparent dissociation constant
LB	Luria-Bertani medium
LC-MS/MS	Liquid chromatography-tandem mass spectrometry
LC_{99}	Lethal concentration to kill 99%
MALDI-TOF	Matrix-assisted laser desorption/ionization time-of-flight mass spectrometer
min	Minutes
MMC	Mitomycin C
MMR	Mismatch repair
MMS	Methyl methanesulfonate
Nal	Nalidixic acid
NER	Nucleotide excision repair
NHEJ	Non-homologous end joining
Ni-NTA	Nickel-nitrilotriacetic acid
nt	Nucleotides
OD	Optical density
PAGE	Polyacrylamide gel electrophoresis
PDE	Phosphodiesterase
PEI	Polyethyleneimine
RNA	Ribonucleic acid
Rpm	Revolutions per minute
SDS	Sodium dodecyl sulphate
ssDNA	Single-stranded DNA
SSG	Single-strand gap
TAE	Tris-acetate EDTA
TLS	Translesion synthesis
wt	Wild-type
YFP	Yellow fluorescent protein

Table of contents

List of figures

List of tables

Introduction

1. Introduction

1.1. Genetic instability and the DNA-damage response

In all living cells, the elementary component of the genetic material, DNA, is constantly subjected to alterations, in the molecule (chemistry), sequence (mismatches), or structure (breaks) level (Figure 1). Most of these modifications arise as a consequence of errors introduced during replication, DNA repair or recombination. Products of cellular metabolism, such as reactive oxygen species, or environmental factors, e.g. UV radiation, represent an additional source of DNA damage. Specific error-free DNA repair pathways are activated (such as base excision repair, nucleotide excision repair, mismatch repair, etc.) as the primary mechanism to remove damaged DNA that does not compromise nucleoid integrity (reviewed in Friedberg et al, 2005b).

When not repaired, these lesions are mutagenic or even lethal, being the principal source of genetic instability (e.g. cancer), but also necessary for genetic variability (when not lethal). One of the major consequences of unrepaired damages in dividing cells is the arrest of the replication fork machinery. Thus, in order to survive, cells must activate a DNA damage response (DDR) system, which involves the bypass or repair of the lesion, followed by the restart of DNA replication (reviewed in Hoeijmakers, 2001). It is known that cells slow down replication when the damage is encountered, via a checkpoint system, in order to give enough time for the cell to remove the lesion. An alternative is to bypass the damage and complete replication, which is still better than dying (reviewed in Osborn et al, 2002). DNA damage bypass is promoted by specialized low-fidelity error-prone DNA polymerases that can incorporate a nucleotide opposite to the damaged site, a mechanism known as translesion synthesis (TLS) (reviewed in Tippin et al, 2004).

1.2. DNA repair systems

Specific repair pathways have evolved for each type of lesion. Although differences exist, it is evident that DNA repair mechanisms have been conserved in both prokaryotic and eukaryotic systems. In *Bacillus subtilis*, a broad variety of DNA repair pathways take place and, therefore, it represents an attractive model for the study of the DDR in prokaryotes. *B. subtilis* is a Gram-positive soil bacterium that undergoes sporulation and natural competence under stress conditions. The genus *Bacillus* belongs to the Phylum Firmicutes and includes rod-shaped bacteria that grow in the presence of oxygen, which distinguishes them from the strictly

anaerobic *Clostridium* spp. When not otherwise stated, all genes and products mentioned during this work are of *B. subtilis* origin.

The nucleotide excision repair (NER) pathway removes bulky DNA adducts, such as thymine dimers, generated by UV light or a variety of drugs (Figure 1). Defects in NER are associated with many human diseases, such as xeroderma pigmentosum (Cleaver, 1969). The UVR system is the best-characterized example of NER in *B. subtilis*, being regulated by the SOS response in this bacterium. When bulky lesions are recognized, endonucleolytic cleavage takes place, removing a short ssDNA region that contains the lesion, leaving a gap that is later filled by a DNA polymerase and then sealed by DNA ligase finishing the repair process. While damaged nucleotides are repaired via NER, non-bulky lesions are specifically removed by the base excision repair (BER) system. These types of damage are caused by chemical insults, such as alkylation, oxidation, deamination, etc. (Figure 1). The BER pathway starts with the detection and removal of the damaged base by a glycosylase, producing an apurinic/apyrimidinic site (known as AP site). These sites are highly mutagenic and have the potential to cause ssDNA breaks, when not processed by specific BER enzymes that remove the damage and fill the gap. The third specific error-free DNA repair system is mismatch repair (MMR). MMR specifically eliminates errors introduced during DNA synthesis, such as base mispairing or insertions (Figure 1). MutS recognizes the mismatch and together with MutL are the main proteins involved in this repair pathway that is coupled to DNA synthesis (reviewed in Lenhart et al, 2012; Yasbin et al, 1993).

Double-strand breaks (DSBs) represent the most lethal type of DNA damage, being originated from environmental sources (e.g. X rays) or chemical agents (e.g. nalidixic acid) (Figure 1). These insults can be repaired via three mechanisms in *B. subtilis*: error-free homologous recombination (HR), error-prone single-strand annealing and non-homologous end joining (NHEJ). The latter two pathways only plays a role when error-free HR is impaired or during stationary phase and, therefore, will not be further discussed.

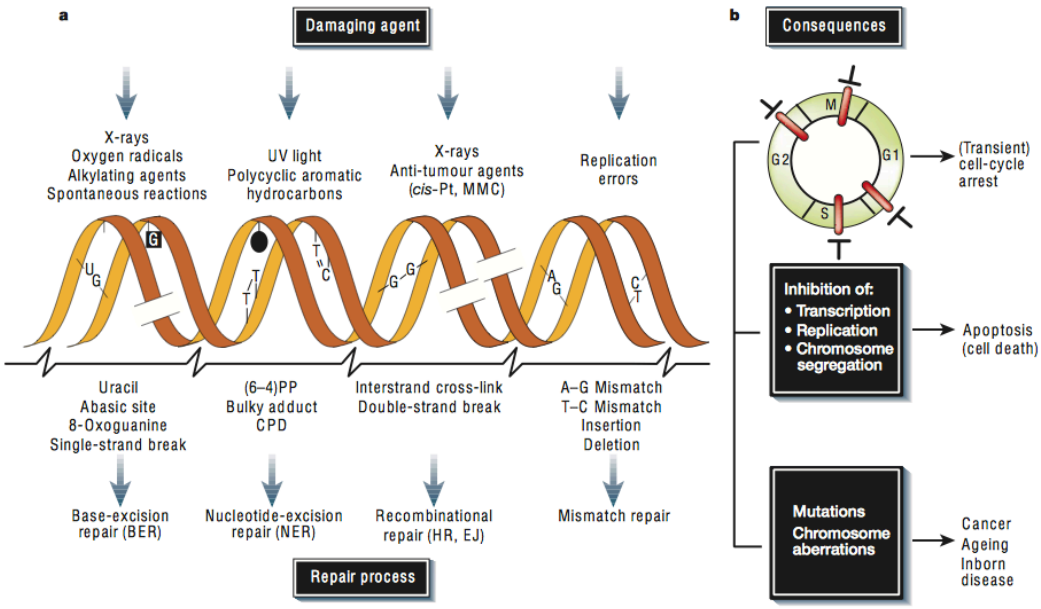

Figure 1. Summary of the types of lesions caused by different DNA damaging agents.
Each lesion can be repaired by a specific pathway or 'repair process'. When not repaired, DNA damage can lead to cell death, mutagenesis or DNA replication blockage in bacteria (in eukaryotes that would be cell-cycle arrest). *Figure extracted from* (Hoeijmakers, 2001).

Error-free HR uses an intact sister chromosome as the template to initiate recombination and re-establish replication (Figure 2). In HR-mediated one-ended DSB repair, RecN in concert with PNPase is one of the first responders, recognizing the DSB and establishing a 'repair centre' (Cardenas et al, 2009; Cardenas et al, 2011; Kidane et al, 2004). Then, long-range end-resection takes place with the action of the AddAB complex or RecJ in concert with a RecQ-like DNA helicase (RecQ and/or RecS) and SsbA, generating a 3'-ssDNA tailed duplex substrate. With the help of accessory (recombinase mediators) SsbA, RecFOR, RecX and RecU proteins, RecA is recruited onto the ssDNA region. RecA mediates strand exchange, forming a D-loop that allows the DNA polymerase to use the homologous strand as a template for DNA synthesis. The translocase RuvAB complex facilitate migration of the D-loop and the formation of a Holliday junction (HJ) that is finally resolved by RecU (reviewed in Alonso et al, 2013; Ayora et al, 2011; Lenhart et al, 2012).

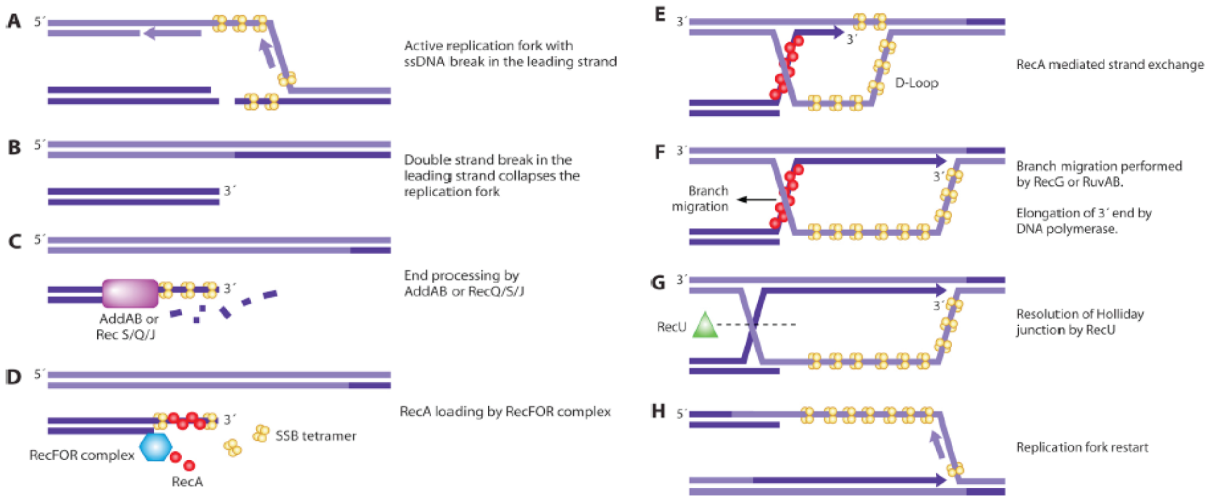

Figure 2. Model of one-ended DSB repair via homologous recombination in *B. subtilis*.
Collapsed replication fork by an ssDNA break leads to one-ended DSB formation (A and B); recognition and processing of DSB (C); RecA loading and nucleoprotein filament formation (D); RecA-mediated strand exchange (E); HJ branch migration and processing (F and G) and; replication restart (H). *Figure extracted from* (Lenhart et al, 2012).

Upon DNA damage that do not affect nucleoid integrity, the generation of ssDNA regions activate the expression of a set of genes, including some of the representatives of the DNA repair system, via a RecA- and LexA-dependent mechanism (SOS response). Whereas lesions that compromise nucleoid integrity, such as double strand breaks (DSBs), cause replication fork collapse and can trigger, besides the SOS response, a more complex DDR (Cardenas et al, 2014) that is RecA-dependent, but LexA-independent (DSB response). In eukaryotes, two DNA damage checkpoint pathways have been described: the ataxia telangiectasia mutated (ATM) or the ATM-Rad3-related (ATR) pathway, which responds to double-strand breaks (DSBs) or mainly to single-strand regions in stalled replication forks, respectively (reviewed in Osborn et al, 2002).

1.2.1. Stalled or collapsed replication forks

In this work, the DDR in dividing cells has been studied, more specifically in exponentially growing cells. Therefore, it is relevant to review what types of DNA damage can stall or collapse the progression of DNA replication forks (Figure 1), as well as the mechanisms that promote DNA replication re-initiation (Figure 3). The use of synthetic agents that produce types of DNA damage recognized by different repair mechanisms enables the study of a variety of DDR pathways. In this work, methyl methanesulfonate (MMS), mitomycin C (MMC),

hydrogen peroxide (H_2O_2) and nalidixic acid (Nal) were selected as the DNA damaging agents to study the role of different proteins in the DDR of exponentially growing *B. subtilis* cells.

MMS introduces alkyl groups in the nitrogen atoms of purine residues to cause base mispairing and replication fork stalling (Beranek, 1990; Sedgwick, 2004). MMS alkylates mostly the N^7 position of the guanine (Friedberg et al, 2005b). The removal of alkylated bases is predominantly performed by the BER system, although stalled forks leading to single strand gaps (SSG) or regressed forks (formation of a Holliday junction, HJ) can be generated (Lundin et al, 2005; McGlynn & Lloyd, 2001). MMC produces interstrand and intrastrand DNA crosslinks, depending if the damage sites are on opposite or the same polynucleotide chain, respectively (Friedberg et al, 2005b). DNA crosslinks block replication and transcription, and the excision of these adducts, which is promoted by the NER pathway, leads mainly to one-ended DSBs (De Silva et al, 2000; Lee et al, 2006). H_2O_2 generally reacts with ferrous iron (Fenton reaction) to generate highly reactive hydroxyl radicals. Endogenously, they are formed as by-products of aerobic respiration. Fenton oxidants may occur at the DNA bases or sugars, causing different types of DNA damage, including strand breaks and crosslinks. Hydroxyl radicals react with C^8 of the guanine generating the C8-OH adduct (8-oxoG), which is regarded as the most abundant oxidative damage. Repair of oxidative damage is promoted by BER, NER or recombinational repair; the latter when one- or two-ended DSBs are produced (reviewed in Henle & Linn, 1997; Krwawicz et al, 2007). Finally, Nal is a synthetic quinolone commonly used as an antibiotic that inhibits a subunit of the DNA gyrase (topoisomerase II) and topoisomerase IV, preventing the tertiary negative structure supercoiling of bacterial DNA and leading to an accumulation of cleavage complexes (i.e. two-ended DSBs) (Crumplin & Smith, 1976; Pommier et al, 2010).

To restore replication and maintain genome integrity, cells have evolved different mechanisms. Fork reversal has broadly been described as a major DNA damage tolerance (DDT) and repair mechanism of stalled forks in dividing cells, with intriguing implications for replication completion (Neelsen & Lopes, 2015). It consists in the coordinated annealing of the two newly synthesized strands into a “chicken-foot structure” that resembles a HJ, when the replication machinery encounters a blockage in the leading strand that stalls its progression. This structure can be processed by different pathways (Figure 3, pathways a and b). It could represent an ‘emergency break’ that transiently protects replication forks and/or allow the lesion to become accessible to the repair machinery and subsequently to be removed (Figure 3, pathway a). Alternatively, the lesion could be bypassed (Figure 3, pathway b.1) or the regressed

fork could be processed by a HJ resolvase. In the latter case, one-ended DSB is formed which will then be repaired via HR, restoring replication fork progression (Figure 3, pathway b.2).

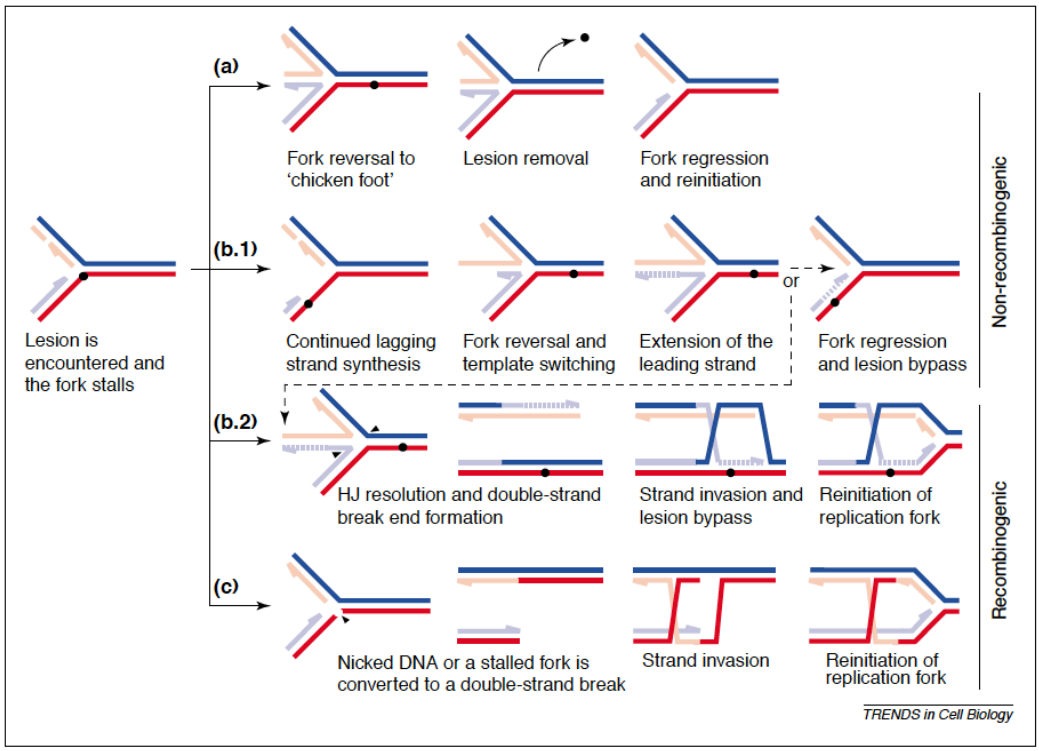

Figure 3. Alternative mechanisms that promote DNA replication restart in stalled or collapsed forks.
Replication forks can stall or collapse when a lesion (represented as a black dot) is encountered on the DNA template. Three pathways have been described to promote replication reinitiation: (a) Fork reversal and lesion removal by the DNA repair machinery; (b) Fork reversal and lesion bypass (1) or (2) HJ resolution and recombination-mediated lesion bypass or; (c) DSB repair via recombination. *Figure extracted from* (Osborn et al, 2002).

HR also plays a central role in collapsed forks, i.e. when one of the DNA strands is broken, which is converted in one-ended DSB when encountered by the replisome (Figure 3, pathway c). If the damage is blocking the lagging strand progression, it can be bypassed by re-priming lagging strand synthesis leaving an ssDNA gap that triggers the recruitment of RecA, activating the SOS response and the gap repair machinery.

1.3. DNA integrity scanning protein A (DisA)

In *B. subtilis*, the last gene of six that compose the clpC operon encodes for the DisA protein (formerly known as YacK) (Figure 4). Among the roles played by the proteins encoded from this operon there are transcription activation induced by heat shock (CtsR), protein phosphorylation (McsA and McsB), protein degradation (ClpC), competence (McsA, McsB and

ClpC) and DNA repair (RadA/Sms and DisA) (Krüger et al, 1997). Three promoters regulate co-transcription of the clpC operon: the vegetative and general stress sigma factors σ^A and σ^B, respectively (positive regulation), and CtsR (negative regulation). During exponential growth, transcription modulated by σ^A contributes to the basal level expression to a greater extent than σ^B. Interestingly, σ^A could also be activated by stress conditions such as amino acid starvation or H_2O_2, when σ^B was absent (Kruger et al, 1996). The CtsR regulon induce gene expression, including those of the clpC operon, in response to heat shock (Kruger & Hecker, 1998). The first four genes of the clpC operon participate in this regulation: McsA and McsB interact with ClpC, but in heat stress conditions this interaction is abolished and McsB is activated. Upon heat activation, the arginine-kinase McsB targets CtsR that is degraded by ClpP-ClpC, inactivating this transcription repressor (Elsholz et al, 2011; Elsholz et al, 2010; Fuhrmann et al, 2009). McsB also phosphorylates RecA, but the role of phosphorylated RecA is poorly understood (Elsholz et al, 2012).

A more complex regulation is found in the clpC operon. The two distal genes, *radA* and *disA,* showed lower levels of induction by heat (Helmann et al, 2001), which is consistent with the data indicating that these genes are part of a separate operon, regulated by the extracytoplasmic function sigma factor σ^M, which is mostly activated under cell envelope stress (Eiamphungporn & Helmann, 2008). Most σ^M-dependent promoters are located nearby the regulated gene (not more than 200 nt upstream), but an exception is *disA*, whose expression is controlled by a σ^M promoter that is located 890 nt upstream of *disA*, within the *radA* gene (Jervis et al, 2007) (Figure 4). It is possible that a truncated RadA/Sms protein is also translated from this promoter, although this possibility has never been addressed. Downstream *disA* lays the *yacL* gene. This genomic organization is conserved in *Dictyoglomi* and *Clostridium*, while *yacL* locates downstream *radA* in *Listeria* and *Staphylococcus* species, which lack the *disA* gene. YacL function is still unknown.

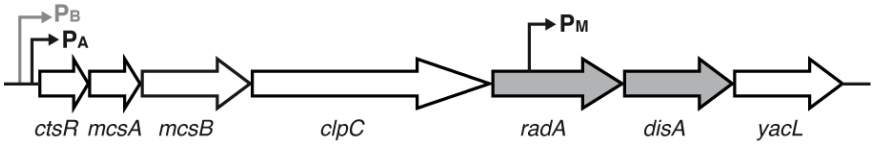

Figure 4. Schematic representation of the *clpC* operon with its promoter regions and neighbour genes.
The big arrows represent the transcription direction and relative size of each gene. The localization of each promoter region is marked with a small arrow identified by a capital letter that represents its sigma factor (P_B for σ^B, P_A for σ^A and P_M for σ^M). The *radA* and *disA* genes are highlighted in grey.

DisA was also found in a screening for proteins that interact with RacA, which is the protein that anchors the chromosome to the cell pole at the onset of sporulation. Axial filament formation was not impaired in Δ*disA* cells, suggesting that DisA should have another function (Ben-Yehuda, 2002). As a mechanism to ensure chromosome integrity before asymmetric division, *B. subtilis* cells fail to enter sporulation in the presence of DNA damage (Ireton & Grossman, 1994). However, in the absence of DisA, cells were able to initiate sporulation even in the presence of DNA damage. Furthermore, it was demonstrated that DisA formed highly dynamic focal assemblies at the onset of sporulation that paused at sites where DSB were produced by the HO endonuclease. This loss of movement was predicted to induce a signal cascade that culminates with a delay in Spo0A activation and therefore a temporary block in sporulation (Bejerano-Sagie et al, 2006) (Figure 5).

When the DNA damage is not repaired upon entry into sporulation, DisA could also act as a damage checkpoint before spores return to vegetative growth (outgrowth). It was observed that DisA plays a role in arresting DNA replication during *B. subtilis* spore outgrowth until the chromosome is free of damage (Campos et al, 2014).

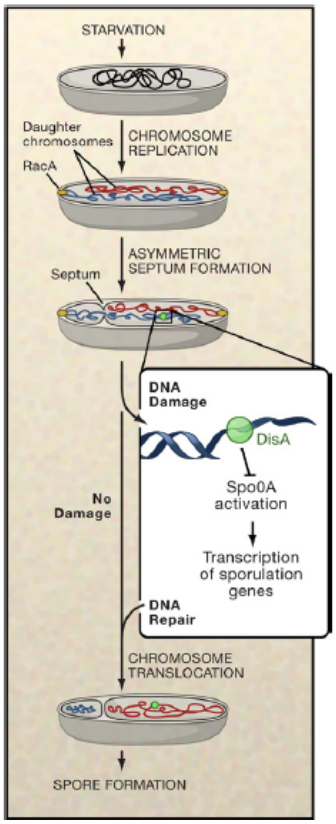

Figure 5. DisA delays entry into sporulation to ensure spore genome integrity.
At starvation, *B. subtilis* cells undergo sporulation, which begins with chromosome duplication and ends up with spore formation. DisA is a highly dynamic protein that scans the chromosome and pauses at DNA lesion sites. DisA delays asymmetric division, possibly to enable the DNA repair machinery to act removing the damage before the spore is formed.

Not all species that harbour DisA undergo sporulation, as for example *Thermotoga*, *Dictyoglomi* and *Fusobacteria* (Figure 9A), suggesting that DisA could play a more general role. Plasmidic and chromosomal transformation were shown to be affected in a *disA* null mutant, which proposed DNA repair or competence functions for DisA (Krüger et al, 1997).

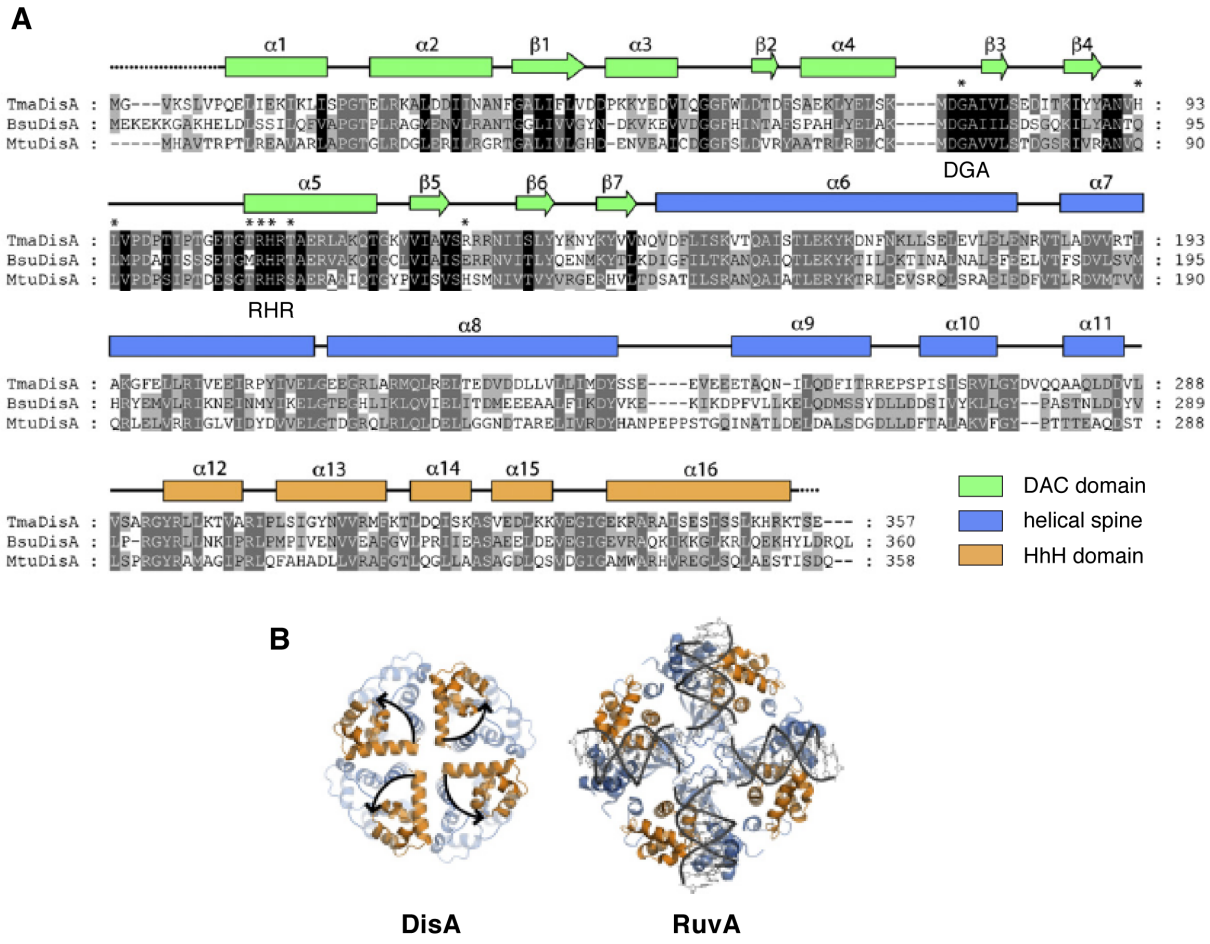

Figure 6. Secondary and quaternary structure of DisA.
(A) Sequence alignment of DisA proteins from *Thermotoga maritima* (Tma), *Bacillus subtilis* (Bsu) and *Mycobacterium tuberculosis* (Mtu). The secondary structure is shown on top of the alignment and conserved residues are shaded. Location of DGA and RHR motifs is highlighted. Notable functional residues are indicated (*). (B) Comparison of the DisA octamer model with the RuvA tetramer model. The four HhH domains are colored orange. *Modified figure from* (Witte et al, 2008).

DisA forms a large molecular complex in solution, as revealed by gel filtration and sedimentation equilibrium experiments. The obtained molecular weight (~370 kDa) corresponds to a large assembly that in both assays was predicted to be an octamer (Witte et al, 2008). The 2.1 Å crystal structure of *Thermotoga maritima* DisA, which shares 41% and 60% amino acid sequence identity and similarity, respectively, with *B. subtilis* DisA (Figure 6A), exhibited a dumbbell-shaped molecule with dimensions of 80 Å x 55 Å x 30 Å (Witte et al, 2008). Three structural domains were detected: an amino-terminal globular domain, renamed

DAC, which binds ATP and metal ions to synthetize c-di-AMP; a spine-liker domain that connects the DAC and HhH domains; and a carboxy-terminal helical HhH domain that provides nonspecific DNA-binding activity (Figure 6A). DisA octamer model was predicted using small-angle X-ray scattering (SAXS), which showed that two DisA tetramers interact via the DAC domain. Interestingly, the four HhH domains are arranged in both sides of the DisA octamer in a geometry that resembles the structure of the four HhH domains found in the HJ binding protein RuvA (Witte et al, 2008) (Figure 6B).

Strikingly, the crystal of a bis-(3', 5')-cyclic dimeric adenosine monophosphate (c-di-AMP) was found within the DisA DAC domain. The motifs RHR and DGA, which are conserved in all DAC proteins, were found to be important for this interaction (Witte et al, 2008). In the presence of divalent cations, DisA possesses specific diadenylate cyclase (DAC) activity, which consists in the hydrolysis of 2 ATP molecules into c-di-AMP (Witte et al, 2008). In *Mycobacterium tuberculosis*, both DAC and HhH domains were shown to be essential for c-di-AMP synthesis (Bai et al, 2012).

Branched DNAs (three- and four-way junctions) were found to specifically inhibit DisA synthesis of c-di-AMP. It was shown that DisA weakly binds ssDNA and dsDNA (Bejerano-Sagie et al, 2006; Witte et al, 2008), but with apparently higher affinity for HJs (Witte et al, 2008). A model was developed to explain the mechanism of DisA checkpoint control (Figure 7). A conformational change in DisA could be the basis for the allosteric regulation of the DAC domain by branched DNA binding. Higher c-di-AMP levels seem to be associated to "normal" DNA, while lower c-di-AMP levels with damaged DNA (Witte et al, 2008).

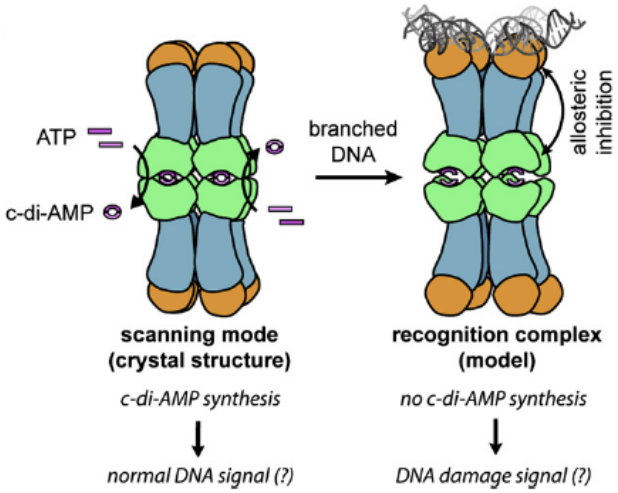

Figure 7. Current model for the role of DisA in DNA damage checkpoint.
In the absence of DNA damage, DisA moves dynamically while synthesizes c-di-AMP. The recognition of recombination intermediates or stalled replication forks (e.g. HJs) inhibits c-di-AMP synthesis (possibly via allosteric inhibition), which signals for the presence of DNA damage.

1.3.1. c-di-AMP synthesis and degradation

c-di-AMP is synthesized by the condensation of two ATP molecules, a reaction catalysed by DAC enzymes in the presence of divalent cations (Figure 8). This essential secondary messenger is mostly found in Gram-positive bacteria, but also in Gram-negative bacteria such as *Chlamydia trachomatis* (Barker et al, 2013), Bacteroidetes, Cyanobacteria, Fusobacteria and δ-proteobacteria, and in Archaea of the phylum Euryarchaeota (Corrigan & Grundling, 2013; Romling, 2008). Most bacteria have only one predicted DAC enzyme (Witte et al, 2008). This is in contrast to c-di-GMP production, for which most organisms encode multiple enzymes. An exception is *B. subtilis*, where three DAC enzymes are functional: two of them are active during vegetative growth and sporulation (DisA and CdaA), while CdaS is only expressed in the forespore (Figure 9B). Finally, in eukaryote and other bacteria (e.g. *E. coli*), c-di-AMP is not produced.

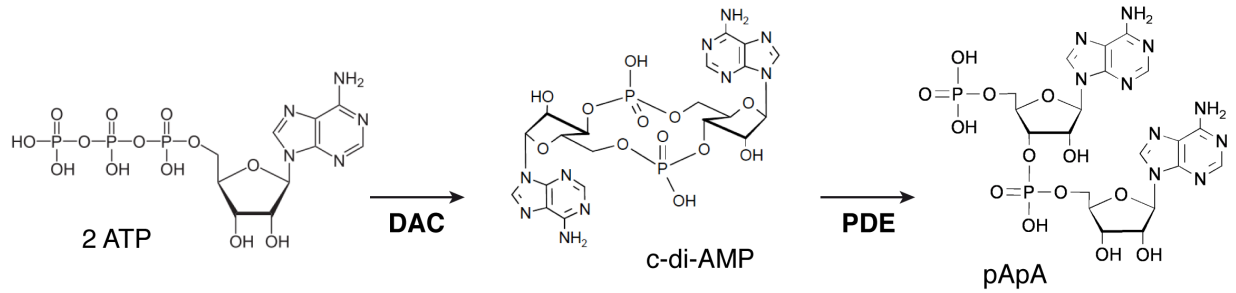

Figure 8. c-di-AMP synthesis and degradation.
Diadenylate cyclase (DAC) enzymes hydrolyse 2 ATP molecules into a cyclic di-AMP (c-di-AMP). Phosphodiesterase (PDE) enzymes degrade c-di-AMP into 2 AMP molecules (pApA). DAC and PDE enzymes control the intracellular c-di-AMP pool.

CdaA (previously known as YbbP) is a functional DAC enzyme in *B. subtilis*, predicted to localize in the membrane and to be involved in cell wall metabolism (Luo & Helmann, 2012a; Mehne et al, 2013). The activity of CdaA is stimulated by interaction with CdaR (formerly known as YbbR), a protein encoded by the gene located downstream *cdaA* (Figure 9A), which extracellular domains potentially sense environmental changes (Corrigan & Grundling, 2013; Mehne et al, 2013). Strikingly, CdaA activity seems to depend on manganese or cobalt ions (Rosenberg et al, 2015).

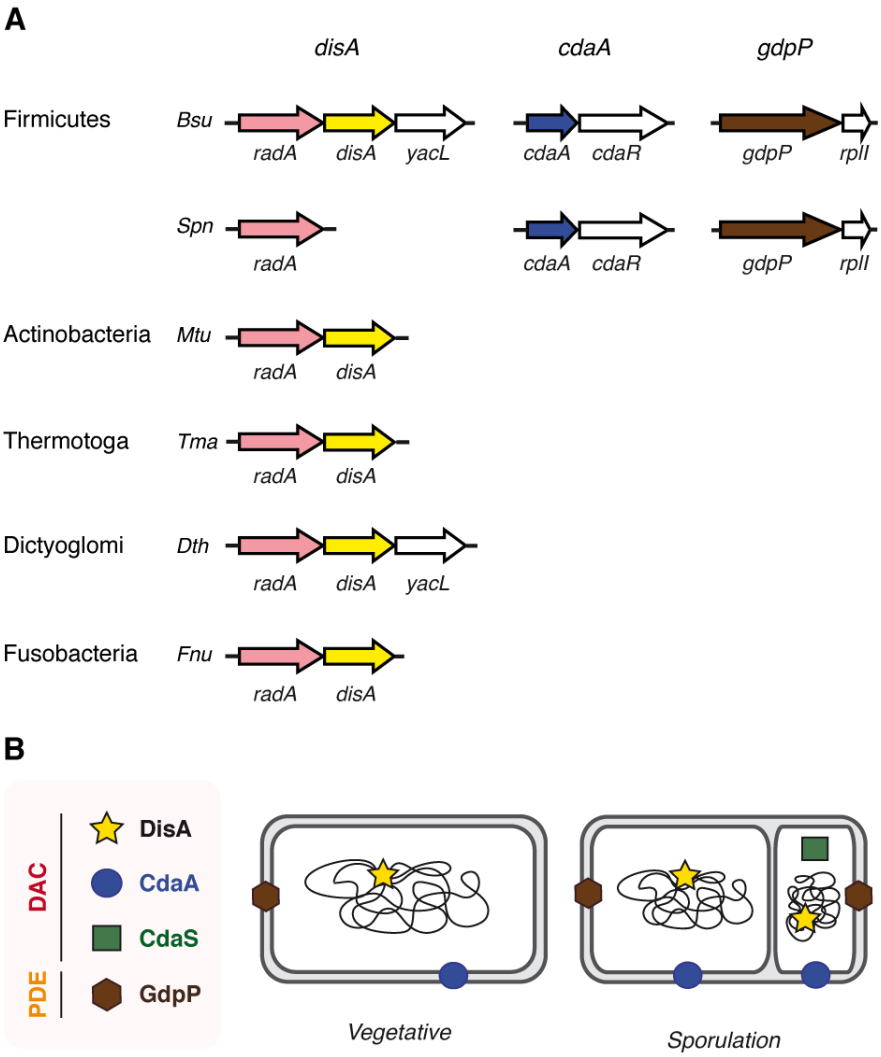

Figure 9. Phylogenetic distribution of *disA*, *cdaA* and *gdpP* genes, and their subcellular localization in *B. subtilis*.
(A) Conserved genomic organization of *disA* among different bacteria Phylum. Abbreviations are based on bacterial genus and species of a representative of each Phylum (*Bsu: B. subtilis, Spn: Streptococcus pneumoniae, Mtu: Mycobacterium tuberculosis, Tma: Thermotoga maritima, Dth: Dictyoglomus thermophilum* and *Fnu: Fusobacterium nucleatum*. (B) Subcellular localization of DAC and PDE enzymes in *B. subtilis* and their temporal expression. DisA colocalizes with the chromosome, while CdaA and GdpP are bound to the membrane. CdaS is only expressed in the forespore.

The *cdaA* gene is the first of a σ^A-regulated operon that also contains the essential *glmM* and *glmS* genes, which are involved in cell wall synthesis (Mehne et al, 2013). In bacteria expressing a single DAC enzyme, the majority of them are very similar to CdaA (e.g. *Listeria monocytogenes*, *Staphylococcus aureus* and *Streptococcus pyogenes*), including its genomic organization (Corrigan et al, 2011; Kamegaya et al, 2011; Woodward et al, 2010). Exceptions are found in Actinobacteria, Thermotoga, Dictyoglomi and Fusobacteria that only express a single DAC enzyme that is homolog to DisA (Figure 9A). Mutation of *cdaA* confers a synthetic lethal phenotype in the Δ*disA* context (Luo & Helmann, 2012a).

CdaS (previously known as YojJ) is the only DAC enzyme exclusively expressed during sporulation (Nicolas et al, 2012) and that are only present in *Bacillus* and *Clostridium spp.* (Corrigan & Grundling, 2013; Romling, 2008). The lack of CdaS affects the ability of spores to germinate in rich media (Mehne et al, 2014). The N-terminal domain modulates the activity of CdaS, which forms a hexamer that when disrupted results in a strong increase of c-di-AMP synthesis (Mehne et al, 2013; Mehne et al, 2014). The functional specialization of the three DAC enzymes (DisA in the chromosome, CdaA in the membrane and CdaS in the forespore) suggests a time- and compartment-specific c-di-AMP production and regulation (Mehne et al, 2013).

Intracellular levels of c-di-AMP are not only regulated by the rate of synthesis but also by the rate of degradation. GppP (formerly known as YybT) is the best-characterized phosphodiesterase (PDE) enzyme that degrades c-di-AMP into pApA (Figure 8). In *B. subtilis*, GdpP is the only PDE enzyme, although is non-essential. The *gdpP* gene forms operon with *rplI*, the gene that encodes for the ribosomal protein L9 (Figure 9A). In other species (e.g. *Listeria* or *Staphylococcus spp.*), *gdpP* can also be found in the same operon of the gene encoding the replicative DNA helicase DnaC. Expression of *gdpP* can be auto-regulated by an antisense RNA under control of σ^D, which is involved among other things with the expression of cell wall autolytic enzymes (Luo & Helmann, 2012b). The GdpP protein contains two transmembrane helices, a degenerate PAS sensory domain, a highly divergent GGDEF domain, a DHH domain and a DHH-associated DHHA1 domain, being the latter domain responsible for the PDE activity (Rao et al, 2009). Proteins with this domain organization are only found in members of the phyla Firmicutes and Tenericutes (Corrigan & Grundling, 2013). However, other PDE enzymes remain unknown. An essential PDE enzyme (renamed DhhP) has been recently characterized in *Borrelia burgdorferi*, which contains only the DHH-DHHA1 domain and was shown to be involved in cell growth and virulence (Ye et al, 2014). Moreover, *gdpP*-mutant strains were more resistant to acid and heat stress in *B. subtilis*, *L. monocytogenes* and *Lactococcus lactis* (Rallu et al, 2000; Rao et al, 2009; Smith et al, 2012; Witte et al, 2013). Interestingly, the stringent response signalling molecule (p)ppGpp inhibits GdpP activity (Rao et al, 2009), increasing the intracellular levels of c-di-AMP under stress conditions (Corrigan et al, 2015). A cross-talk between these two nucleotide-signalling pathways was demonstrated *in vivo* in *S. aureus* (Corrigan et al, 2015).

1.3.2. c-di-AMP function

Signalling nucleotides are well known to have key roles in the regulation of a wide range of cellular pathways in all living cells. In bacteria, c-di-AMP was the second cyclic dinucleotide identified, which recently has been identified to be a crucial signalling molecule that regulate a set of processes that are not necessarily the same as c-di-GMP (reviewed in Corrigan & Grundling, 2013). Accumulation of high concentrations of c-di-AMP, by overexpressing a hyperactive allele of CdaS ($CdaS_{L44F}$) in a strain lacking GdpP, inhibited growth and led to aberrant cell morphology in *B. subtilis* (Mehne et al, 2013). Decreased c-di-AMP levels (by overexpressing GdpP in a strain lacking CdaA) greatly sensitized *B. subtilis* cells to β-lactam antibiotics, suggesting a role for this molecule in cell wall homeostasis (Luo & Helmann, 2012a). Reduction of c-di-AMP levels also decreased growth rates and affected cell wall stability in *L. monocytogenes* (Witte et al, 2013). In *S. aureus*, c-di-AMP was also shown to be involved in cell wall stress and controlling cell size (Corrigan et al, 2011), and to regulate fatty acid synthesis in *Mycobacterium smegmatis* (Zhang et al, 2013). The c-di-AMP secreted by *L. monocytogenes* (Parvatiyar et al, 2012; Witte et al, 2013; Woodward et al, 2010), *C. trachomatis* (Barker et al, 2013) and *M. tuberculosis* (Dey et al, 2015), was shown to specifically trigger host innate immunity. The modulation of immune responses by c-di-AMP could be a powerful weapon to be used in immunotherapeutic strategies against bacterial pathogens.

Finally, c-di-AMP levels act as an indicator of DNA integrity at the onset of sporulation in *B. subtilis*. The intracellular concentration of c-di-AMP was revealed to be 3-fold higher during sporulation, but decreased in the absence of DisA or in the presence of DNA-damaging agents, where the levels of GdpP are increased. External addition of c-di-MP partially rescued the delay in sporulation in cells treated with nalidixic acid. It is likely that upon DNA damage, DisA halts c-di-AMP production, which act as a signal to stop replication until the DNA can be repaired (Oppenheimer-Shaanan et al, 2011).

By using affinity pull-down assays and genome-wide nucleotide protein interaction screens, c-di-AMP receptors have progressively been identified in bacteria (Corrigan et al, 2013; Roelofs et al, 2011). However, only receptors related to metabolic functions have been described so far to be regulated by c-di-AMP: *M. smegmatis* DarR, a transcription repressor of genes that encode fatty acids or cold shock proteins (Zhang et al, 2013); *S. aureus* KtrA and CpaA, and *S. pneumoniae* CabP protein, involved in potassium and/or sodium transport (Bai et al, 2014; Corrigan et al, 2013); the histidine kinase KdpD of *S. aureus*, with a potential role in

potassium uptake (Corrigan et al, 2013); a pyruvate carboxylase (LmPC) from *L. monocytogenes* (Sureka et al, 2014) and; the PII-like signal transduction proteins DarA of *B. subtilis* (Gundlach et al, 2015), PstA of *S. aureus* and *L. monocytogenes*, which are associated with nitrogen metabolism (Campeotto et al, 2015; Choi et al, 2015; Muller et al, 2015). c-di-AMP is also sensed by the *ydaO* riboswitch class and this interaction, in Bacillales, is predicted to modulate the expression of genes involved in sodium/potassium transport, amino acid transport and cell wall homeostasis. Activation of transcription by this riboswitch was observed as c-di-AMP levels decreased (Nelson et al, 2013).

1.4. Radiation-sensitive protein A (RadA/Sms)

The *radA* gene, also termed *sms* ('sensitivity to MMS') (Song & Sargentini, 1996), was first identified in an *E. coli* mutant (*radA100*) that was sensitive to X-ray and UV-radiation and MMS (Diver et al, 1982). In *E. coli*, *radA* is cotranscribed with the phosphoserine phosphatase gene *serB*, although no defect in serine biosynthesis was observed in a *sms* null (*sms*1) strain, whereas increased sensitivity to MMS was confirmed (Neuwald et al, 1992). In *B. subtilis*, the *sms* gene showed 50% amino acid identity with *E. coli radA*. Mutation in *sms* increased sensitivity of cells to MMS, therefore this gene was renamed *sms* (Krüger et al, 1997). To simplify, in this work the *sms* or *radA* gene is referred as *radA* and its product as RadA/Sms. It is important to highlight that the *radA* gene described here is not the same gene as *radA* from Archaea, even though they have the same name and share a similar ATPase domain to *recA* (Haldenby et al, 2009).

B. subtilis RadA/Sms protein is 458 amino acids long and can be divided in several putative domains that are ubiquitous among different eubacterial orthologs (Figure 10): a zinc-finger domain at the N-terminus with a CXXC-X_n-CXXC motif; an extended region with homology to RecA, with Walker A and B boxes, which is characteristic of ATPases; a highly conserved nuclease motif (KNRXG) and; a C-terminal region that is related to the Lon protease. The zinc finger motif seems to play an essential role in the DNA repair function of RadA/Sms, since a single amino acid modification (Cys to Tyr) in the *radA100* strain was sufficient to impair resistance to MMS (Song & Sargentini, 1996). The KNRXG motif is also present in the gp65 protein of the D29 mycobacteriophage. Mutation in this motif led to complete loss of the fork-specific 3'-5'exonuclease activity carried out by gp65 (Giri et al, 2009).

RadA/Sms protein sequence alignments of representatives of different bacteria groups (e.g. Gram-positive or negative, spore or non-spore forming, absence or presence of *disA*) are shown

in Figure 10, where the conserved domains regions are also indicated. Interestingly, in *B. subtilis* (as in *L. monocytogenes*), the putative Lon protease domain lacks the active-site serine that is present in *E. coli* and *M. tuberculosis* RadA/Sms, being substituted by an alanine (Figure 10, red asterisk).

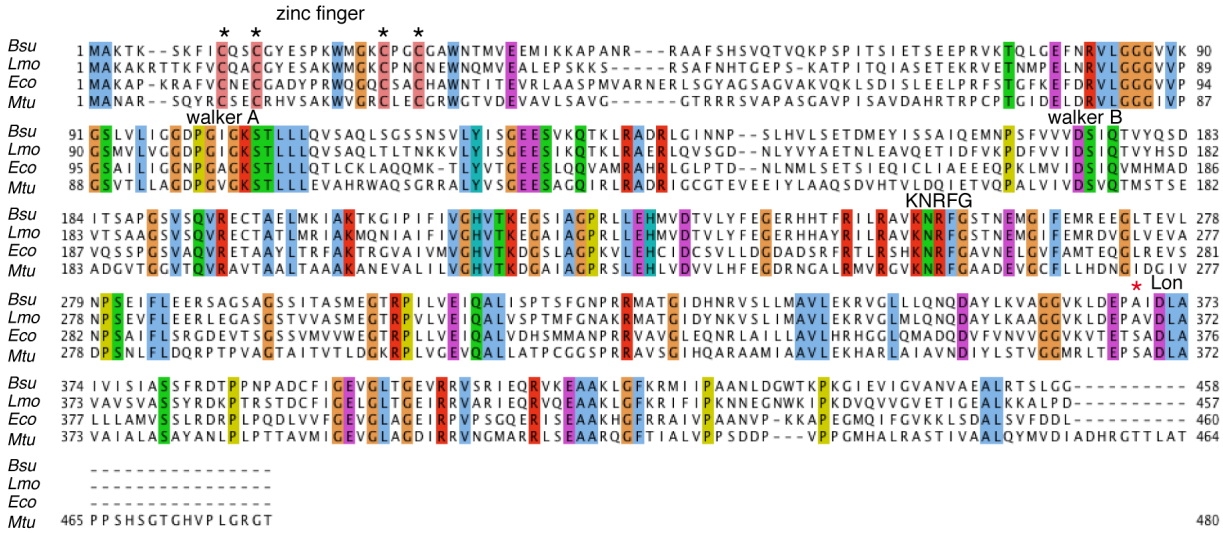

Figure 10. RadA/Sms protein sequence alignments.
Identical amino acids alignments are coloured. *Bsu: Bacillus subtilis* (Gram-positive, spore forming, *disA*$^+$); *Lmo: Listeria monocytogenes* (Gram-positive, non-spore forming, *disA*$^-$); *Eco: Escherichia coli* (Gram-negative, non-spore forming, *disA*$^-$); *Mtu: Mycobacterium tuberculosis* (Gram-positive, non-spore forming, *disA*$^+$). The C-terminal zinc finger region is indicated and the conserved cysteine marked with black asterisks. Walker A and B boxes, as the KNRFG nuclease motif are also indicated. A red asterisk indicates the active-site serine present in Lon proteases, which is substituted by an alanine in *Bsu* and *Lmo*.

The moderate sensitivity to DNA-damaging agents of *E. coli* strains lacking *radA* is highly exacerbated in combination with mutations in *ruvA*, *ruvB* and/or *recG* (Beam et al, 2002; Cooper et al, 2015). Genetic analysis of *E. coli* revealed that all the conserved domains of RadA (zinc finger, walker A, KNRXG and Lon protease homology) are required for DNA damage survival (Cooper et al, 2015). Moreover, the lack of *radA* impaired the recovery of genetic rearrangements induced by the replication fork helicase DnaB (Lovett, 2006). In *Deinococcus radiodurans*, resistance to ionizing radiation requires RadA (Slade et al, 2009), which is also important for gene conversion perhaps via HJ processing functions together with RuvB and RecG in *Rhizobium etli* (Castellanos & Romero, 2009; Martinezsalazar et al, 2009). RadA/Sms also plays a role in chromosomal transformation in *S. pneumoniae* (Burghout et al, 2007) and in *B. subtilis* (Carrasco et al, 2002; Krüger et al, 1997). Taken together, a role of RadA/Sms in recombination and DNA repair, more specifically in the resolution and stabilization of regressed forks or branched intermediates during HR has been proposed.

The first association of RadA/Sms with DisA was suggested in *Mycobacterium smegmatis* (Zhang & He, 2013). In this bacterium, RadA/Sms physically interacts with DisA, modulating negatively the synthesis of c-di-AMP. This regulation was proposed to be a conserved mechanism among eubacterial species that expresses *radA* and *disA* (such as *B. subtilis*), as demonstrated by bacterial two-hybrid interaction assays. Taking into account that *disA* exists exclusively downstream *radA* and that both protein products have been related to DNA repair functions and to functionally interact in another gram-positive bacteria, it is unavoidable to question whether DisA and RadA/Sms play a role in the DDR of *B. subtilis*.

Objectives

2. Objectives

The general aim of this work was to study the role of DisA in the DDR of exponentially growing *B. subtilis* cells. Specific objectives were to:

I. Genetically characterize the contribution of DisA, RadA/Sms and variation of c-di-AMP levels to the DDR in exponentially growing *B. subtilis* cells;
II. Investigate the involvement of DisA with homologous recombination functions;
III. Study *in vivo* the localization and dynamics of DisA-YFP and RadA-YFP in damaged and undamaged vegetative *B. subtilis* cells;
IV. Characterize biochemically the DisA protein and its involvement with HJ processing and DNA strand exchange functions;
V. Study the role played by RadA/Sms in the DisA function.

Materials and methods

3. Materials and methods

1.5. Materials

1.5.1. Strains

The strains used in this work are detailed in the following tables:

Table 1. *E. coli* strains

Strain	Genotype	Use
XL1 Blue	*recA1 endA1 gyrA96 thi-1 hsdR17 supE44 relA1 lac [F' proAB lacI^q ZΔ M15 Tn10 (Tet)]* (Stratagene)	Host for plasmid construction and maintenance
BL21 (DE3)	pLysS B F- *dcm omp T hsdS* (rB-mB-) *gal* (DE3) [pLysS Cat] (Stratagene)	Host for overexpression of *Bacillus subtilis* proteins

Table 2. *B. subtilis* strains

Strain	Relevant mutant genotype	Reference
BG214	*trpCE metA*5 *amyE1 ytsJ*1 *rsbV*37 *xre*1 *xkd*A1 *att*$^{SP\beta}$ *att*^{ICEBs1}	Laboratory strain
BG703	+ Δ*ruvAB*	(Sanchez et al, 2005)
BG855	+ Δ*recU*	(Sanchez et al, 2005)
BG1131	+ Δ*recG*	(Sanchez et al, 2007a)
BG190	+ Δ*recA*	(Ceglowski et al, 1990)
BG1221	+ Δ*disA*	This work
BG1245	+ Δ*radA*	This work
BG1363	+ $P_{spac(hy)}$ *radA*	This work
BG1413	+ $P_{spac(hy)}$ *radA* Δ*disA*	This work
BG1415	+ $P_{spac(hy)}$ *radA* Δ*radA*	This work
BG1319	+ Δ*radA* Δ*disA*	This work
BG1253	+ Δ*recU* Δ*disA*	This work
BG1395	+ Δ*recU* Δ*radA*	This work
BG1255	+ Δ*ruvAB* Δ*disA*	This work
BG1355	+ Δ*ruvAB* Δ*radA*	This work
BG1257	+ Δ*recG* Δ*disA*	This work
BG745	+ Δ*recG* Δ*radA*	This work
BG1307	+ Δ*gdpP*	This work
BG1303	+ Δ*cdaA*	This work
BG1305	+ Δ*cdaS*	This work

BG1309	+ $P_{spac(hy)}$ *gdpP*	This work
BG1327	+ *disA-yfp*	This work
BG1333	+ *radA-yfp*	This work
BG1405	+ *disA-yfp* Δ*recU*	This work
BG1407	+ *disA-yfp* Δ*recN*	This work
BG1409	+ *radA-yfp* Δ*recU*	This work
PY79	prototroph	Laboratory strain
YA5	+ Δ*disA*	(Bejerano-Sagie et al, 2006)
YA127	+ *disA*77	(Oppenheimer-Shaanan et al, 2011)
168	*trpC*2	Laboratory strain
GP1323	+ Δ*disA* Δ*cdaS* P_{xylA} *cdaS*	(Mehne et al, 2013)
GP1354	+ Δ*disA* Δ*cdaA* Δ*cdaS* P_{xylA} $cdaS_{E46K}$	(Mehne et al, 2014)
GP1334	+ Δ*disA* Δ*cdaA* Δ*cdaS* P_{xylA} $cdaS_{L44F}$	(Mehne et al, 2014)

1.5.2. Reagents

The chemical products and the different compounds used in this project are specified in the following table:

Table 3. Chemicals and compounds

Component	Manufacturer
Micro bio-spin columns, Hydroxyapatite, Gel-dryer Model 583	Bio-Rad
IPTG	Calbiochem
Casein hydrolysate	Fluka
Sephadex G-50 DNA grade, Q sepharose fast flow, SP sepharose fast flow, anti-rabbit IgG-horseradish peroxidase	GE Healthcare
SDS, Ammonium sulphate, Tris	ICN
Medical film (x-ray film)	Konica Minolta
Sodium acetate trihydrate, Hydrochloric acid, Formic acid, Coomasie blue, Magnesium chloride hexahydrate, Dimethyl sulfoxide, Absolute ethanol, Imidazole, Isopropyl alcohol, Glycine, Sodium hydroxide, D/L Tryptophan, L-Methionine, Calcium chloride, Titriplex (EDTA)	Merk
Millex filters (0.22 µm), VM filters (0.05 µm), HAWP filters (0.45 µm)	Millipore
Glycerol	MP Biomedicals
Restriction enzymes, T4 polynucleotide kinase (PNK), T4 DNA ligase	New England Biolabs
Acetic acid, Vaseline	Panreac
[α^{32}P]-ATP, [γ^{32}P]-ATP	Perkin Elmer
Agarose, Tryptone, Bacteriological agar, Yeast extract	Pronadisa
Ni-NTA agarose, Plasmid extraction kits	Quiagen

Proteinase K	Roche
Acrylamide, Bisacrylamide, Nalidixic acid (Nal)	Serva
Ampicillin, Chloramphenicol, Mytomycin C (MMC), Glutaraldehyde, Methyl Methanesulfonate (MMS), Hydrogen peroxide (H_2O_2), 1,4-Dithiothreitol (DTT), Suberic acid, Triton X-100, Lysozyme, Ethidium bromide, deoxynucleotides diphosphate (dNDPs), Urea	Sigma
Dialysis membranes	Spectrum
LB broth	USB

1.5.3. Oligonucleotides

In the following table are shown the sequences of oligonucleotides used in this work:

Table 4. Oligonucleotides

ID	Sequence 5' – 3'
J3-1	CGCAAGCGACAGGAACCTCGAGAAGCTTCCGGTAGCAGCCTGAGCGGTG GTTGAATTCCTCGAGGTTCCTGTCGCTTGCG
J3-2	CGCAAGCGACAGGAACCTCGAGGAATTCAACCACCGCTCAACTCAACTG CAGTCTAGACTCGAGGTTCCTGTCGCTTGCG
J3-3	CGCAAGCGACAGGAACCTCGAGTCTAGACTGCAGTTGAGTCCTTGCTAG GACGGATCCCTCGAGGTTCCTGTCGCTTGCG
J3-4	CGCAAGCGACAGGAACCTCGAGGGATCCGTCCTAGCAAGGGGCTGCTAC CGGAAGCTTCTCGAGGTTCCTGTCGCTTGCG
J3-5	CGCAAGCGACAGGAACCTCGAGTCTAGACTGCAGTTGAGTTGAGCGGTG GTTGAATTCCTCGAGGTTCCTGTCGCTTGCG
170	CTAGAGACGCTGCCGAATTCTGGCTTGGATCTGATGCTGTCTAGAGGCCT CCACTATGAAATCGCTGCA
173	CCGGGCTGCAGAGCTCATAGATCGATAGTCTCTAGACAGCATCAGATCC AAGCCAGAATTCGGCAGCGTCT
345	GCGATTTCATAGTGGAGGCCTCTAGACAGCACGCCGTTGAATGGGCGGA TGCTAATTACTATCTC
346	GAGATAGTAATTAGCATCCGCCCATTCAACGGCGTGCTGTCTAGAGACT ATCGATCTATGAGCTCTGCAGC
J50-1	GACGCTGCCGAATTCTGGCGTTAGGAGATACCGATAAGCTTCGGCTTAA
J50-4	ATCGATGTCTCTAGACAGCACGAGCCCTAACGCCAGAATTCGGCAGCGT
J50-6	CTTAAGCCGAAGCTTATCGGTATCTGCTCGTGCTGTCTAGAGACATCGAT
16-M	GACGCTGCCGAATTCTACCAGTGCCTTGCTAGGACATCAGTCCTTACCTG CAGGTTCAC
17-M	GGGTGAACCTGCAGGTAAGGGGCTGCTCATCGTAGGTTAGTTGGTAGAA TTCGGCAGC
19-M	TAAGAGCAAGATGTTCCTCAACTGATGTCCTAGCAAGGCAC
21	ACTAACCTACGATGAGCAGCC
Fb-1	AGAGGATCCCCGGGTACCGAGCTCGAATTC
Fb-2	GAATTCGAGCTCGGTACCCGGGGATCCTCT

F-2	AAAAAAAAAAAAAAAAAAAAAAAAAAAAAAGAATTCGAGCTCGGTACC CGGGGATCCTCT

1.5.4. Media

The composition of each growth medium used in this work is listed in the following table:

Table 5. Media

Name	Composition
LB Broth (Luria-Bertani broth)	10 g/l casein peptone, 5 g/l yeast extract, 5 g/l NaCl
LB Agar (Luria-Bertani agar)	10 g/l casein peptone, 5 g/l yeast extract, 5 g/l NaCl, 12 g/l Agar
GM1	1X SBase (2 g/l ammonium sulphate, 14 g/l K_2HPO_4, 6 g/l KH_2PO_4, 1 g/l sodium citrate), 0.5 % glucose, 0.1 % yeast extract, 0.02 % casein hydrolysate, 0.8 mM $MgSO_4$, 25 µg/ml D/L tryptophane, 50 µg/ml L-methionine
GM2	GM1 medium supplemented with 3.3 mM $MgSO_4$ and 0.5 mM $CaCl_2$
$S7_{50}$	5 mM potassium phosphate pH 7.0, 10 mM ammonium sulphate, 50 mM MOPS pH 7.0, 1 % gluocose, 0.1 % glutamate monohydrate, 0.7 mM $CaCl_2$, 2 mM $MgCl_2$, 50 µM $MnCl_2$, 5 µM $FeCl_3$, 1 µM $ZnCl_2$, 40 µg/ml tryptophane, 40 µg/ml methionine

1.5.5. Plasmids

A list of the plasmids used in this work is provided in the following table:

Table 6. Plasmids

Name	Derived from	Description and Reference
pCB837	pGEM-T	Contains the *disA::six-cat-six* fragment used to construct the *disA* null mutant (This work)
pCB919	pGEM-T	Contains the *radA::six-cat-six* fragment used to construct the *radA* null mutant (This work)
pCB946	pGEM-T	Contains the *radA-disA::six-cat-six six* fragment used to construct the *radA-disA* null mutant (This work)
pCB947	pSG1164	Contains the *disA-yfp* fusion used to construct the strain expressing DisA-YFP (This work)
pCB950	pSG1164	Contains the *radA-yfp* fusion used to construct the strain expressing RadA/Sms-YFP (This work)
pCB875	pET24b	Plasmid to overexpress DisA-6xHis protein (Bejerano-Sagie et al, 2006)
pCB959	pET3a	Plasmid to overexpress RadA/Sms protein (This work)
pCB954	pDR111	Contains the *amyE::*$P_{spac(hy)}$*-radA* fragment used to construct the *B. subtilis* strains overexpressing RadA/Sms (This work)

1.5.6. Buffers

A list of the buffers, and their composition, used in this work is given in the following table (Table 7). The concentrations described are the final volume concentration.

Table 7. Buffers

Buffer	Composition
A	50 mM Tris-HCl (pH 7.5), 50 mM NaCl, 1 mM DTT, 0.5 mg/ml BSA, 0.1% Triton
B	50 mM potassium phosphate buffer (pH 7.6), 10% glycerol, 500 mM NaCl, 20 mM imidazole
C	50 mM potassium phosphate buffer (pH 7.6), 10% glycerol, 20 mM imidazole
D	50 mM Tris-HCl (pH 7.5), 300 mM NaCl, 50% glycerol
E	50 mM Tris-HCl (pH 7.0), 1 M NaCl, 10% glycerol, 1 mM DTT
F	50 mM Tris-HCl (pH 7.5), 1 M NaCl, 50% glycerol, 1 mM DTT
G	50 mM Tris-HCl (pH 7.5), 80 mM NaCl, 10 mM MgOAc, 50 µg/ml BSA and 5% glycerol

1.6. Methods

1.6.1. Cells manipulation

E. coli was only used in this work for cloning, plasmid maintenance and overexpression of *B. subtilis* proteins. The *E. coli* strains used are listed in Table 1. *B. subtilis* laboratory strain (BG214) and its isogenic derivatives, as well as the PY79 and 168 strains and their derivatives, are all listed in Table 2. Except otherwise stated, bacteria cultures were grown in LB broth and when specified in the text, $S7_{50}$ minimal medium was used. The composition of each medium is detailed in Table 5.

1.6.1.1. Preparation of *E. coli* competent cells

E. coli cells were grown at 37°C under agitation until exponential phase (OD_{600} = 0.4), harvested by centrifugation and treated with ice cold 0.1 M $MgCl_2$ and 0.1 M $CaCl_2$. In this condition, pores are produced in the cell membrane that allow for extracellular DNA uptake. Cells aliquots (0.2 ml) were prepared if competent cells were not used immediately and stored at -80°C with 20% glycerol (Hanahan, 1983).

1.6.1.2. Preparation of *B. subtilis* competent cells

B. subtilis cells have the advantage of developing natural competence at certain conditions (e.g. starvation). Competent cells were obtained by growing an overnight culture in GM1 (See Table 5) at 30°C without agitation. The overnight culture was diluted in a fresh GM1 medium

to an OD_{560} of 0.04 and allowed to grow at 37°C with vigorous aeration. Aliquots (1 ml) were taken 30, 60 or 90 min after cells reached stationary phase and stored at -80°C with 20% glycerol for further use (Bott & Wilson, 1968).

1.6.1.3. Bacterial transformation

E. coli cells were transformed using the heat shock method (Hanahan, 1983). Plasmidic DNA (max. 100 ng) was added to each 0.2 ml aliquot of pre-thawed competent cells and incubated for 30 min on ice. Then, they were submitted to heat shock of 42°C for 1 min and allowed to cool again on ice. Preferentially, cells were incubated at 37°C with agitation for about one hour, then pelleted and plated in LB agar containing the selective antibiotic.

B. subtilis cells were transformed using the method described by Bott and Wilson (1968). Stored aliquots (1 ml) of previously prepared natural competent cells were added to 10 ml fresh GM2 medium and allowed to grow for two hours at 37°C with agitation. Then, small aliquots (0.2 ml) of competent cells were taken and incubated for another hour with 100-200 ng DNA. Cells were pelleted and plated in LB agar containing the selective antibiotic.

1.6.1.4. Bacterial transduction using bacteriophage SPP1

B. subtilis cells were transducted using the method modified from (Yasbin & Young, 1974). First, SPP1 phages containing random chromosomal segments were obtained by infecting a *B. subtilis* mid-log phase culture with SPP1 bacteriophage stock, in a multiplicity of infection (MOI) of 10 phages/cell. Cells were spun down and the phage-rich supernatant was filtered (0.45 μm) and stored at 4°C. In this step, bacterial cells were infected and lysed by the stock lysate that also contain defective SPP1 phages that encapsidated random segments of chromosomal DNA. When working with SPP1, the LB broth was supplemented with 10 mM $MgCl_2$. Then, these phages were titrated and used to infect the receptor *B. subtilis* culture in a MOI of around 1 phage/cell. Cells were pelleted and plated in LB agar containing the selective antibiotic.

1.6.1.5. Construction of *B. subtilis* mutant strains

The majority of *B. subtilis* strains used in this study, which are listed in Table 2, are isogenic to the BG214 strain, except for some strains that are derived from the 168 and PY79 backgrounds. For gene disruption, the method previously described was used (Sanchez et al, 2007b). A 2-kb *six-cat-six* cassette containing two directly repeated copies of β-site-specific recombinase target site (*six*) surrounding the chloramphenicol acetyl transferase (*cat*) gene was used to replace the coding sequence of *ruvAB*, *recG*, *disA* or *radA* gene. These disruptions were

transferred into the chromosome of *B. subtilis* via bacterial transformation or SPP1 transduction to generate null mutants. Then, expression of the β-recombinase was used to remove the *cat* gene from *ΔdisA* and *ΔruvAB* strains. Strains expressing the DisA-YFP or RadA/Sms-YFP fusion proteins from the native locus and promoter(s) were constructed using plasmids pCB947 and pCB950, respectively. Some of the strains used in this work (*ΔgdpP*, *ΔcdaA*, *ΔcdaS*, $P_{spac(hy)}$-GdpP) derived from strains kindly provided by Dr. John D. Helmann (Cornell University, USA) (Luo & Helmann, 2012a) and the strains overexpressing *cdaS* (GP1323, GP1354 and GP1334) were generously sent by Dr. Jörg Stülke (Mehne et al, 2014). Finally, *B. subtilis* strains overexpressing *radA* were obtained by transforming wild-type cell with pCB954 (*amyE::*$P_{spac(hy)}$*-radA*).

1.6.2. Survival assays (chronic and acute)

B. subtilis wild type or mutant strains disrupted in one or more genes (See Table 2) were submitted to survival assays against agents that induce different types of DNA damage: MMC, MMS, H_2O_2 and Nal. Survival assays were divided into chronic or acute. In the chronic assay, cells were exposed to a DNA damaging agent overnight, while in the acute, cultures are treated for a short period of time (15 min). The latter represents a more quantitative test since an estimated number of viable cells were obtained.

1.6.2.1. Chronic assays

The sensitivity of cells to chronic exposure to MMS, H_2O_2, Nal or MMC was determined by growing cultures to an OD_{560}= 0.4 and spotting 10 μl of serial 10-fold dilutions (1 x 10^{-3} to 1 x 10^{-6}) on freshly prepared LB agar plates supplemented with the indicated concentrations of the DNA damaging agent, as described (Sanchez et al, 2005). Plates were incubated overnight at 37ºC. The drug concentration used in each experiment was the highest dose to give the clearest phenotype.

1.6.2.2. Acute assays

Acute survival assays were performed as previously described (Cardenas et al, 2009). Briefly, *B. subtilis* cells were grown to an OD_{560} = 0.4 at 37°C in LB broth, and exposed to different concentrations of MMS**.** After 15 min, cells were diluted and plated on LB agar plates. The large majority of cells are one and two non-separated tweens with an average of ~1.6 cell/ colony forming unit (CFU), suggesting that the proportion of cells is similar to CFUs. CFUs were counted and plotted against the concentration of damaging agent, giving the survival

curve. For experiments in which external c-di-AMP was provided, cells were pre-treated with polyamines, as previously described (Bejerano-Sagie et al, 2006).

1.6.3. Mutation frequency analysis

An overnight culture derived from a single colony was used to inoculate 20 ml of LB, giving an OD_{560} of 0.04 and grown at 37°C until it reached an OD_{560} of 0.8. At this point, 10 ml of cells was harvested by centrifugation, resuspended in 0.2 ml of LB and plated onto LB plates containing 10 μg/ml rifampicin. From the same culture, a 10^{-6} dilution was plated onto LB without antibiotic, in order to obtain the total number of viable cells. The plates were incubated overnight at 37°C and the CFUs counted on the following morning. Mutation frequencies were calculated as the number of rifampicin resistant colonies / total number of cells.

1.6.4. DNA manipulation

1.6.4.1. DNA isolation and quantification

Plasmidic DNA was isolated from *E. coli* using DNA purification kit (Qiagen). The DNA concentration was estimated using NanoDrop ND-1000 Spectrophotometer (Thermo Scientific) by measuring the sample's absorbance at 260 nm and its purity was determined by the ratio 260/280 nm. Results were confirmed by loading the samples in an agarose gel. The plasmids used in this work are listed in Table 6.

1.6.4.2. DNA radiolabeling

Oligonucleotides were radiolabeled with [γ-^{32}P]-ATP using the enzyme polynucleotide kinase from T4 (T4 PNK) that catalyses the transfer and exchange of Pi from the γ position of ATP to the 5'-hydroxyl terminus of polynucleotides. The reaction was incubated for 45 min at 37°C and heat inactivated for 20 min at 65°C. Non-incorporated γP^{32}-ATP was removed by passing the sample through a Sephadex G-50.

1.6.4.3. Preparation of DNA substrates for biochemical assays

Annealing of oligonucleotides was performed to obtain different types of DNA substrates. The oligonucleotide mix was incubated for 5-10 min at 95°C and then allowed to cool in the same thermoblock for at least 3 hours. At this point the oligonucleotides should have re-annealed, forming the desired structure that was further confirmed by native PAGE.

1.6.4.4. Purification of DNA substrates for biochemical assays

Quite often the DNA substrate annealed contains a proportion of free oligonucleotides or intermediate structures. In order to purify these substrates, samples were separated in a non-denaturing polyacrylamide gel. Then, the band corresponding to the desired DNA structure was cut from the gel and incubated for at least 4 hours in buffer containing 0.5 M NH_4Ac, 0.1% SDS and 1 mM EDTA. The DNA should go to the supernatant that will then be collected and ethanol precipitated.

1.6.4.5. c-di-AMP isolation from cell extracts

c-di-AMP were isolated from cell extracts using the following protocol (Burhenne & Kaever, 2013). *B. subtilis* strains were grown in $S7_{50}$ minimal medium (See Table 5) to an OD_{560} of 0.4 at 37ºC with agitation. The cells were centrifuged, washed with growth medium and resuspended in extraction buffer (acetonitrile/methanol/water, 2/2/1, v/v/v) and metabolites heat extracted for 10 min at 95ºC. Extracts were normalized according to the CFUs and protein concentration. Once c-di-AMP extractions were performed, the samples were sent to the Research Core Unit Mass Spectrometry (Hannover, Germany) to be quantified. The intracellular c-di-AMP levels of different *B. subtilis* strains were quantified by LC-MS/MS. The concentration of c-di-AMP from each strain was interpolated from the purified c-di-AMP standard curve, the number of CFUs per vial and assuming an average cell volume of 1.2 fL.

1.6.5. Protein manipulation

1.6.5.1. Proteins overexpression

a) DisA

E. coli BL21 (DE3) pLysS carrying the plasmid pCB875 was used to overexpress *B. subtilis* DisA protein. pCB875 derives from the pET24b expression vector, where a copy of the *disA* gene was cloned downstream the T7 promoter and ribosomal binding site, and upstream the sequence for a C-terminal His-tag (Bejerano-Sagie et al, 2006). *E. coli* BL21 (DE3) pLysS is a commercial strain lysogenic for λ-DE3, which contains the T7 bacteriophage gene I, encoding T7 RNA polymerase under control of the lac_{UV5} promoter. This strain also contains a plasmid, pLysS, which carries the gene encoding T7 lysozyme that lowers the background expression level of the targeted gene, being an advantage especially in the expression of toxic proteins. Upon IPTG addition, this host will then express the T7 RNA polymerase that specifically recognizes the T7 promoter, to finally induce the transcription of the *disA-6xhis* fusion. Cells were grown overnight in presence of kanamycin (10 μg/ml, PCB875) and chloramphenicol (15

μg/ml, pLysS). The next day, the culture was diluted to an OD of 0.04 and grown at 37ºC. Once the culture reached mid-exponential phase (OD=0.4), 0.5 mM IPTG was added. After 3 hours, cells were harvested by centrifugation and stored at -20ºC. Culture aliquots before and after IPTG addition were taken to confirm overexpression.

b) RadA/Sms

E. coli BL21 (DE3) pLysS carrying the plasmid pCB959 was used to overexpress *B. subtilis* RadA/Sms protein. pCB959 derives from the pET3a expression vector, where a copy of the *radA* gene was cloned downstream the T7 promoter sequence and the ribosomal binding site. In this strain, as described above for DisA, expression of *radA* was controlled by IPTG addition. Cells were first grown overnight in presence of ampicillin (100 μg/ml) and chloramphenicol (15 μg/ml). The next day, the culture was diluted to an OD of 0.04 and grown for 20 min at 30ºC. The culture was transferred to 20ºC and 100 μM IPTG was added once cells reached mid-exponential phase (OD=0.3). After 16 hours, cells were pelleted and stored at -20ºC. Alternatively, cells were grown at 30ºC and induced for 3 hours with 50 μM IPTG. Culture aliquots before and after IPTG induction were taken to confirm overexpression.

1.6.5.2. Protein purification

In this work, new purification protocols for DisA and RadA/Sms proteins have been established. Other proteins, used in this work, were kindly provided by Dr. Begoña Carrasco (RecU, SsbA, RecO and RecA) and Dr. Silvia Ayora (RecG, RuvA and RuvB). In this thesis, DisA, RadA/Sms, RecA, RecU and RecG protein concentrations are expressed as moles of monomers, RecO as moles of dimers, RuvA and SsbA as moles of tetramers and RuvB as moles of hexamers, except otherwise stated. If not mentioned, all protein purification steps were performed at 4ºC.

a) DisA purification

The DisA protein overexpressed in this work was soluble and due to the presence of a 6xHis-tag, affinity chromatography using a Ni^{+2} column was the purification method used. *E. coli* BL21(DE3) cells bearing the pCB875-borne *disA* were grown for 3 hours at 37°C after IPTG induction, harvested by centrifugation, resuspended in buffer B (with 20 mM imidazole), sonicated and centrifuged (35,000 x *g* for 30 min). The supernatant was collected and polyethyleneimine (PEI) added (0.25% PEI, for an OD_{260} = 120) in order to retain and separate the nucleic acids from the protein extract. After 30 min of incubation, the solution was centrifuged (20,000 x *g* for 15 min) and the proteins remaining in the supernatant were precipitated with 70% ammonium sulphate (AS) saturation. The AS pellet was resuspended in

buffer C (without NaCl), until a final concentration of 1 M salt. The extract was loaded onto a Ni-NTA agarose column that had been previously packed and equilibrated with buffer C containing 1 M NaCl. The column was washed several times with buffer C containing a salt concentration (from 1 to 0.05 M). DisA was eluted from the Ni^{+2} column by increasing the imidazole concentration to 150 mM. Traces of other proteins eluted with DisA were removed from the sample with a Q sepharose column. DisA eluted from the Q sepharose at 600 mM NaCl. Finally, the protein was submitted to an overnight dialysis step in buffer D containing 50% glycerol. Purified protein aliquots were stored at -20ºC and -80ºC for further use. The protein concentration was determined by UV absorption applying the formula [Protein conc, μg/ml = 144 x (A_{215} – A_{225})] (Walker, 2002).

b) RadA/Sms purification

The RadA/Sms overexpression resulted in a very insoluble protein. Many approaches were tested in an attempt to increase solubility: lower IPTG concentrations (from 1 to 0.02 mM), lower induction temperatures (from 37 to 16°C), alternative growth medium (ZY auto-induction medium), use of french press instead of sonication to disrupt the cells, addition of metal ions to the lysis buffer (Mg^{+2} or Zn^{+2}), etc. None of the approaches improved RadA/Sms solubility. Thus, urea was used as the denaturing agent for the purification of RadA/Sms. *E. coli* BL21(DE3) cells bearing the pCB959-borne *radA* were grown for 3 hours at 30°C after IPTG induction, harvested by centrifugation, resuspended in buffer E supplemented with lysozyme (4 mg/ml). After 20 min of incubation at 37°C, cells were disrupted by sonication and centrifuged (35,000 x *g* for 30 min). The pellet was resuspended in buffer E containing 2 M urea, then 4 M urea, in order to clean the extract and solubilize the protein of interest, respectively. In the following steps, 4 M urea was added to all buffers. The traces of nucleic acid were removed by loading the sample in a tandem of Q/SP-sepharose at 200 mM NaCl. Under this salt condition, RadA/Sms does not bind to these columns. The sample was diluted again until the salt concentration reached 40 mM, and then loaded onto a SP sepharose (GE Healthcare), where it eluted at 500 mM NaCl. Then, it was used Bio-Gel HT Hydroxyapatite (HA, Bio-Rad) to improve the purification and finally elute clean fractions of the protein. Several refolding methods were tested: (i) in the HA column, by progressively decreasing the urea concentration during the column washing steps; (ii) before extract purification, by step-by-step dialysis, then proceeding with the purification protocol without urea or (iii) after final HA elution, by step-by-step dialysis in presence of 0.5% CHAPS. The CHAPS was removed by a final dialysis step in buffer F containing 50% glycerol. The latter refolding method gave the highest yield and purity,

in addition to being the most active protein obtained. Thus, this was the RadA/Sms protein used in all biochemical assays performed in this work.

1.6.5.3. Protein identification

All the proteins purified had their identity confirmed by peptide mass fingerprinting analysis (MALDI-TOF/TOF mass spectrometry), carried out in the Proteomics Facility of the CNB.

1.6.5.4. Analysis of RecA protein expression

RecA protein expression in exponential growing *B. subtilis* cells was measure according to the method described in (Cardenas et al, 2012). Briefly, cells at OD_{560}=0.4 were treated with increasing concentrations of MMC for 30 min. Then, cells were harvested by centrifugation, resuspended in buffer D (5% of glycerol instead of 50%), and lysed by sonication. Extracts with normalized total protein concentration and purified RecA protein with known amounts (10 to 500 ng) were separated on 10% SDS-PAGE. Gels were transferred to PVDF membranes and probed against anti-RecA antibodies. Protein bands corresponding to RecA were quantified using Quantity One. Purified RecA protein was used to build a standard curve and to calculate the amount of RecA from each extract.

1.6.6. Biochemical assays

1.6.6.1. Protein-DNA interaction:

a) Electrophoretic mobility shift assay (EMSA)

To visualize protein-DNA complex formation, EMSAs were performed. A reaction was typically performed at 37°C for 15 min with radiolabeled DNA and the protein of interest, mixed in buffer A, in a final volume of 20 µl. Reactions containing no protein were performed to control the mobility of the free DNA (negative controls). Samples were immediately loaded and separated in 6% native polyacrylamide gel electrophoresis (PAGE) and run at 200 V for about 2 hours. The gel was dried using a Gel-dryer (Bio-Rad) and exposed overnight to a medical film (Konica Minolta). Mobility shifts were observed when protein-DNA complex formation occurred.

b) DNase I footprinting

DNase I footprinting is a widely used method for studying the interaction between proteins and DNA. The areas protected from DNase I attack (footprints), give the specific areas where the protein is bound to the DNA. For these assays, reactions were performed as before (See EMSA), except that in the end, when not added before, 10 mM $MgCl_2$ was included which is

required for the endonuclease activity of DNase I. The enzymatic reaction was stopped by EDTA addition and the DNA was ethanol precipitated and resuspended in 10 µl formamide buffer (80% formamide, 8 mM EDTA, 0.1% bromophenol blue and 0.1% xylene cyanol). The samples were finally loaded in a 6% denaturing PAGE (dPAGE) containing urea, run at 1500 V and exposed overnight to a medical film.

For a size marker sequencing ladder, the Maxam-Gilbert G+A ladder was used, produced by partial acidic hydrolysis of DNA, in the presence of diphenylamine (Belikov & Wieslander, 1995). The radiolabeled oligonucleotide used to form the HJ was mixed to 10 µl of 3% diphenylamine (dissolved in formic acid) and left for 4 min at room temperature. The reaction was stopped by adding 100 µl of 0.3 M sodium acetate (pH 5.5). The 'milky' solution formed was then extracted 3 times with water-saturated ether. Then, the ether was removed by incubating the tube at 37°C with an open lid and the DNA precipitated by addition of 2.5 volumes of ethanol. Finally, the DNA pellet was resuspended in 20 µl formamide buffer.

1.6.6.2. Resolution assays

Resolution reactions were performed in the presence of the HJ-specific endonuclease RecU from *B. subtilis*. [γ-^{32}P]-ATP labelled HJ was incubated at 37°C with RecU in buffer A containing 10 mM $MgCl_2$. Samples were deproteinized after 30 min of reaction with the addition of 20 µg proteinase K, 20 mM EDTA and 0.8% SDS, and further 20 min of incubation. Then, alkaline loading buffer (with formamide and NaOH) was added, samples were heated for 10 min at 95°C and finally loaded into a denaturing 15% PAGE containing 6M urea, which run at 1600 V for about 3 hours.

1.6.6.3. Strand exchange reactions

The 3,197-bp KpnI-cleaved pGEM3Zf(+) dsDNA (20 µM) and homologous circular 3,197-nt ssDNA (10 µM) were incubated in buffer G containing 5 mM (d)ATP and 1.2 µM RecA, at 37°C for a variable time, in a 20-µl reaction volume. The RecA-mediated DNA strand exchange was analysed in presence of different protein combinations, involving SsbA (300 nM), RecO (100 nM) and DisA (25-200 nM), as indicated in the figures. The samples were deproteinized and separated by 0.8% agarose gel electrophoresis with ethidium bromide staining. Signals of DNA bands were quantified using Quantity One.

1.6.6.4. ATPase assays

a) Spectrophotometer

To investigate whether RadA/Sms protein hydrolyses ATP or whether DisA modulates RecA (d)ATPase activity, a coupled spectrophotometric enzyme assay was used (Hobbs et al, 2007; Morrical et al, 1986). Absorbance measurements were taken with a Shimadzu CPS-240A dual-beam spectrophotometer equipped with a temperature controller and 6-position cell chamber. The cell path length and band pass were 1 cm and 2 nm, respectively. The regeneration of ATP from ADP and phosphoenolpyruvate driven by the oxidation of NADH can be followed by a decrease in absorbance at 340 nm (Yadav et al, 2012). Rates of (d)ATP hydrolysis was measured in buffer G containing 5 mM (d)ATP and RecA (0.8 μM) or RadA/Sms (160 nM), for 30 min at 37°C in a 50-μl reaction volume. A (d)ATP regeneration system (0.5 mM phosphoenolpyruvate, 10 U/ml pyruvate kinase) and a coupling system (0.25 mM NADH, 10 U/ml lactate dehydrogenase, 3 mM potassium glutamate) were also included. When indicated, homologous circular 3,197-nt ssDNA (10 μM) and/or 3,197-bp KpnI-cleaved pGEM3Zf(+) dsDNA (20 μM) were also added to the reaction.

b) Thin-layer chromatography (TLC)

The diadenylate cyclase (DAC) activity of DisA was studied by monitoring the formation of c-di-AMP in the presence of [α-^{32}P]-ATP, using thin-layer chromatography (TLC) with a modified protocol from (Witte et al, 2008). DAC reactions were performed at 37°C using a range of protein concentrations at variable times, in buffer A containing 1 or 10 mM $MgCl_2$, and with/out DNA, in a 20 μl reaction volume. The reaction started when 100 μM ATP was added, in a ratio of 1:2000 [α^{32}P]-ATP:ATP, and stopped by adding 25 mM EDTA. 5-10 μl of each reaction was spotted in a 20x20 cm TLC PEI cellulose F plates and run for about 2 hours in a TLC chamber containing running buffer [1:1 (v/v) 1.5 M KH_2PO_4 (pH 3.6) and 70% AS]. Dried TLC plates were analysed by phosphor imaging. Spots were quantified using Quantity One (Bio-rad).

1.6.6.5. Mass spectrometry for c-di-AMP detection *in vitro*

Reactions were performed in buffer A containing 1 mM $MgCl_2$ and 100 μM ATP at 37°C, in presence or absence of DisA. Samples were collected and analysed by negative mode MALDI-TOF on a Bruker Ultraflex III, using the 2', 4', 6'-trihydroxyacetophenome matrix (THAP) prepared with ammonium citrate. This analysis was performed in the Mass Spectrometry Lab (Science Faculty of the 'Universidad Autónoma de Madrid' - UAM).

1.6.7. Cytological studies

1.6.7.1. DisA and RadA/Sms localization and dynamics

Exponentially growing cells were obtained by inoculating overnight cultures in fresh $S7_{50}$ minimal media and grown to an OD_{560} = 0.4 at 30 ºC. Cells were loaded on agarose pads on object slides and analysed by fluorescence microscopy (Axio Observer A1, Plan Fluar objective, NA: 1.45, Zeiss) as previously described (Kidane et al, 2004). Mid-log phase cells were either untreated or exposed to 100 ng/ml MMC, 10 mM MMS or 350 μg/ml Nal for variable time at 30 ºC. For foci velocity quantification, 400 ms stream image acquisitions (frames are at 7 -30/s) were collected 60 min after MMC addition. These experiments were performed in the LOEWE-Zentrum für Synthetische Mikrobiologie (Marburg, Germany) in collaboration with Peter Graumann's laboratory.

Results

4. Results

1.7. Effect of *disA* mutation and variation of c-di-AMP levels

1.7.1. Survival of Δ*disA* after DNA damage induction

It has been demonstrated that DisA halts sporulation when DNA is damaged, acting in the DNA-damage checkpoint response at the onset of sporulation in *B. subtilis* (Bejerano-Sagie et al, 2006). However, the role of DisA during vegetative development, which is also present in non-sporulating bacteria, is still unknown. In order to answer this question, a *B. subtilis* BG214 strain disrupted in the *disA* gene (BG1221) was constructed (See Table 2). To investigate the contribution of DisA to the DNA damage response, viability assays using agents that cause DNA damage repaired via different mechanisms were performed. Cells were exposed chronically (overnight) or acutely (for 15 min) to different DNA damaging agents. A detailed description of how the viability assays were performed can be found in the 'Material and methods' section (page 28). The damaging agents selected generate different types of DNA damage that can be removed by specific repair mechanisms, each one for a given type or a group of lesions (reviewed in 'Introduction'). The drug concentration used in each experiment was the minimal dose that showed the clearest phenotype.

The absence of DisA did not impair cell growth (Figure 17 and Figure 11A, No drug). Chronic exposure to MMC, H_2O_2 and Nal, which cause a replication fork collapse, only marginally affected Δ*disA* survival, whereas MMS, which cause a replication fork stalling, clearly reduced cell viability (Figure 11A and Figure 11B). The *disA* mutation reduced about 100-fold the rate of survival to MMS (2 mM) when compared to the wild-type (wt) strain. In order to confirm this phenotype and quantitate the sensitivity to the DNA damaging agent, Δ*disA* cells were exposed to increasing concentrations of MMS for 15 min and the surviving fraction was quantified. Interestingly, the Δ*disA* strain was also sensitive to acute exposure to MMS, showing a lethal concentration to kill 99% (LC_{99}) of ~25.5 mM, compared to the wt strain that had a LC_{99} of ~41.3 mM MMS (Figure 11C). Taken together, these results suggest that DisA could play a role in vegetative cells in the response to alkyl DNA damage caused by MMS.

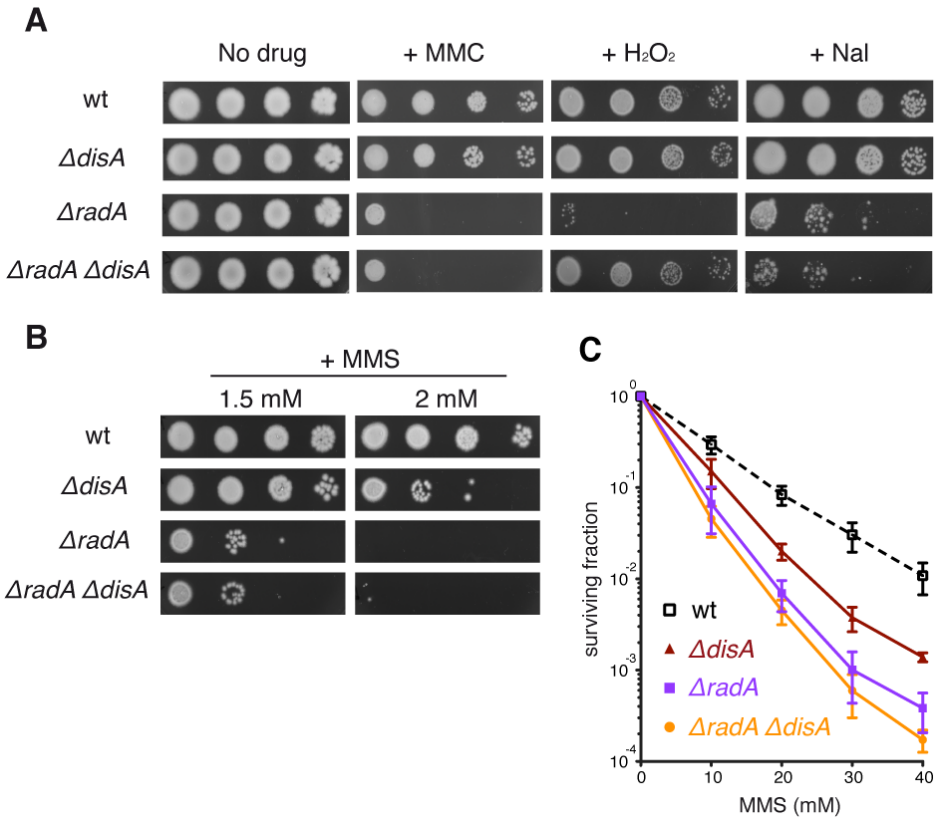

Figure 11. Viability assays of the Δ*disA*, Δ*radA* and Δ*radA* Δ*disA* mutants.
(A) Serial dilutions (10^{-3} to 10^{-6}) of each exponential growing culture were spotted in LB plates containing MMC (50 ng/ml), H_2O_2 (0.8 mM), NaI (0.95 µg/ml) or (B) MMS (1.5 or 2 mM). No drug, in the absence of drug. (C) Exponential growing cultures of the indicated strains were submitted to increasing concentrations of MMS (10, 20, 30 and 40 mM). After exacts 15 min, appropriated dilutions of each culture were platted in LB agar and the colony-forming units were counted the next day. The results are the average of at least four independent experiments and standard errors of the mean are indicated.

1.7.2. Mutation frequency in Δ*disA*

Cells also use strategies to deal with replication-blocking damages without removing the DNA lesions. This process is promoted by the DDT pathway, which overcomes unrepaired DNA lesions that interfere with the progression of replication forks, helps cells to ensure the completion of chromosome replication and the maintenance of genome stability. Translesion DNA synthesis (TLS) is a direct mechanism of bypassing unrepaired DNA lesions. Here, the stalled replicative DNA polymerase is replaced by a specialised non-processive low-fidelity DNA polymerase, which lacks proofreading exonuclease activity and possesses flexible active sites that can accommodate modified DNA bases to replicate over the DNA lesion. TLS polymerases insert either incorrect or correct bases opposite the DNA lesion, which is followed by an extension from the inserted base that can be carried out by either the same or another TLS

polymerase. Following extension, the TLS polymerase is replaced by the high-fidelity replicative polymerase to continue DNA replication (reviewed in Friedberg et al, 2005a).

To gain insights into the role of DisA in the DDR of exponentially growing cells, it was tested whether DisA contributes to lesion bypass by measuring the frequency of mutation to rifampicin in cells lacking DisA. The mutation frequency in wild-type cells was $7.9x10^{-9}$ (Figure 12), which is in strong agreement with published results (Walsh et al, 2014). In exponentially growing Δ*disA* cells, a modest 1.5-fold decrease in mutation frequency was observed, as measured by counting rifampicin-resistant colonies after MMS induction. This result indicates that during vegetative growth DisA could be occasionally favouring lesion bypass, stimulating replication fork progression and cell survival even in presence of damaged sites. Alternatively, DisA reduces error-free homologous recombination and indirectly favours the bypass of DNA lesions.

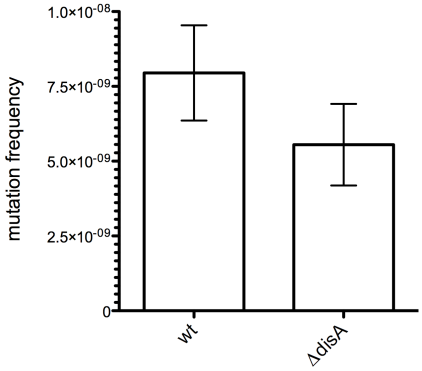

Figure 12. Mutation frequency of wt and Δ*disA* cells.
10 individual colonies of each strain were grown in LB medium. At late exponential phase (OD = 0.8), DNA damage was induced by addition of 6 mM MMS. The mutation frequency was obtained by dividing the number of rifampicin-resistant colonies by the total number of cells.

1.7.3. Contribution of the *radA-disA* operon to DNA repair

The *radA* gene is ubiquitous among Bacteria and it can be found in many different genomic contexts. Interestingly, when *disA* gene is present, *radA* is always located upstream it, forming an operon. For this reason, it was proposed that RadA/Sms could play a role with DisA, and this possibility is still being explored. In *M. smegmatis*, it was suggested that RadA/Sms regulates negatively DisA DAC activity and that this interaction could be conserved in other bacteria species (Zhang & He, 2013). It has also been proposed recombination and DNA repair functions for RadA/Sms in *E. coli* (Beam et al, 2002; Cooper et al, 2015; Lovett, 2006) *B. subtilis* (Carrasco et al, 2002), *Rhizobium etli* (Martinezsalazar et al, 2009) and *Streptococcus pneumoniae* (Burghout et al, 2007). Taking all this information into account, we asked what is exactly the contribution of RadA/Sms in DNA repair in *B. subtilis* and if it could modulate the activity of DisA. To start answering this question, a *radA* null mutant (Δ*radA*) was constructed.

Cells lacking *radA* had normal growth in the absence of induced DNA damage (Figure 11, No drug). However, Δ*radA* showed a strong reduction in viability when submitted to chronic exposure to all DNA damage agents tested (MMC, H_2O_2, Nal and MMS) (Figure 11A and B). These results confirm the involvement of RadA/Sms in recombinational repair of different types of DNA damage.

To evaluate the interaction between *radA* and *disA*, a strain lacking both genes was constructed (Δ*radA* Δ*disA*). Under conditions in which the survival of Δ*disA* was only slightly affected (+MMC, +H_2O_2, +Nal and 1.5 mM MMS), Δ*radA* was clearly sensitive (Figure 11B). The same phenotype was observed with the Δ*radA* Δ*disA* double mutant, except when cells were exposed to H_2O_2, where the absence of *disA* seemed to suppress the Δ*radA* defect (Figure 11A). This could be explained by the absence of a toxic intermediate produced by DisA, which is processed by RadA/Sms. Therefore, even in the absence of RadA/Sms, the cells would not have problems in repairing the damage produced by H_2O_2. Since DisA is only required to repair alkyl DNA damages, the defect of the double mutant in MMS acute assays was analysed. The single Δ*radA* mutation rendered cells very sensitive to MMS (LC_{99} of ~19.2 mM) and the double mutant showed a very similar defect (LC_{99} of ~17.2 mM) (Figure 11C). These results suggest that RadA/Sms could work together with DisA in the repair of alkyl DNA damage, although RadA/Sms might have additional functions in recombination-mediated DNA repair that remain to be elucidated.

1.7.4. Overexpression of RadA/Sms is not sufficient to overcome the Δ*disA* defect in DNA repair

To test whether the lack of DisA could be compensated by overexpressing RadA/Sms protein and that the Δ*disA* defect is not due to a destabilization of the entire operon *radA-disA* functions, a strain (BG1363) with an ectopic copy of *radA* cloned downstream an IPTG inducible promoter [$P_{spac(hy)}$] was constructed ($P_{spac(hy)}$-*radA*). The overproduction of RadA/Sms was confirmed because the Δ*radA* defect was supressed in the $P_{spac(hy)}$-*radA* Δ*radA* strain (Figure 13B). Overexpression of RadA/Sms did not impair cell growth, neither in presence or absence of MMS (Figure 13A, No drug and +MMS). Interestingly, increased levels of RadA/Sms were not enough to complement the lack of *disA* to repair lesions caused by alkyl groups (Figure 13A). This also suggests that the phenotype observed in Δ*disA* is not due to disruption of the upstream *radA* gene.

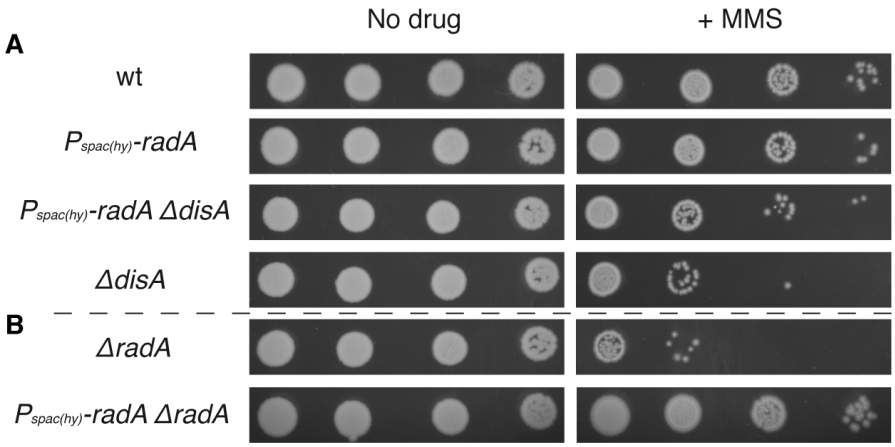

Figure 13. RadA/Sms do not complement Δ*disA* defect in DNA repair.
Exponentially growing wt, $P_{spac(hy)}$-*radA*, $P_{spac(hy)}$-*radA* Δ*disA*, Δ*disA*, Δ*radA* and $P_{spac(hy)}$-*radA* Δ*radA* cultures were tested for survival against chronic exposure to (A) 2.2 mM and (B) 1.6 mM MMS.

1.7.5. The absence of RadA/Sms does not affect RecA induction

DNA lesions activate a broad range of responses that have in common RecA accumulation (Au et al, 2005; Cardenas et al, 2014; Goranov et al, 2006; Simmons et al, 2009). To study whether the absence of *radA* (or *radA-disA*) has an effect in the RecA-dependent SOS response, cells were exposed to increasing concentrations of MMC for 30 min and the level of RecA was quantified. The basal level of RecA was similar in Δ*radA* and wt cells (estimated to be ~ 4,500 monomers/CFU) and had an increase of 4- to 6-fold in both strains after MMC induction (Figure 14). These results suggest that the lack of RadA/Sms (or both RadA/Sms and DisA) do not affect the DNA damage-dependent RecA induction.

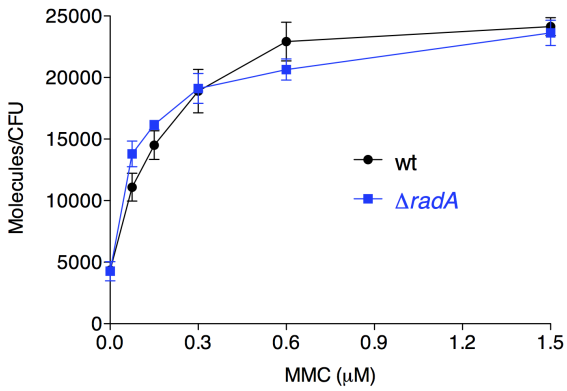

Figure 14. RecA accumulation upon SOS induction in wt and Δ*radA* cells.
The number of RecA molecules in exponential growing wt and Δ*radA* cells, in presence or absence of increasing MMC concentrations, were quantified from Western blots using α-recA antibodies and known amounts of purified RecA protein. The results are the average of at least four independent experiments and standard errors of the mean are indicated.

1.7.6. Involvement of DisA and RadA/Sms with HJ processing functions

Previously, it was shown that DisA binds branched DNA structures (e.g. HJs) *in vitro* and that HJ-bound DisA produces lower amounts of c-di-AMP compared to DNA-free DisA (Witte

et al, 2008). HJs are formed presynaptically after the regression of a stalled replication fork or post-synaptically as intermediates of DSB repair (Atkinson & McGlynn, 2009; Holliday, 1964). In *B. subtilis*, the formation and resolution of HJ intermediates involves a set of genuine recombination proteins: the RecG helicase stimulates replication fork regression and branch migration; RuvAB is the main HJ translocase and RecU specifically cleaves these branched intermediates (Ayora et al, 2004; Canas et al, 2014; Sanchez et al, 2007a). To test the hypothesis that DisA could be involved with functions related to HJ processing at the presynaptic stage, the efficiency of Δ*recU*, Δ*recG* or Δ*ruvAB* mutants to repair alkyl DNA damage in the Δ*disA* context was analysed. Strains BG1253 (Δ*recU* Δ*disA*), BG1257 (Δ*recG* Δ*disA*) and BG1255 (Δ*ruvAB* Δ*disA*) were constructed as described in 'Materials and methods' (page 27) and submitted to chronic and acute assays.

Untreated Δ*recU*, Δ*recG* and Δ*ruvAB* cultures were impaired in cell growth (Figure 15A-C, No drug), in agreement with previous publications that reported 21%, 26% and 28% of propidium-iodide-stained cells and defects in chromosome segregation with 4.4%, 7.4% and 5.1% of anucleate cells in each of these strains, respectively (Carrasco et al, 2004; Sanchez et al, 2005). Low doses of MMS (50 and 70 μM) were sufficient to produce a strong phenotype in Δ*recU*, Δ*recG* and Δ*ruvAB* when compared to the wt, Δ*disA* and Δ*radA* strains. In the chronic assays, the absence of *disA* did not change the phenotype of the single mutants (Figure 15A-C). However, in the acute assay (Figure 15D-F), which is more quantitative and takes into account the differences in the initial number of cells, the lack of *disA* exacerbated the defect of Δ*ruvAB* cells in repairing damages caused by MMS (Figure 15F). The double Δ*recG* Δ*disA* and Δ*recU* Δ*disA* mutants showed similar survival curves (Figure 15D and E). These results suggest that DisA could be involved in recombinational DNA repair functions, playing a role in the same pathway as RecU and RecG (epistasis), but in a different route than RuvAB (non-epistasis).

In the previous section, it was proposed that DisA and RadA/Sms could be partners in the repair of alkyl DNA damage (Figure 11). To test whether RadA/Sms could also be involved in the processing of HJ intermediates, the following double mutants were constructed: BG1395 (Δ*recU* Δ*radA*), BG745 (Δ*recG* Δ*radA*) and BG1355 (Δ*ruvAB* Δ*radA*). As shown in Figure 15, absence of *radA* produces a similar effect to the lack of *disA*: epistasis with RecU and RecG, but non-epistasis with RuvAB. Taken together, these results reveal new players during recombinational DNA repair, where DisA and RadA/Sms may participate at the same level as RecU and RecG.

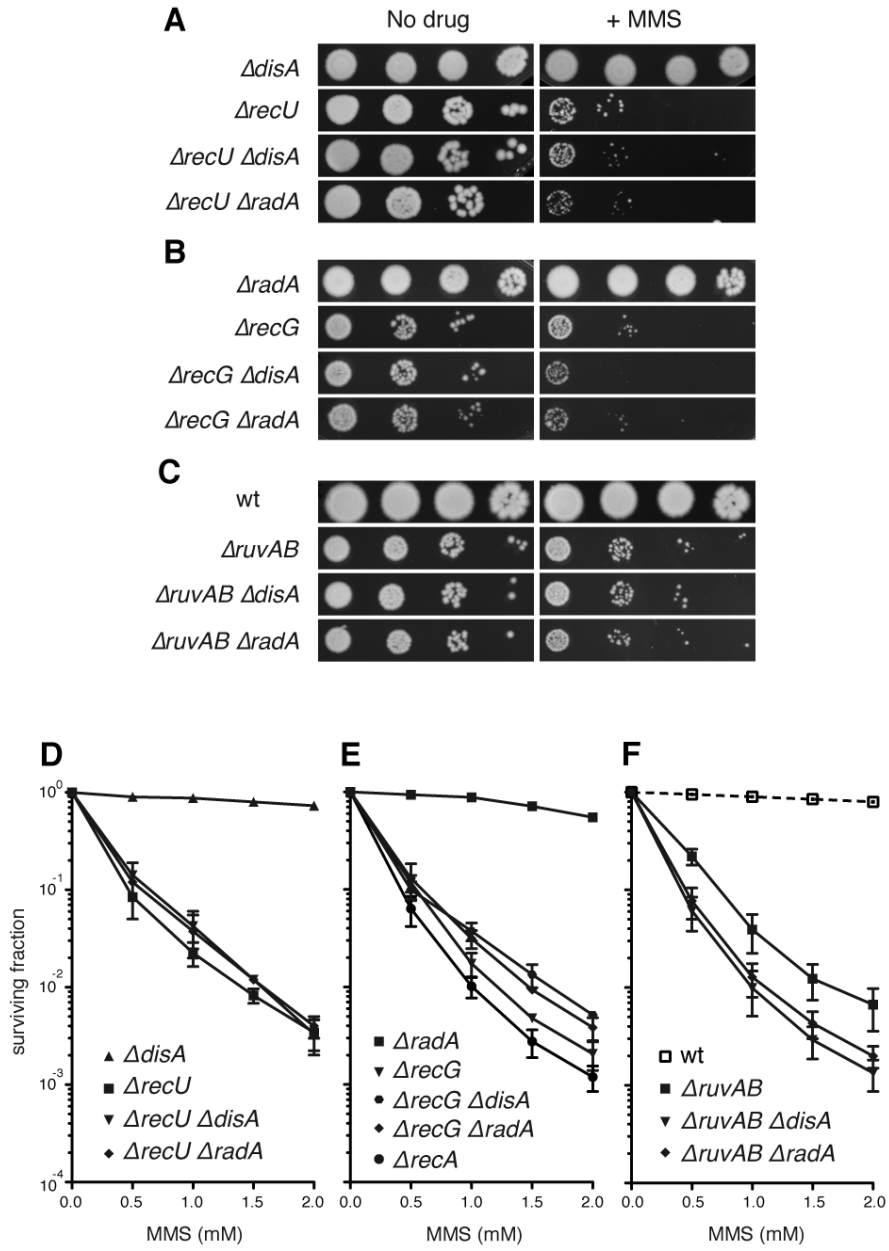

Figure 15. *disA* and *radA* are epistatic with *recU* and *recG*, but non-epistatic with *ruvAB*.
Survival of Δ*disA*, Δ*recU*, Δ*recU* Δ*disA*, Δ*recU* Δ*radA* (A and D), Δ*radA*, Δ*recG*, Δ*recG* Δ*disA*, Δ*recG* Δ*radA* (B and E), wt, Δ*ruvAB*, Δ*ruvAB* Δ*disA*, Δ*ruvAB* Δ*radA* (C and F) to chronic exposure to 50 µM MMS (A and B) or 70 µM MMS (C) and acute exposure to increasing concentrations of MMS (D-F). The results are the average of at least four independent experiments and standard errors of the mean are indicated.

1.7.7. Analysis of the c-di-AMP pool during vegetative growth

The presence of c-di-AMP is essential for life in Firmicutes. The intracellular concentration of c-di-AMP has been quantified before in vegetative *B. subtilis* PY79 (~1.7 µM) (Oppenheimer-Shaanan et al, 2011) and in *Staphylococcus aureus* (2 to 3 µM) (Corrigan et al, 2011). However, the contribution of DisA DAC and GdpP PDE to the c-di-AMP pool in exponentially growing *B. subtilis* has never been addressed before. As shown in (Figure 16), the

levels of c-di-AMP in wt BG214 cells was ~3.8 μM and decreased to ~2.8 μM in the absence of *disA*. In cells lacking the PDE (Δ*gdpP*), the concentration of c-di-AMP increased to ~4.3 μM and when *gdpP* was overexpressed by an IPTG induction, the levels of c-di-AMP reached ~2.7 μM, which is similar to the obtained for Δ*disA*. These results demonstrate that DisA is not the only protein that contributes for the c-di-AMP pool during vegetative growth in *B. subtilis* and that there seems to be a minimal level of c-di-AMP necessary for cell viability (~2.7 μM). Moreover, it can be concluded that during vegetative growth the c-di-AMP pool varies in a very narrow range, from ~2.7 μM to ~4.3 μM. This suggests a tight regulation, being small changes sufficient to produce a noticeable effect.

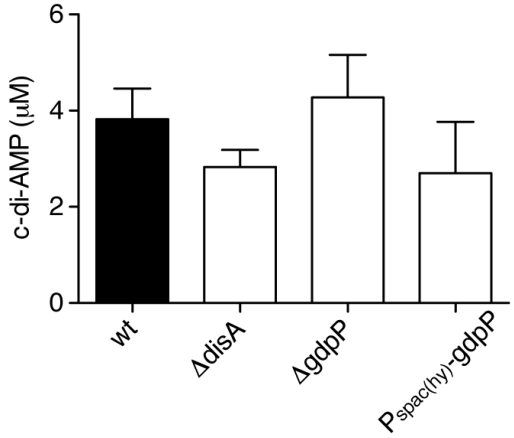

Figure 16. Quantification of the intracellular levels of c-di-AMP in wt, Δ*disA*, Δ*gdpP* and *P*$_{spac(hy)}$-*gdpP* (+IPTG) strains in mid-log phase. Cells were lysed and nucleotide extractions analysed by LC-MS/MS (detailed in 'Materials and methods', page 30). The concentration of c-di-AMP of each strain was determined based on a standard curve performed using purified c-di-AMP. Each value is the mean of three independent experiment and the bars denote the standard deviation.

1.7.8. Contribution of DAC and PDE activities to DNA repair

In the previous sections, it has been revealed that DisA is needed during exponential growth for the repair of damage caused by alkylating agents (Figure 11). To further characterize the role of DisA, it is essential to consider that the absence of DisA not only implies the lack of the protein but also a reduction in the intracellular levels of c-di-AMP (Figure 16) (Oppenheimer-Shaanan et al, 2011). Most Firmicutes have a single DAC enzyme, and since c-di-AMP is an essential molecule, DAC mutants should be incompatible with life in these bacteria (Woodward et al, 2010). However, in *B. subtilis* three DAC enzymes are expressed: DisA and CdaA during vegetative phase and sporulation, and CdaS only in the forespore (Mehne et al, 2013; Nicolas et al, 2012). Another protein that is important in this process is GdpP, which converts c-di-AMP into pApA and finally in AMP, being the only phosphodiesterase (PDE) described to date in *B. subtilis* (Rao et al, 2009). Due to the impossibility of constructing a triple DAC mutant (Luo & Helmann, 2012a), single DAC and PDE mutants were constructed to test whether reduced (Δ*disA*, Δ*cdaA*, P$_{spac(hy)}$-GdpP) or increased (Δ*gdpP*) levels of c-di-AMP play a role in the

response to alkylating damage during vegetative growth. Since CdaS is only expressed during sporulation, Δ*cdaS* was used as a negative control.

Untreated Δ*disA*, Δ*cdaA*, Δ*cdaS* and Δ*gdpP* mutants, or over-expression of GdpP ($P_{spac(hy)}$-*gdpP*), rendered similar number of cells compared to the wt strain, suggesting that these mutations or over-expression did not impair cell growth (Figure 18A, No drug). Each strain was also grown for 5 hours in LB and showed similar growth curves compared to the wt, except for Δ*cdaA* that had a slightly slower growth (Figure 17). These results indicate that single disruption of DAC or PDE genes (or variations in the levels of c-di-AMP) do not impair cell proliferation.

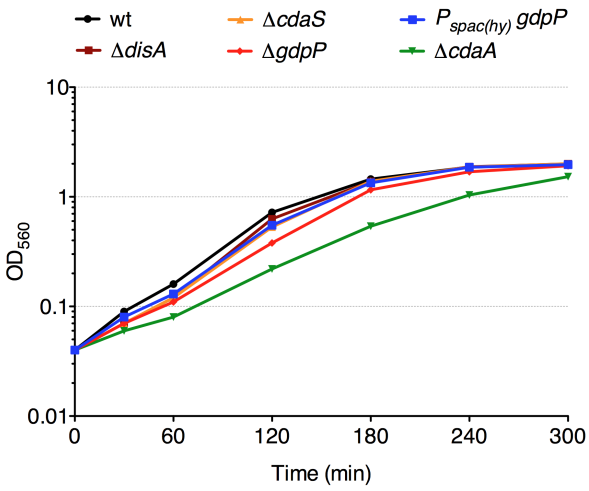

Figure 17. Growth curves of DAC and PDE mutant strains.
Cells were grown in LB at 37°C with 250 rpm agitation. Samples were collected at each indicated time point and the absorbance at 560 nm was measured using a spectrophotometer.

As expected, Δ*cdaS* viability was not affected by MMS treatment, since CdaS is not expressed during vegetative growth. As revealed before (Figure 11), Δ*disA* was sensitive to MMS but not to H_2O_2 exposure (Figure 18A). Surprisingly, a different outcome was observed in Δ*cdaA*. Cells lacking CdaA were extremely affected by chronic treatment with H_2O_2, but only a modest difference was observed in Δ*cdaA* survival to MMS compared to the wt (Figure 18A). To determine the highest concentration of H_2O_2 sufficient to provide a clear repair deficiency in Δ*cdaA*, lower concentrations of H_2O_2 were used (Figure 19). Upon chronic exposure to 0.5 mM H_2O_2, Δ*cdaA* cells were already affected, implying a strong sensitivity to this agent. H_2O_2 promotes different types of DNA lesions, which are mainly repaired via BER and other specific repair pathways, although at high concentrations produces DSBs repaired via HR (Barzilai & Yamamoto, 2004). In order to test whether CdaA is involved in the repair of DSBs, another agent, MMC that generates one-ended DSBs was used. Upon chronic exposure to MMC, Δ*cdaA* cells were as resistant as the wt strain (Figure 19). Interestingly, overexpression of GdpP by IPTG addition rendered cells as sensitive to MMS as Δ*disA*, and a

moderate sensitivity to H_2O_2 was observed (Figure 18A). Whereas, deletion of *gdpP* made cells more resistant to both agents tested. These results were confirmed in the acute assay (Figure 18B), where Δ*disA* and overexpression of GdpP ($P_{spac(hy)}$-*gdpP*) had similar survival curves, decreased when compared to wt, Δ*cdaA* and Δ*cdaS* strains, while Δ*gdpP* showed more resistance to increasing concentrations of MMS.

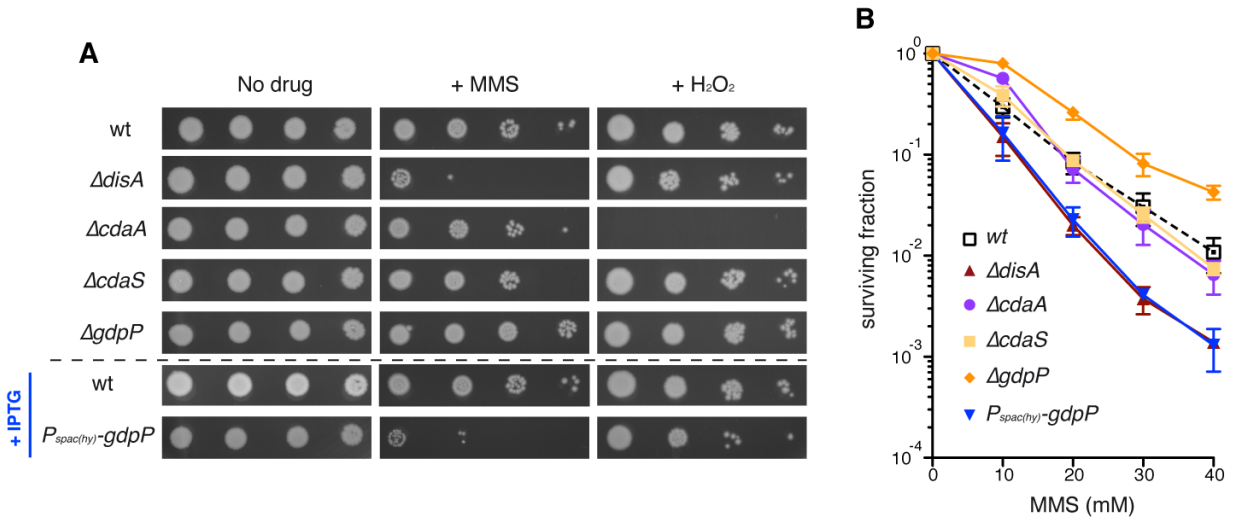

Figure 18. Reduced c-di-AMP levels, DisA and CdaA are involved in the DNA damage response during vegetative growth.
(A) Chronic assays were performed to compare the survival of wt, Δ*disA*, Δ*cdaA*, Δ*cdaS*, Δ*gdpP* and *Pspac(hy)-gdpP* to 2.4 mM MMS and 1.3 mM H_2O_2 exposure. + IPTG, when the plates were supplemented with 0.5 mM IPTG. (B) wt, Δ*disA*, Δ*cdaA*, Δ*cdaS*, Δ*gdpP* and *Pspac(hy)-gdpP* cultures were tested for survival to MMS acute exposure. The results are the average of at least four independent experiments and standard errors of the mean are indicated.

Taken together, these results reveal the importance of c-di-AMP to trigger the DNA damage response to alkyl groups (e.g. MMS) and oxidative stress (e.g. H_2O_2), via DisA or CdaA, respectively. Lowering drastically the levels of c-di-AMP seems to decrease cell survival, whereas increasing it enhances resistance do DNA damage.

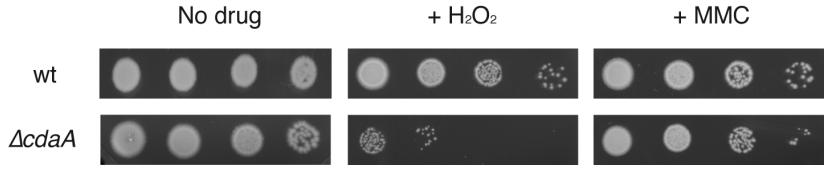

Figure 19. CdaA plays a role in the response to oxidative stress.
Survival of wt and Δ*cdaA* strains to chronic exposure to 0.5 mM H_2O_2 and 50 ng/ml MMC. No drug, in the absence of a DNA damaging agent. Serial dilutions (10^{-3} to 10^{-6}) of each exponential growing culture were spotted in LB agar plates supplemented with the indicated concentration of drug.

1.7.9. C-di-AMP is involved in DNA repair during vegetative growth

The importance of c-di-AMP in reporting DNA integrity in *B. subtilis* undergoing sporulation has been proposed in previous reports (Bejerano-Sagie et al, 2006; Oppenheimer-Shaanan et al, 2011). However, the role of c-di-AMP in DNA repair during vegetative growth is still unknown. In the previous section, it was shown how the absence of the vegetative DAC enzymes (DisA and CdaA) and the drastic reduction in the levels of c-di-AMP (by overexpressing GdpP) impaired viability in the presence of DNA damaging agents. To confirm the role played by c-di-AMP produced by DisA, chronic assays were performed with a strain expressing a DisA variant (*disA77*) where only one amino acid of the DAC active site was mutated (D77N). Interestingly, *disA77* sensitivity to MMS was comparable to the phenotype observed when *disA* is not expressed (Figure 20A). This result suggests an essential role for the c-di-AMP produced by DisA in the response to alkyl DNA damages, although DisA77-GFP did not form foci properly (Oppenheimer-Shaanan et al, 2011).

The addition of external c-di-AMP in sporulating *B. subtilis* cells led to a bypass of the DNA damage checkpoint response (Oppenheimer-Shaanan et al, 2011). To test whether externally added c-di-AMP could suppress the DNA repair defect of Δ*disA* cells, exponential growing culture of this mutant was supplemented with 1.4 μM c-di-AMP (Biolog) and survival to increasing concentrations of MMS was measured. The wt strain was used as a control to rule out any adverse effect produced by c-di-AMP addition. Surprisingly, Δ*disA* cells supplemented with c-di-AMP were as resistant to MMS treatment as the wt cells (Figure 20B). The addition of c-di-AMP in wt cultures did not produce any effect. This suggests that the externally added c-di-AMP *per se* can overcome the DNA repair defect produced by the absence of DisA.

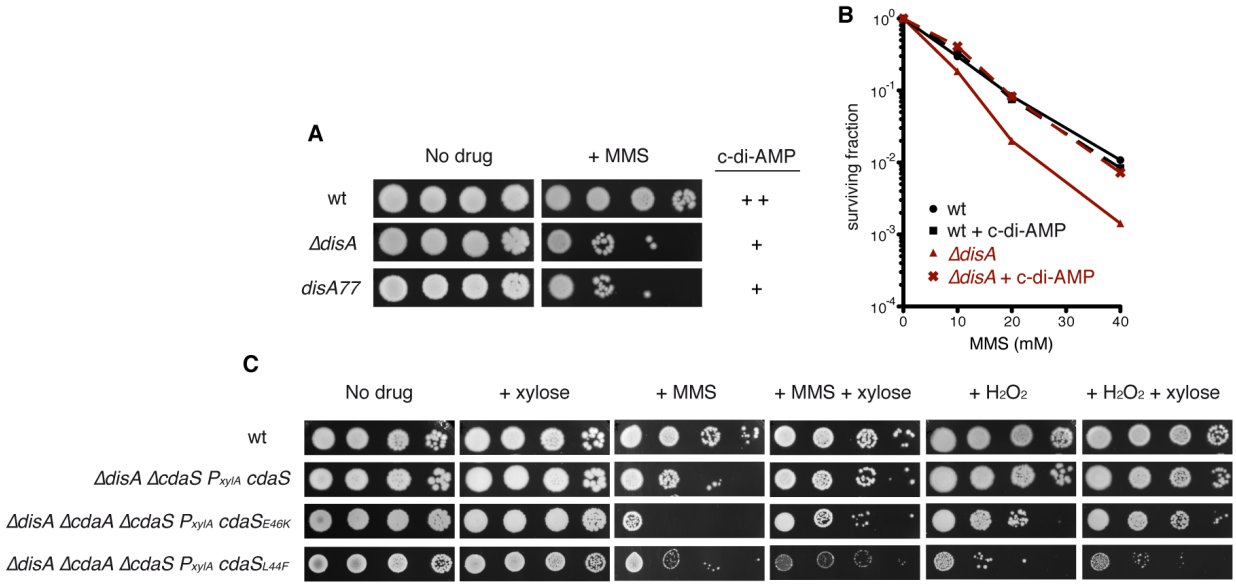

Figure 20. C-di-AMP plays a role in DNA repair during vegetative growth.
(A) Wt, Δ*disA* and *disA77* strains were grown to middle exponential phase when serial dilutions were taken and spotted in LB agar plates in the absence (No drug) or presence of 2 mM MMS (+MMS). The c-di-AMP column represents the relative amount of c-di-AMP produced by each strain. (B) Surviving fractions of wt and Δ*disA* cells supplemented with 1.4 µM c-di-AMP (Biolog) to acute exposure to increasing concentrations of MMS. (C) Chronic assays with different DAC mutants expressing an ectopic allele of *cdaS* and its variants (E46K and L44F) from a xylose inducible promoter (P_{xylA}). Serial dilutions of each vegetative culture were spotted in LB agar plates containing, when indicated, 0.5% xylose (+xylose), 2.2 mM MMS (+MMS) or 0.9 mM H_2O_2 (+H_2O_2). No drug, in the absence of any supplement.

It is known that c-di-AMP is essential for viability and that absence of DisA and CdaA is lethal for *B. subtilis* (Luo & Helmann, 2012a). Moreover, expression of CdaS during vegetative growth from a xylose inducible promoter (P_{xylA}) was shown to be sufficient to rescue the viability of Δ*disA* Δ*cdaA* (P_{xylA}-*cdaS*) or Δ*disA* Δ*cdaA* Δ*cdaS* (P_{xylA}-*cdaS*) triple mutant strain (Mehne et al, 2013). However, in the absence of the xylose inducer, suppressor mutants that express hyperactive forms of CdaS ($CdaS_{E46K}$ and $CdaS_{L44F}$) were observed (Mehne et al, 2014). To test whether the c-di-AMP produced by CdaS overexpressed ectopically and its hyperactive variants supported DNA repair in the absence of DisA and CdaA, chronic assays were performed with double Δ*disA* Δ*cdaS* (P_{xylA}-*cdaS*) or triple Δ*disA* Δ*cdaA* Δ*cdaS* (P_{xylA}-$cdaS_{E46K}$) and Δ*disA* Δ*cdaA* Δ*cdaS* (P_{xylA}-$cdaS_{L44F}$) strains.

Untreated cultures did not show impaired cell growth in LB plates with or without 0.5% xylose (Figure 20C, No drug and +xylose). As expected (Figure 18), all strains were sensitive to MMS, and Δ*disA* Δ*cdaA* Δ*cdaS* (P_{xylA}-$cdaS_{E46K}$) and Δ*disA* Δ*cdaA* Δ*cdaS* (P_{xylA}-$cdaS_{L44F}$) to H_2O_2, due to the lack of DisA and CdaA, respectively. However, in the presence of xylose, all strains rescued completely or at least partially the defect observed in the absence of the inducer,

when compared to the wt, except for Δ*disA* Δ*cdaA* Δ*cdaS* (P_{xylA}-$cdaS_{L44F}$), which remained sensitive to H_2O_2 after xylose induction (Figure 20C). All together, this results support the idea that c-di-AMP is involved in the DNA damage response during log-phase, through a mechanism that needs to be further investigated.

1.8. Cytological study of DisA and RadA/Sms

1.8.1. Localization and dynamics of DisA-YFP

DisA-GFP protein fusion formed a discrete and highly dynamic focus that moved along the chromosome at the onset of sporulation (Bejerano-Sagie et al, 2006). In order to study the behaviour of DisA during exponential growth, a strain expressing a fused DisA-YFP (Venus) protein from its native locus and promoter was constructed (BG1327). Venus is an improved version of the yellow fluorescent protein (YFP), with better efficiency of maturation and an increased resistance to environment stresses (Nagai et al, 2002). This strain did not show sensitivity to MMS, suggesting that the *disA-yfp* gene encoded a wt-like protein. Cells were grown in $S7_{50}$ minimal medium to slow down the cellular events and reduce the background levels produced by LB medium. Once the culture reached mid-log phase (OD_{560}=0.4), the cells were mounted on agarose pads containing $S7_{50}$ growth medium on object slides and visualized on a Zeiss fluorescence microscope (Axio Observer A1, Plan Fluar objective, NA: 1.45). When indicated, DAPI (1 μg/ml) was added for nucleoid staining. Time-lapse images were taken in order to characterize the movement of DisA and determine its foci velocities.

In exponential growing *B. subtilis* cells, DisA-YFP formed multiple bright foci, which were highly dynamic throughout the cell (Figure 22A). The foci movement did not show any specific pattern, being rather random. The overlay images of DisA-YFP and DAPI suggested that DisA foci colocalize with the chromosome (Figure 21A). These results indicate that during exponential growth DisA protein displays a different behaviour, being more widely distributed than during sporulation, where only one focus per cell was observed (Bejerano-Sagie et al, 2006). Alternatively, the use of a more modern microscope and therefore images with higher resolution allowed the distinction of multiple foci, when before it was seen as a single large focus.

DisA foci were visible even in the absence of DNA damage induction (Figure 22A). In order to study DisA foci dynamics in the presence of different types of DNA lesions, cells were treated with MMS (10 mM), MMC (100 ng/ml) or Nal (350 μg/ml) for 60 min, which is the

time point when HJs are formed during DSB repair (Sanchez et al, 2005). Surprisingly, no apparent differences in DisA-YFP behaviour, in the presence or absence of the mentioned drugs, were observed (data not shown). To quantify the speed of DisA-YFP foci movement in growing cells treated or not with MMC, individual foci were tracked and their speed measured using the ImageJ software. For an average of 50 tracks from at least 2 individual experiments, an average speed of 0.58 μm/s was determined (Figure 23A). Unexpectedly, the average speed of DisA-YFP was about 20% faster after MMC addition compared to its absence. However, the standard deviations in this analysis were very large due to the highly static/dynamic shift characteristic of DisA-YFP's movement, and therefore this increase was not considered significant.

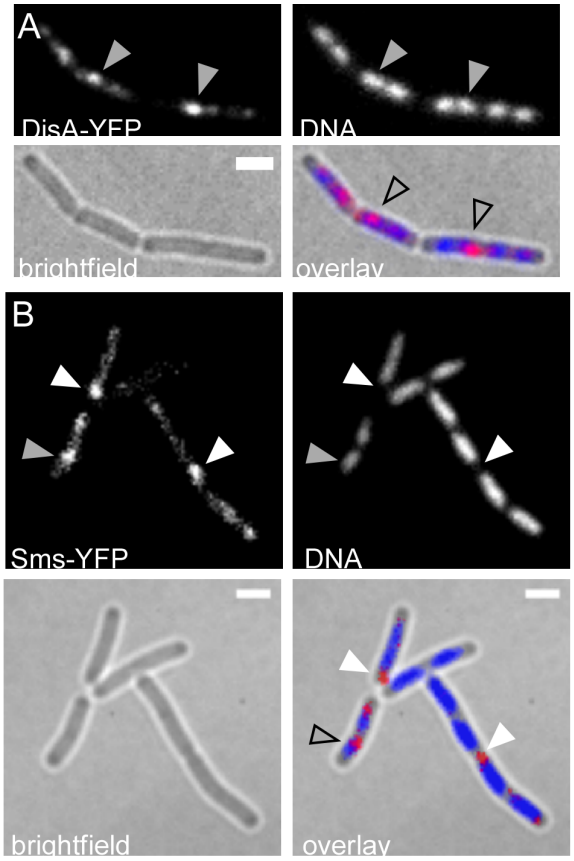

Figure 21. DisA-YFP foci colocalize with the chromosome in vegetative *B. subtilis*.
Cells expressing (A) DisA-YFP or (B) RadA/Sms-YFP were grown to mid-logarithm phase (OD_{560}=0.4), mounted on agarose pads and analysed by florescence microscopy. Left panels, YFP fluorescence images and brightfield; right panels, DAPI and YFP/DAPI overlays. Grey arrows indicate foci that overlap with the nucleoid. White arrows indicate foci that do not colocalize with the nucleoid. Scale bar corresponds to 2 μM.

To corroborate these results, *disA-yfp* gene was moved to a strain lacking RecU (BG1405, *disA-yfp* Δ*recU*), the *B. subtilis* HJ resolving enzyme and analysed by fluorescence microscopy. The absence of RecU leads to chromosomal segregation defects (4% of anucleate cells) and to an accumulation of unresolved HJs (Carrasco et al, 2004; Pedersen & Setlow, 2000; Sanchez et al, 2007a). Moreover, *recU* was epistatic with *disA* and *radA* (Figure 15), suggesting that these genes could encode for proteins related to the same DNA repair pathway. In the strain *disA-yfp* Δ*recU,* static patched structures were visible (Figure 22B), which were absent in the *disA-yfp*

background. Altogether, these results support the idea that: i) DisA protein forms highly dynamic foci that travel along the chromosome during vegetative growth; ii) DisA protein is able to recognize branched DNA intermediates *in vivo* (e.g. HJs), which are accumulated in the absence of RecU; and iii) in the presence of HJs, DisA losses its dynamicity. This phenomenon was not observed in the presence of DNA damaging agents, perhaps because DisA forms a very dynamic molecule and the method used was not sensitive enough to detect static DisA proteins. However, by inducing an accumulation of HJs, these events were more easily visualized.

1.8.2. Localization and dynamics of RadA/Sms-YFP

In the previous section, it was suggested that RadA/Sms and DisA could work in the same DNA repair pathway. Additionally, it has been proposed that *M. smegmatis* RadA/Sms and DisA physically interact and possibly functionally as a conserved mechanism in several bacteria (Zhang & He, 2013). If these data are correct, the two proteins should have the same or at least a similar localization pattern. To test this hypothesis, the *radA* native gene in BG214 was replaced by the *radA-yfp* fusion (BG1333). In this construction it cannot be ruled out whether *radA-yfp* fusion is affected or that the downstream *disA* gene is not affected, because this strain was slightly more sensitive to MMS than the wt in viability chronic assays (data not shown).

RadA/Sms-YFP protein was much less bright than DisA-YFP, but the formation of many discrete foci could still be observed in the absence of DNA damage induction (Figure 21B). Interestingly, RadA/Sms-YFP foci appeared in the cytosol in areas with or without DNA, unlike DisA that preferentially colocalized with the chromosome (Figure 21A and B). RadA/Sms-YFP foci moved without a discernible specific pattern throughout the cell but with a visually similar behaviour to DisA-YFP. Exponential growing *radA-yfp* cells were then submitted to MMS (10 mM) treatment for 60 min. As observed for DisA-YFP, the RadA/Sms-YFP foci remained dynamic even after DNA damage induction.

The approach employed to visualize static DisA-YFP foci was also tested in RadA/Sms-YFP. For this purpose, the *radA-yfp* fusion was moved to the Δ*recU* background and analysed by fluorescence microscopy. Interestingly, static RadA/Sms-YFP foci were observed, although they were much more sporadic than in Δ*recU* DisA-YFP (Figure 22). Altogether, these results suggest that RadA/Sms and DisA move dynamically and in a similar fashion throughout the cell, with an interaction of the two proteins *in vivo* being possible.

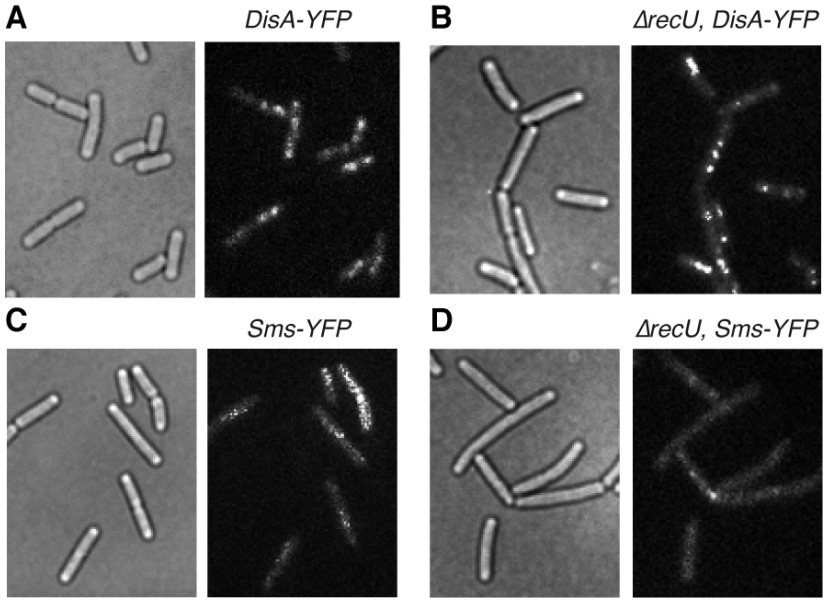

Figure 22. Localization of DisA-YFP and RadA/Sms-YFP in exponential growing *B. subtilis*.
(A) DisA-YFP, (B) DisA-YFP in the Δ*recU* background, (C) RadA/Sms-YFP and (D) RadA/Sms-YFP in the Δ*recU* background. Left panels are brighfield images.

1.8.3. The absence of RecN does not impair DisA-YFP expression and movement

The DNA damage response to DSBs involves the recruitment of complex molecular machinery mediating DNA repair (Alonso et al, 2013). Among the first responders is RecN, which in concert with PNPase activates the DSB repair (Cardenas et al, 2011; Cardenas et al, 2014; Kidane et al, 2004). RecN foci are visible 20 min after MMC induction, RecO, RecR and RecA after 30 min, RecF and RecX after 60-90 min and RecU after 60-120 min (Cardenas et al, 2012; Kidane et al, 2004; Manfredi, 2009; Sanchez et al, 2005).

To test whether the absence of RecN affects the expression and dynamic behaviour of DisA, *disA*-y*fp* was moved into the Δ*recN* background (BG1407, *disA-yfp* Δ*recN*). In the absence of RecN, *disA-yfp* still encoded bright and dynamic foci with a localization pattern very similar to what was seen in the wt strain (Figure 23B). The average velocity of DisA-YFP foci was slightly faster in the Δ*recN* background (0.68 μm/s), but within the same range of what was observed in the wt strain (0.58 ± 0.4 μm/s), suggesting that this difference is not significant (Figure 23A). These results indicate that DisA is not related to, nor affected by, an impairment of the initial steps of DSB repair, which are promoted by RecN. The same outcome was observed in cells expressing RecU-YFP, whose foci formation after MMC induction was not affected by the absence of RecN (Sanchez et al, 2005). Altogether, these results strongly support the idea that DisA and RadA/Sms could be involved in the recognition of recombination intermediates that are further processed by RecU, RecG and RuvAB.

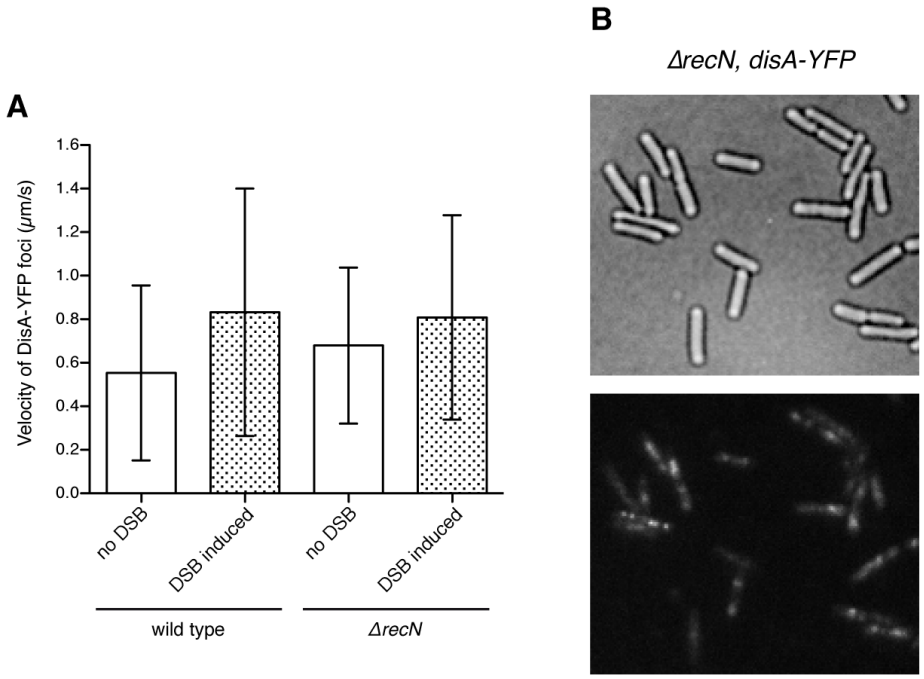

Figure 23. DisA-YFP foci velocity in the presence or absence of DSBs in the wt or Δ*recN* background.
(A) DSBs were induced in vegetative wt or Δ*recN* cells expressing DisA-YFP by addition of 100 ng/ml MMC for 60 min. Cells were analysed by fluorescence microscopy (B) and foci velocities obtained from time lapse images using ImageJ software.

1.9. Biochemical study of the DisA protein

1.9.1. Purification of *B. subtilis* DisA

To further study the role of DisA in DNA repair, an *in vitro* characterization of the protein was carried out, focusing on the DAC and DNA binding activities. For this purpose, the C-terminal His-tagged DisA recombinant protein from *B. subtilis* was expressed and purified. The protein overexpression was conducted in *E. coli* BL21 (DE3) pLysS and induced with 0.5 mM IPTG for 3 hours at 37°C. A high concentrated fraction of DisA protein (10 mg/ml) was purified from the cell extracts using a Ni-NTA resin (for more details see 'Materials and methods' page 31). The apparent molecular mass of DisA protein was about 43 kDa on a SDS-PAGE (Figure 24), which is consistent with the calculated molecular mass (41.6 kDa). The gel purified 43 kDa and the slight 44 kDa bands were sent for protein identification by peptide mass fingerprinting analysis (MALDI-TOF/TOF mass spectrometry), carried out in the Proteomics Facility of the CNB. The analysis confirmed that both proteins were DisA from *B. subtilis*.

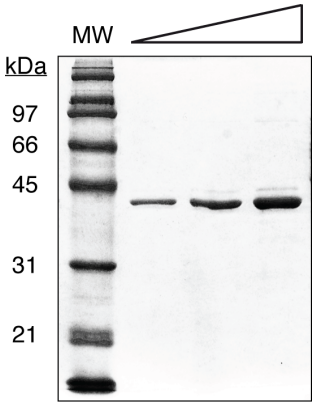

Figure 24. Purified *B. subtilis* DisA.
12.5% SDS-PAGE with increasing concentrations of purified DisA. Lane MW, protein ladder of the indicated molecular weights.

1.9.2. Purified DisA is functional and synthesizes c-di-AMP

It is known that DisA protein possesses DAC, which catalyses the hydrolysis of two ATP molecules into a cyclic diadenosine monophosphate (c-di-AMP) (Witte et al, 2008). To test whether the DisA purified was a functional protein, its DAC activity was analysed by thin-layer chromatography (TLC). In a reaction with ATP (including radiolabeled [α^{32}P]-ATP) and increasing concentrations of DisA, the progressive hydrolysis of ATP concomitant with the formation of two products with lower mobility was observed (Figure 25).

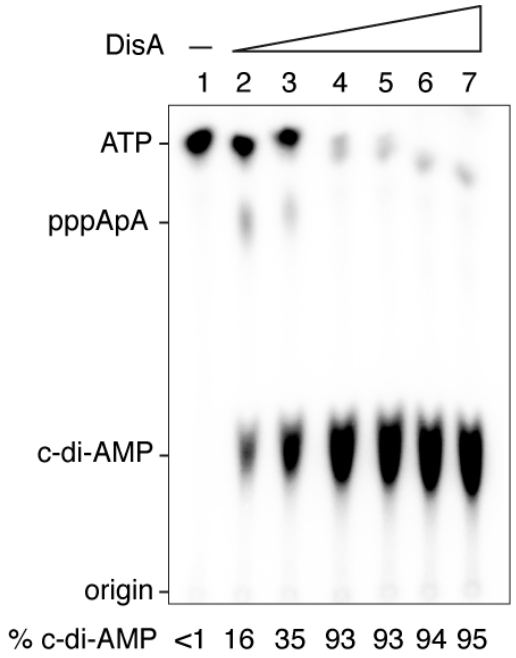

Figure 25. DisA converts ATP into c-di-AMP.
All reactions were performed at 37°C in buffer A containing 1 mM $MgCl_2$ and 100 µM ATP (and 0.05 µM [α-^{32}P]-ATP). From *lanes 2-7*, increasing concentrations of DisA (110, 220, 440, 870, 1750 and 3500 nM) was added and incubated for 30 min to the reaction mixture. In *lane 1*, reaction mixture without protein. The TLC was developed using Phosphorimager. The amount of c-di-AMP produced in each reaction is indicated as percentages (% c-di-AMP) relative to the total amount of ATP.

To verify the identity of the product that was accumulated in a protein concentration-dependent manner in the reaction of purified DisA and ATP, the same reaction was performed

and a sample taken for MALDI-TOF analysis. The reaction with ATP only was used as a control, and formed ions at *m/z* = 506 and 528, that corresponds to [ATP-H^+] and [ATP-$2H^+$+Na^+], respectively (Figure 26A). Whereas, when DisA was included in the reaction, the appearance of new peaks was significant at *m/z* = 657 and 679, and the peak corresponding to ATP were much smaller (Figure 26B). The new peaks corresponded precisely to the expected mass of c-di-AMP, in the forms of [c-di-AMP-H^+] and [c-di-AMP-$2H^+$+Na^+], respectively. Therefore, this analysis confirmed that c-di-AMP was the main product formed in the reaction of DisA and ATP.

The presence of a molecule that migrates faster than c-di-AMP, but slowly than ATP was also detected (Figure 25). Surprisingly, this molecule was identified by mass spectrometry as being an ATP-AMP dimer (pppApA), corresponding to the ions formed in the range of *m/z* = 835 to 915 (Figure 26B).

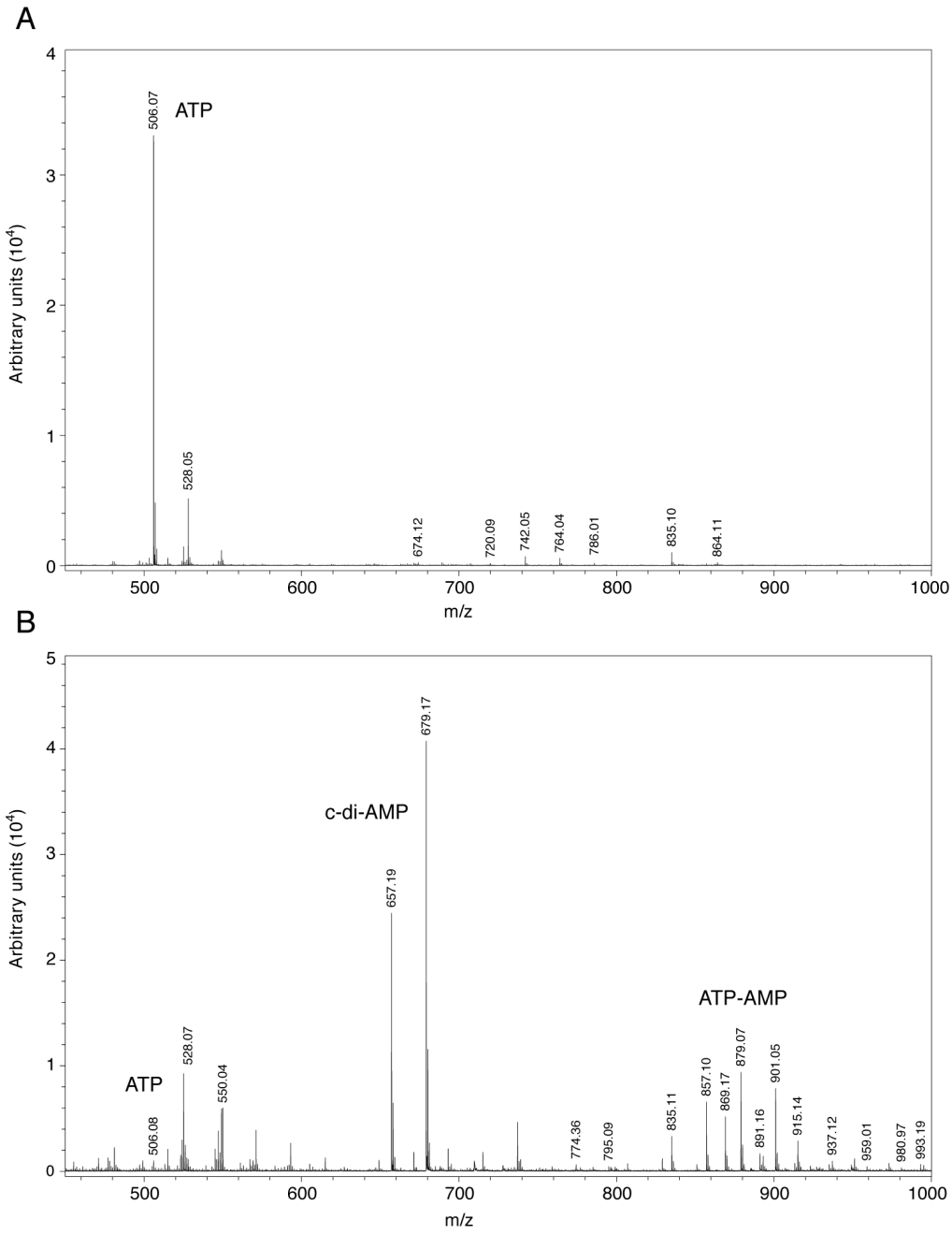

Figure 26. MALDI-TOF analysis of the DAC reaction products.
Reactions were performed in buffer A containing 1 mM $MgCl_2$ and 100 μM ATP at 37°C for 30 time, in the absence (A) or presence of 100 nM DisA (B). Samples were analysed by negative mode MALDI-TOF on a Bruker Ultraflex III. Peaks corresponding to [ATP-H^+] (*m/z*=506), [ATP-$2H^+$+Na^+] (*m/z*=528), [c-di-AMP-H^+] (*m/z*=657), [c-di-AMP-$2H^+$+Na^+] (*m/z*=679) and ATP-AMP variants (*m/z*=835, 857, 869, 879, 901 and 915) are indicated in the figure.

1.9.3. dATP is not substrate for DisA

Previously, it has been demonstrated that DisA specifically hydrolyses ATP, rather than other nucleotides triphosphates, like GTP, CTP, UTP or ITP (Witte et al, 2008). However, the activity of DisA towards dATP has never been addressed before. dATP is an essential molecule

for DNA synthesis and in *B. subtilis* is the preferred nucleotide for RecA DNA strand exchange reaction in the absence of accessory factors (Carrasco et al, 2008). Surprisingly, no DAC activity was detected in a reaction at 37°C with 500 nM DisA for up to 30 min (Figure 27B). The same reaction using ATP rather than dATP converted nearly 100% of the ATP into c-di-AMP in less than 30 min, 76% of it already being hydrolysed in the first 5 min (Figure 27A). These results indicate that ATP, but not dATP, is the preferred substrate for DisA to produce c-di-AMP.

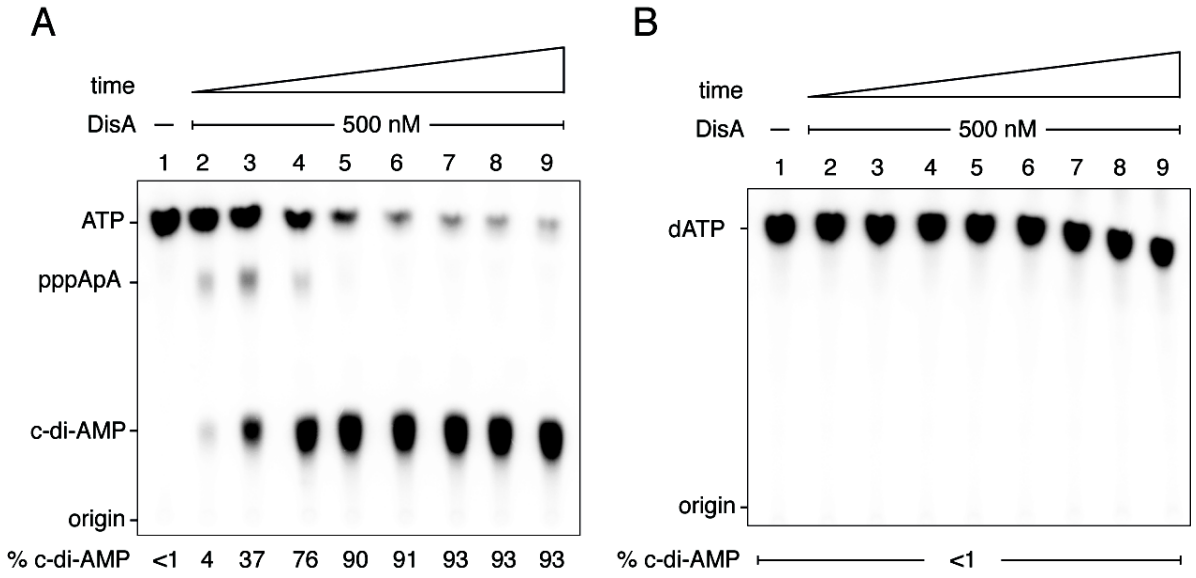

Figure 27. ATP (but not dATP) is the substrate for DisA DAC activity.
Purified DisA (500 nM) was incubated at 37°C for a variable period of time (*lanes 2-9*: 0.5, 1, 5, 10, 15, 20, 25 and 30 min) with 100 µM ATP (0.05 µM [α-^{32}P]-ATP) (A) or 100 µM dATP (0.05 µM [α-^{32}P]-dATP) (B). In *lane 1*, reaction mixture without protein.

1.9.4. pppApA is an intermediate of DisA DAC reaction

In a reaction performed with dATP and higher amounts of DisA (1.75 µM), 9% of pppApA was formed in the first 10 min of the reaction. Only when the reaction reached 120 min did the levels of pppApA start to decrease while the amount of c-di-dAMP increased to 9% of the total amount of dATP. As a control, the same reaction was performed in presence of ATP rather than dATP, and, as expected, c-di-AMP was rapidly formed in less than 10 min (Figure 28). Altogether, these results suggest that pppApA is an intermediate product of the DAC reaction performed by DisA.

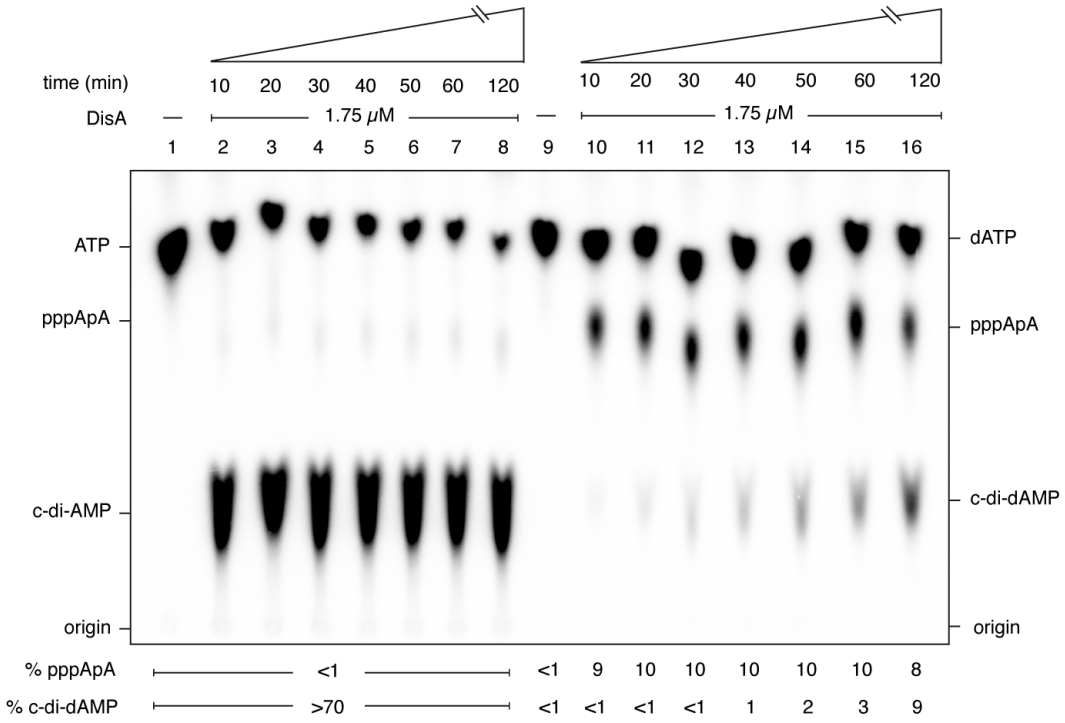

Figure 28. pppApA is the intermediate of the DAC reaction.
Purified DisA (1.75 μM) was incubated in buffer A containing 1 mM $MgCl_2$ at 37°C up to 120 min in the presence of ATP (*lanes 2-8*) or dATP (*lanes 10-16*). In *lanes 1 and 9*, no protein was added to the reaction. The relative amount of pppApA and c-di-AMP produced in each reaction is indicated as percentages to the total amount of ATP.

1.9.5. Characterization of DisA DAC activity

DisA from *T. maritima* and *B. subtilis* were the first DAC enzymes to be characterized, back in 2008 by Dr. Karl-Peter Hopfner's group (Witte et al, 2008). Before that, it was unknown that c-di-AMP existed *in vivo*. In order to further characterize DisA enzyme's activity, different reaction conditions (variations in metal ion or salt concentrations) were tested and kinetics assays were performed. DisA displayed maximum activity in presence of 1-10 mM Mg^{+2} or 1-5 mM Mn^{+2}, while no ATP hydrolysis was observed in the absence of metal ions (Figure 29A). Variations in NaCl concentrations from 30 to 150 mM did not produce a strong effect in c-di-AMP synthesis, although lower salt concentrations (30 and 50 mM) resulted in higher c-di-AMP production than 100-150 mM NaCl (Figure 29B).

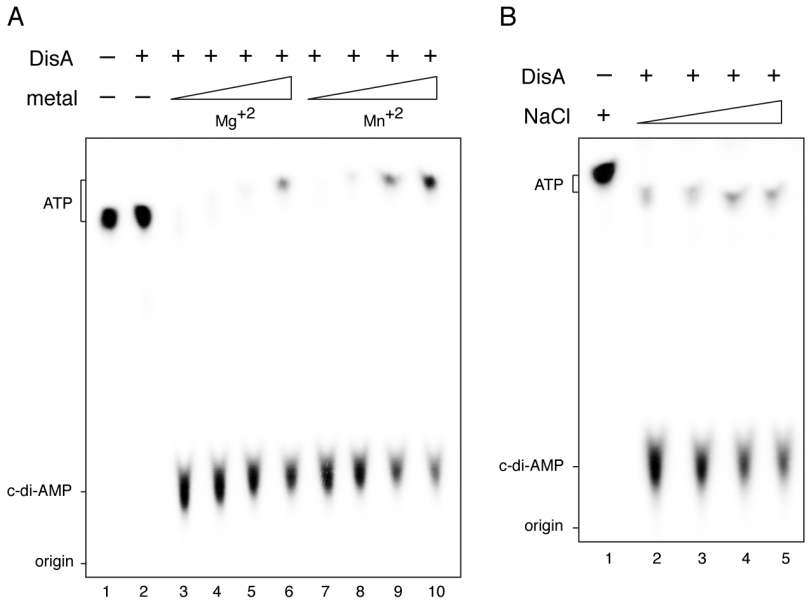

Figure 29. Effect of different metal ion and salt concentrations on DisA DAC activity.
TLC of DAC reactions performed at 37°C for 30 min in buffer A containing 50 µM ATP and 1.5 µM DisA. The effect of increasing concentrations of (A) metal ions (1, 5, 10 and 15 mM Mg^{+2} or Mn^{+2}) or (B) NaCl (30, 50, 100 and 150 mM) on c-di-AMP synthesis was analysed.

Kinetics assays were performed with increasing concentrations of the substrate (ATP), a fixed amount of protein (500 nM DisA and a fixed reaction time of 10 min. This is the time point in which DisA produced c-di-AMP at an initial rate that is approximately linear (data not shown). As shown in Figure 30, the activity of DisA was saturated at 400 µM ATP. Steady-state kinetic measurement yielded a turnover number (K_{cat}) of 1.18 s^{-1} and a Michaelis-Menten constant (*Km*) of 247.7 ± 64.7 µM for ATP. These data indicate that 250 µM ATP is needed for DisA to reach its half-maximal velocity (given by the *Km*), and that DisA has a fast turnover, given by the low k_{cat} value (1.18 s^{-1}).

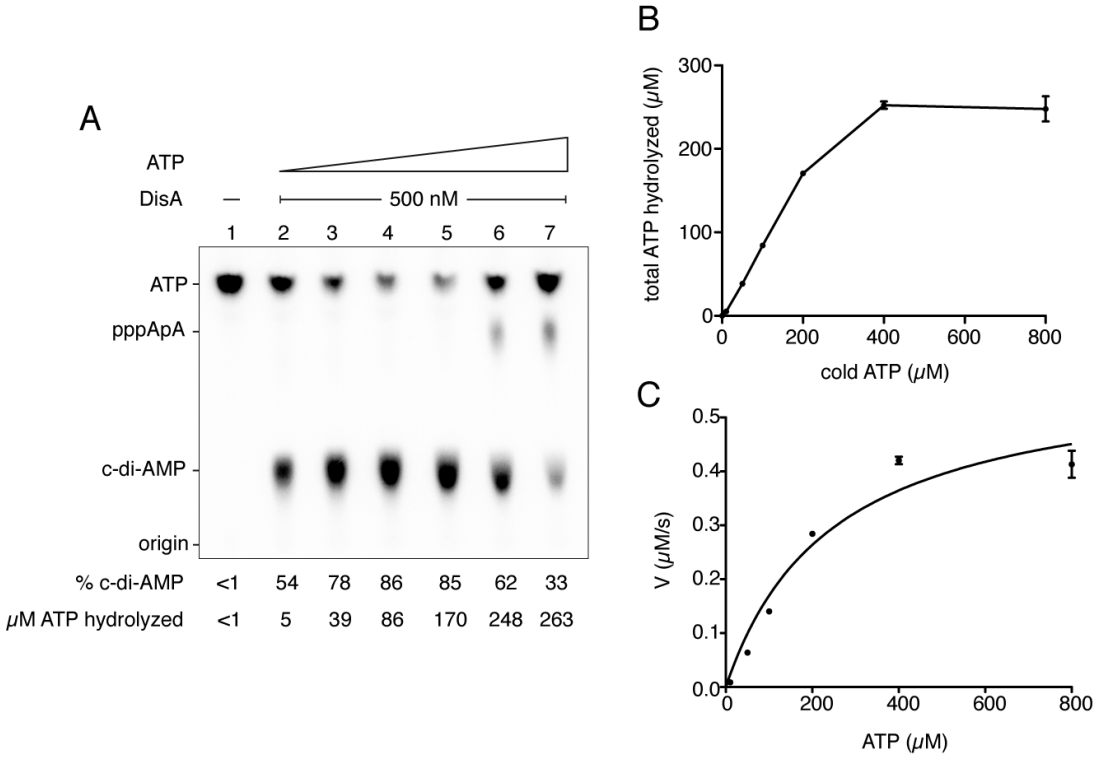

Figure 30. DisA enzyme kinetics.
(A) DAC reactions were performed at 37°C with 500 nM DisA and increasing concentrations of ATP (10, 50, 100, 200, 400 and 800 μM), and a fixed concentration of [α^{32}P]-ATP (0.05 μM). After 10 min, reactions were stopped by EDTA addition. The concentration (μM) of ATP hydrolysed by DisA in each reaction is indicated. (B) Graphic representation of the ATP saturation curve with the values extracted from part A. (C) Steady-state kinetic analysis of the hydrolysis of ATP catalysed by DisA, which exhibited a *Km* of 247.7 ± 64.7 μM and *Kcat* of 1.18s^{-1}. The results are the average of at least three independent experiments.

1.9.6. DisA forms large complexes with Holliday junctions

B. subtilis DisA binds DNA through its HhH domain, which has slightly more affinity for HJs rather than for dsDNA or ssDNA (Witte et al, 2008). In order to confirm these results and further characterize the affinity of DisA for HJs, electrophoretic shift mobility assays (EMSAs) were performed. DisA bound HJs (HJ-J3) in a concentration-dependent manner, forming large complexes that did not enter the gel, but stayed on the wells. The apparent dissociation constant (K_{Dapp}) estimated for DisA-HJ complexes was of ~350 nM in the presence of 1 mM $MgCl_2$ (Figure 32A). The HJ used in these experiments is composed of 4 arms of 80-nt each, and forms a fixed substrate, not supporting translocation. Affinity for the mobile HJ DNA (HJ_M) was also tested, but DisA shows similar K_{Dapp} values for both fixed and mobile HJs (Table 8).

It has been described that 4-way junctions can adopt different conformations according to the concentration of metal ions (e.g. Mg^{+2}) applied. The presence of 80 μM Mg^{+2} was shown to be enough to fold the extended HJ (open form) into a 2-fold-symmetric X-shape (stacked X-

structure) in which the DNA helices lie in an anti-parallel sense to each other (Figure 31) (Duckett et al, 1993; Duckett et al, 1988; Duckett et al, 1990). There are potentially two conformers of the stacked X-junction, *iso I* and *iso II*, that differ in the choice of stacking partners. The transition rates between conformers decrease with increased Mg^{+2} concentration and the open form is a necessary intermediate in conformer transition (McKinney et al, 2003; Yu et al, 2004). In the presence of Mg^{+2}, the fixed HJ, used in most of the experiments performed with DisA, mainly adopts stacked *iso II* conformation, while the mobile HJ has nearly equal populations of each conformer.

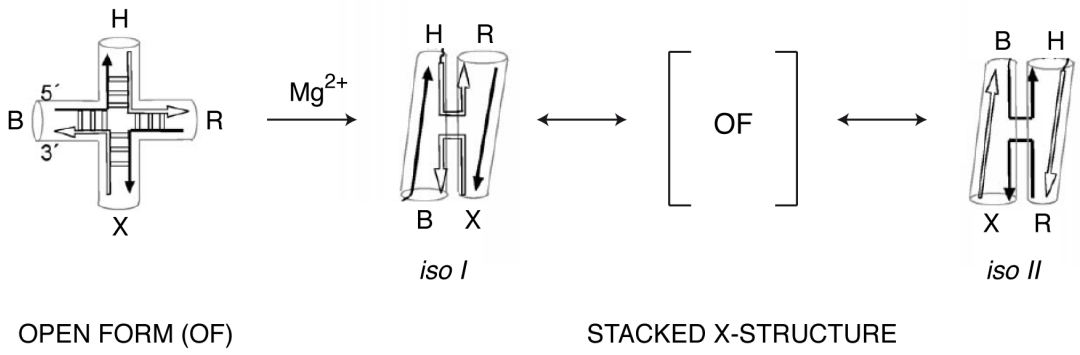

Figure 31. Metal ion-dependent HJ conformational switch.
Schematic representation of a HJ DNA in the extended form (open form) and in the stacked conformation. In the absence of metal ions, the junction adopts the open conformation, minimizing the repulsion between the negatively charged phosphates. Magnesium folds the 4-way junction into a stacked X-structure at concentrations higher than 80 μM. Two folded conformers are possible (*iso I* and *iso II*), and an open form intermediate is necessary to allow conformers transition. This figure was modified from (McKinney et al, 2003).

To test whether DisA could bind with the same affinity unfolded and folded HJs, reactions were performed in the absence (5 mM EDTA) or presence of low (1 mM Mg^{+2}) or high (10 mM Mg^{+2}) magnesium concentrations. In the presence of low or high Mg^{+2} concentrations, DisA bound HJs with a similar affinity, which was only slightly reduced in the absence of Mg^{+2} (Figure 32B). This result indicates that DisA has slightly more affinity for stacked X-structures, but that it can also bind the unfolded HJ conformation.

To examine whether DisA bound to ATP or in the presence of c-di-AMP could form complex with HJ, EMSA experiments were performed. DisA binds similarly HJ in the presence or absence of ATP, but with lower affinity in the presence of c-di-AMP (Figure 32C). In summary, the binding of DisA to HJs was obtained with 100-fold lower protein concentrations than the previously published (0.35 μM vs. 35 μM, respectively). Moreover, it was shown that DisA could bind open or stacked HJs, in the presence or absence of nucleotide cofactors.

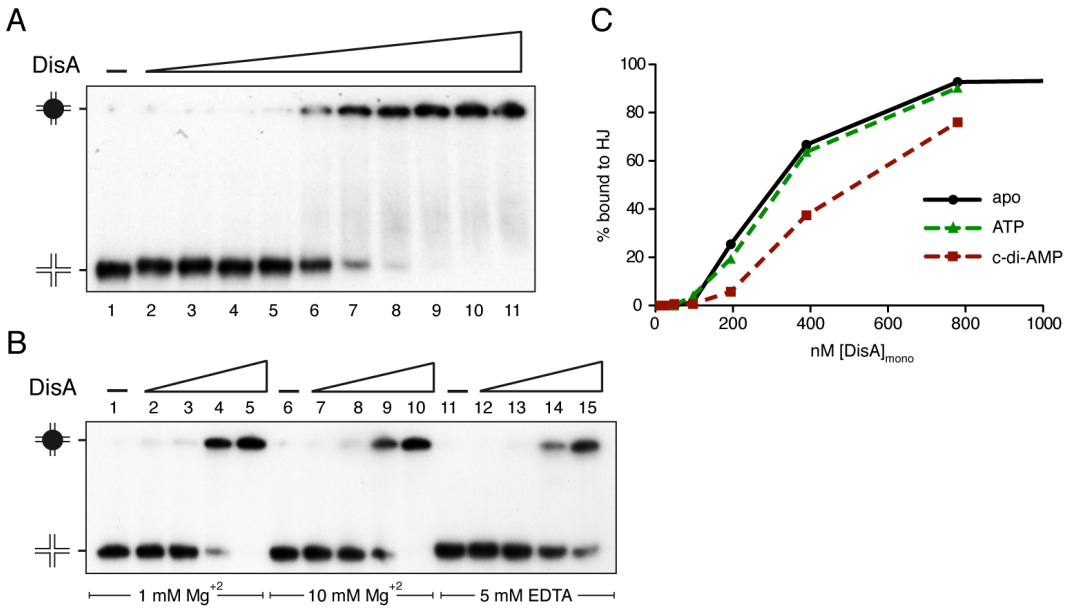

Figure 32. Characterization of the DisA-HJ complex.
To separate DisA-HJ complexes from free DNA, EMSAs were performed using 6% native PAGE. (A) 80-nt fixed HJs [γ-^{32}P]-HJ-J3 (0.05 nM) was incubated with increasing concentrations of DisA (12, 24, 48, 97, 190, 390, 770, 1550, 3100 and 6200 nM; *lanes 2-11*) for 15 min in buffer A containing 1 mM $MgCl_2$. In *lane 1*, no protein was added. (B) The same reaction was performed, but different metal concentration was used (1 mM, 10 mM or no $MgCl_2$). The DisA concentration in this experiment was 100, 200, 400 and 800 nM. In *lane 1, 6 and 11*, no protein was added. (C) Fractions (%) of DisA bound to HJ in presence of 200 μM ATP, c-di-AMP or no nucleotide (apo). These reactions were performed in buffer A containing 1 mM $MgCl_2$. The results are the average of at least three independent experiments.

1.9.7. DisA shows little preference among different DNA structures

To gain insight into the role of DisA in DNA repair, it was analysed whether DisA could bind other DNA than HJs, including those that are also produced during HR (D-loops, replicated D-loop, ssDNA, etc.). Each DNA structure was radiolabeled and a series of EMSAs were performed with increasing concentrations of DisA (100, 200, 400 and 800 nM), considering that 100 nM is the concentration that no complex with HJ was observed and that at 800 nM all 4-way junction was bound to DisA (Figure 32). In general, DisA bound all DNA substrates tested, with rather similar K_{Dapp} that ranged from 250 nM to 350 nM (Table 8). DisA bound ssDNA and dsDNA with slightly lower affinity (Table 8). These results strongly support the idea that DisA is a DNA binding protein with little preference for DNA structures, being demonstrated for the first time its capability of interacting with a wide range of DNA structures that are found *in vivo*.

Table 8. DisA binding affinity for different DNA substrates

Substrate code	Substrate description	Structure + oligonucleotide composition	K_{Dapp} (nM)*
HJ	fixed Holliday Junction J3	J3-1 J3-4 J3-2 J3-3	≈ 350
HJ_M	mobile Holliday Junction	173 345 170 346	≈ 350
Flayed	50-nt flayed DNA	J50-1 J50-4	≈ 350
Y-Fork	50-nt Y-fork DNA	J50-1 J50-6 J50-4	≈ 400
D-loop	D-loop	19-M 17-M 16-M	≈ 250
RD-loop	replicated D-loop	19-M 17-M 21 16-M	≈ 250
80-dsDNA	80-bp dsDNA	J3-2 J3-5	≈ 400
80-ssDNA	80-nt ssDNA	J3-2	≈ 400
5' tail	30 + 60-nt with ssDNA 5'-AAA tail	Fb-1 F-2	≈ 600
30-dsDNA	30-bp dsDNA	Fb-1 Fb-2	≈ 800

*All K_{Dapp} values are given as moles of DisA monomers.

1.9.8. DisA binds HJ without sequence-specificity

To further characterize the DNA binding activity of DisA towards HJs, footprinting analyses were performed. Footprinting is a protection assay designed to elucidate the sequence-specific binding sites for a protein on DNA (Galas & Schmitz, 1978). In this experiment, DNaseI, which is a double strand-specific endonuclease that makes single strand nicks in the DNA backbone, was used as the cleavage agent. One arm of the fixed (J3-HJ, arm 4) was radiolabeled. The 80-nt [γ-^{32}P]-J3-HJ was incubated with increasing concentrations of DisA (0.5, 1, 2 and 4 μM) at 37°C for 15 min. DNase I was added to the reaction for 5 min, then the DNA was precipitated and finally run in a 6% dPAGE. DisA generated a footprint that was extended throughout the whole strand (Figure 33), suggesting that DisA binds HJ without recognizing any specific sequence.

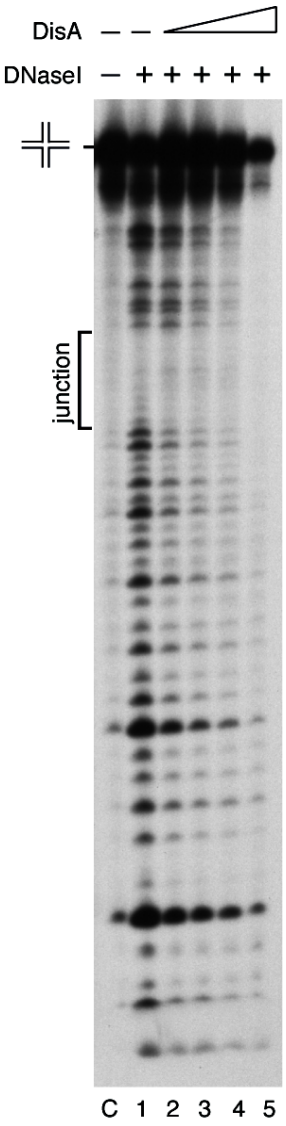

Figure 33. DNase I Footprinting of DisA-HJ complex.
[γ-^{32}P]-J3-4 HJ was incubated with increasing concentrations of DisA (0.5, 1, 2 and 4 μM, *lanes 2-5*) for 15 min at 37°C. Reaction mixtures were then treated with DNase I, and the products were analysed by denaturing PAGE. The position of the DNA crossover is marked as 'junction'. C, in the absence of DNase I.

1.9.9. DisA-DNA complex stability

In vivo, the formation of HJs mainly occurs during stalled replication forks regression or during the final stage of one- or two-ended DSB repair. DisA has a similar affinity for HJ and dsDNA (K_{Dapp} = 350 nM vs. 400 nM, respectively) (Table 8), which raise the question of how DisA can find a HJ between the much more abundant dsDNA. One possibility is that DisA could form a more stable complex with HJ rather than with dsDNA. To test this hypothesis, the DisA-DNA complex was pre-formed, then competitor DNA (unlabelled DNA) was added and the stability of the protein-DNA complex was analysed.

Both DisA-HJ and DisA-dsDNA complexes were very stable (more than 60 min) when analysed by EMSA (Figure 34). This data suggests that DisA forms a long living complex, both with HJ and dsDNA.

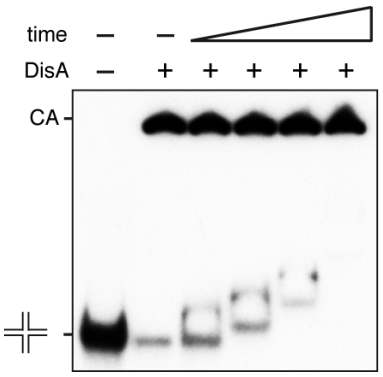

Figure 34. Stability of DisA-HJ complexes analysed by EMSA.
[γ-^{32}P]-HJ DNA (0.1 nM) was incubated with DisA (600 nM) for 15 min in buffer A containing 10 mM Mg^{+2}. Then, 50-fold excess of unlabelled HJ DNA was added to the reaction and samples were collected at different time points (1, 15, 30 and 60 min) and loaded into a 6% native PAGE.

1.9.10. DisA binding to HJ specifically inhibits c-di-AMP synthesis

Previously, it has been revealed that branched DNA could regulate DisA's DAC activity (Witte et al, 2008). To further investigate how DisA is regulated and confirm previous results, DAC assays were performed in presence or absence of DNA, using the conditions described in (Witte et al, 2008). Reactions were performed in buffer A containing 10 mM Mg^{+2}, except that lower amounts of protein (200 nM rather than 3.5 μM) and DNA (up to 250 nM rather than more than 0.65 μM) were used compared to the previous experiments. The c-di-AMP produced was separated by TLC and quantified by phosphor imaging. It was observed that in presence of HJs, c-di-AMP formation decreased in a DNA concentration-dependent manner, reaching more than 60% inhibition with 250 nM HJ (Figure 35A, 'High', *lanes 3-7*, and Figure 35C). On the other hand, the presence of dsDNA did not significantly affect DisA's activity, which decreased no more than 10% (Figure 35 B and C, *lanes 3-7*). Interestingly, no DAC inhibition was observed when the reaction was performed in buffer A containing 1 mM Mg^{+2} (Figure 35A and Figure 35B, 'Low', *lanes 8 and 9*). Altogether, these data corroborate the observation that HJ specifically regulates DisA c-di-AMP production, which was not observed when DisA is incubated with dsDNA. Furthermore, it seems that binding to the open HJ conformation, which are formed in the presence of low Mg^{+2} concentrations, is not sufficient to modulate DisA's DAC activity. This result suggests that not only HJ *per se*, but also a particular HJ conformation (stacked-X shape) is needed to regulate the synthesis of c-di-AMP by DisA, through a mechanism that remains to be studied.

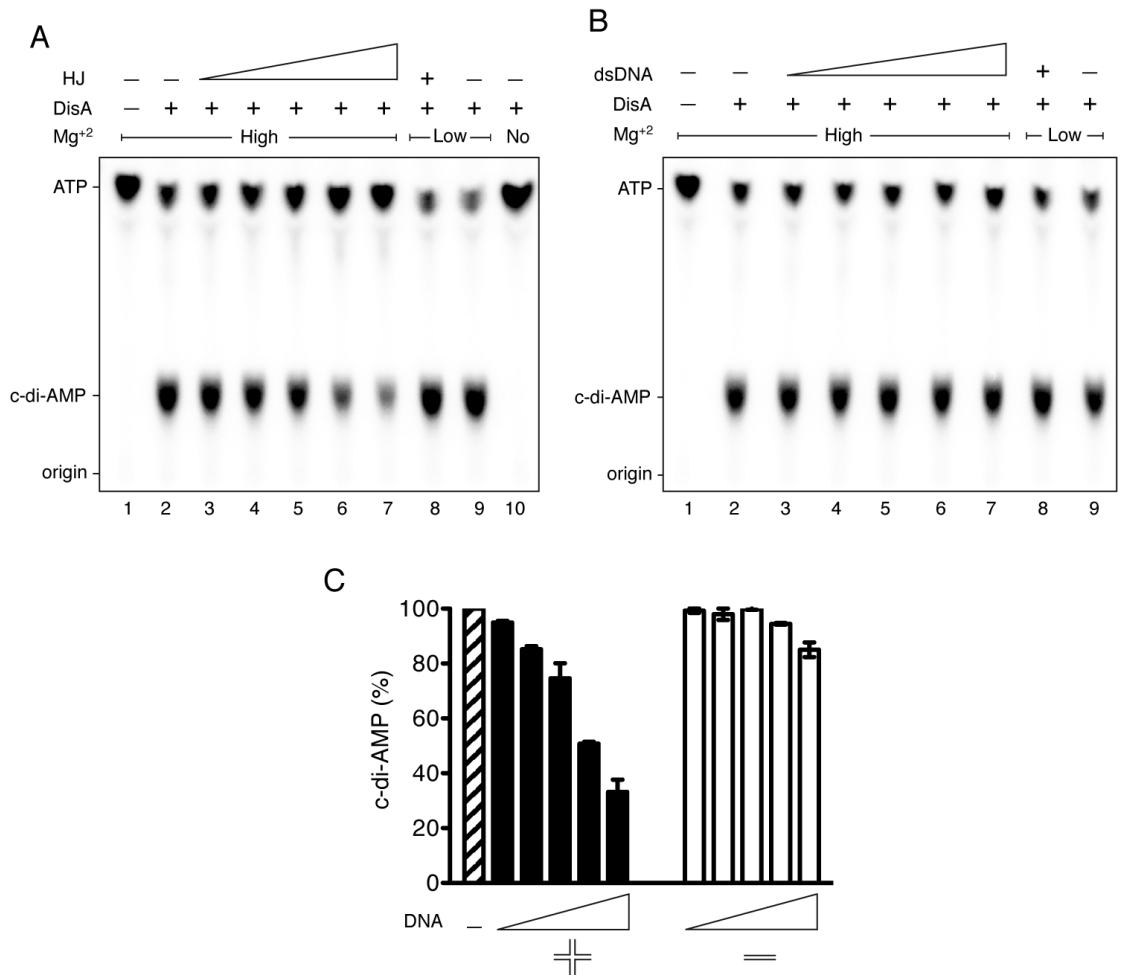

Figure 35. DisA DAC activity is inhibited specifically by binding to HJs.
TLC of the products obtained from the reaction of ATP and 200 nM DisA in the presence or absence of increasing concentrations (12.5, 25, 50, 125 and 250 nM) of HJ (A) or dsDNA (B). Reactions were performed at 37°C for 15 min, in buffer A containing 10 mM Mg^{+2} ('High' condition) or 1 mM Mg^{+2} ('Low' condition). (C) Relative amounts of c-di-AMP synthesized in the reactions shown in part A and B.

1.9.11. DisA inhibits RuvAB and RecG helicase activities

The branch migration translocases RuvA and RuvB form a motor complex (RuvAB) that is essential for the unwinding of a regressed stalled replication fork (Gupta et al, 2014) and for the processing of HJs at late stages of HR (Iwasaki et al, 1992). Together, the RuvAB complex promotes HJ branch migration, an ATP-dependent reaction that increases the length of the heteroduplex DNA (Parsons et al, 1995; Parsons et al, 1992). Reactivation of stalled replication forks represents a major housekeeping function in bacteria (Cox et al, 2000). It has been demonstrated that RecG is the main helicase that promote stalled replication fork regression, producing an HJ-like structure, known as "chicken foot". RecG couples ATP hydrolysis with duplex DNA unwinding and rewinding. It seems that only once RecG has acted and processed the fork into an HJ-like structure, can RuvAB play a role (reviewed in Bianco, 2015).

The lack of *B. subtilis* RuvAB or RecG affects cell proliferation and in the presence of DNA damages strongly impairs colony formation (Figure 15). Moreover, simultaneous disruption of *ruvAB* and *recG* genes was synthetically lethal, suggesting that the activities promoted by RecG and RuvAB do not overlap (Sanchez et al, 2005). Previously (Figure 15), it was revealed that *disA* is epistatic with *recG* and non-epistatic with *ruvAB*, being *recG* and *ruvAB* non-epistatic. It has also been observed that the HhH domain of DisA is arranged in a geometry that resembles the four HhH domains of RuvA (Witte et al, 2008). In order to investigate whether the HJ binding protein DisA can modulate RecG and RuvAB helicase activities, DNA unwinding assays were performed. Reactions were performed at 37°C in presence of 5 mM ATP and 10 mM Mg^{+2}, using a mobile HJ as the DNA substrate rather than a fixed as previously used (Figure 32 to Figure 35).

RecG (15 nM) or RuvAB (15 nM) unwound 75% and 93% of the total HJ amount, generating 42% and 50% flayed DNA, respectively, in a 15 min reaction (Figure 36, *lanes 1 and 12*). It seems that part of the HJ unwound got diffused throughout the gel, being the reason why the percentage corresponding to unwound HJ do not match the obtained fraction of flayed DNA (defined band). DisA did not display helicase activity (Figure 36A, *lanes 9-11*). Surprisingly, however, RecG- or RuvAB-mediated DNA unwinding was strongly inhibited when DisA was added to the reaction, albeit to a different extent (Figure 36, *lanes 2-7 and 13-18*). In both cases, the inhibition modulated by DisA was more efficient when the protein was pre-incubated 5 min with HJs prior RecG or RuvAB addition (Figure 36, *lanes 5-7 and 16-18*). A small stimulation of RecG's activity was observed when low concentrations of DisA were added after the helicase (Figure 36, *lanes 2 and 3*). Since different outcomes were obtained by varying the order of protein addition, it was assumed that the inhibitory effect exerted by DisA was genuine rather than performed by any non-specific effect.

DisA displayed a significant inhibitory effect on RuvAB, even when the helicase was pre-incubated with HJs prior DisA. In general, the inhibition produced by DisA could be attributed to: (i) a physical competition with the helicases for the DNA substrate (HJs); (ii) a poor stability of the RecG-HJ or RuvAB-HJ complexes or (iii) DisA produces a conformational change on RuvAB/RecG or displaces it from the centre of the HJ, abolishing its helicase activity.

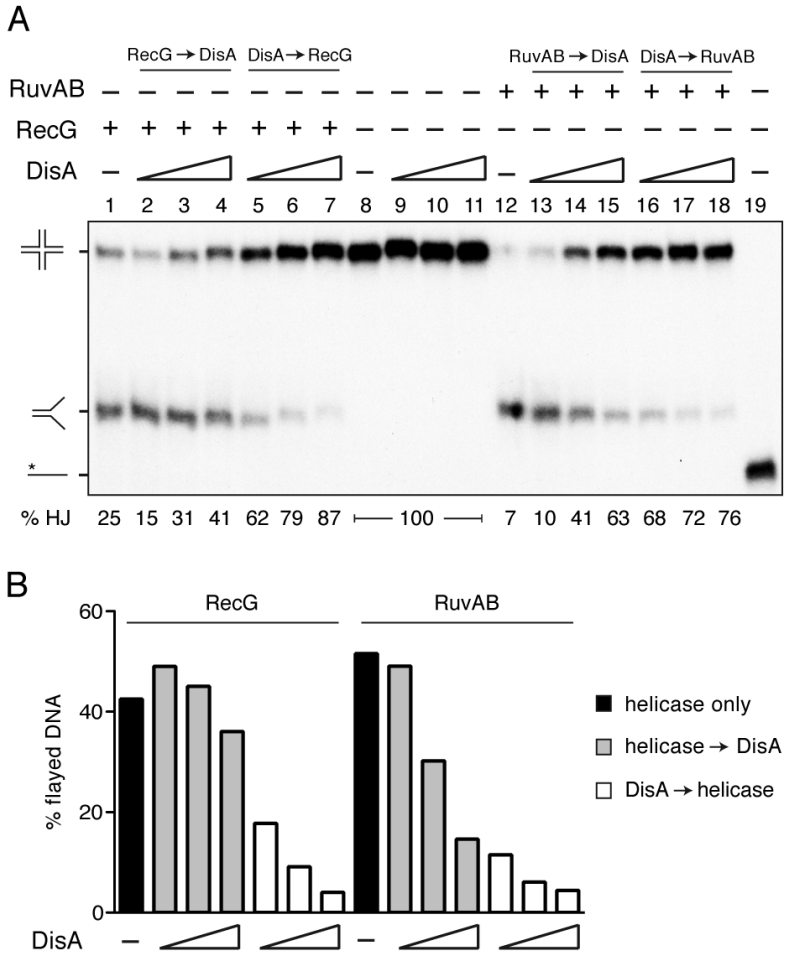

Figure 36. DisA inhibits HJ DNA unwinding catalysed by RecG and RuvAB.
(A) [γ-^{32}P]-labelled mobile HJ DNA (0.1 nM) was incubated with 15 nM of RecG or RuvAB for 15 min, in presence or absence of increasing concentrations of DisA (50, 200 and 400 nM). Reactions with DisA alone were performed as controls (*lanes 9-11*). The order of protein addition is indicated at the top. Reactions were performed in buffer A containing 5 mM ATP and 10 mM Mg^{+2}, and deproteinized (with 20 μg proteinase K, 0.8% SDS and 20 mM EDTA) at the end. Then, the DNA substrates formed in each reaction were visualized using native 6% PAGE by autoradiography. The relative amount of HJ (% HJ) and flayed DNA (B), produced in the reactions showed in panel A, was quantified using Quantity One. In *lane 19*, radiolabeled oligonucleotide was run alone, as a substrate ladder.

1.9.12. RuvAB can bind HJ in the presence of DisA

It has been described that $RuvA_{Eco}$ binds specifically HJs, in which forms tetramers that occupy exclusively the crossover region, that are then sandwiched between two hexameric rings of RuvB (Hiom & West, 1995; Parsons et al, 1995; Parsons et al, 1992). Given the strong inhibition produced by DisA (Figure 36), the ability of RuvAB to bind HJs in the presence of DisA was investigated. RuvA-HJ complexes displayed two shifted bands of different mobility when analysed by EMSA (Figure 37A, *lanes 2 and 3*). In agreement with previous results (Parsons et al, 1992), the band with higher mobility might correspond to a tetramer of RuvA bound to the HJ (Figure 37A, CRA-I), while the band with lower mobility, to a double tetramer

of RuvA bound to each side of the HJ (Figure 37A, CRA-II). In the presence of DisA, the two RuvA-HJ complexes were slightly shifted (Figure 37A, *lanes 6-9*, CRA-III), suggesting that RuvA and DisA could bind simultaneously to the HJ DNA.

Since DisA forms large complexes with HJs that do not enter polyacrylamide gels and that RuvAB-HJ complexes are equally large, EMSAs in the presence of the three proteins would not provide any additional information. Therefore, to study whether DisA and RuvAB can bind together to HJs, DNase I footprinting was performed. To observe only DNA binding and avoid the helicase activity of RuvAB, a non-hydrolysable ATP analog (ATPγS) was used as the nucleotide cofactor. Reactions were performed in buffer A containing 5 mM ATPγS and 10 mM Mg^{+2}. In strong agreement with the previously described (Hiom & West, 1995), RuvA footprints were located around the crossover region (Figure 37B, *lanes 3 and 4*), while RuvAB nearly protected all over the strand analysed (Figure 37B, *lanes 5 and 6*). RuvA and RuvAB also generated a hypersensitive band, located near the 5'-end. As observed before (Figure 33), DisA bound all over the HJ with no sequence specificity (Figure 37B, *lanes 7 and 8*). Different combinations of the three proteins together (DisA, RuvA and RuvB) showed an extended protection of the HJ (Figure 37B, *lanes 9-16*), in which the binding of RuvAB can be clearly verified by the appearance of the hypersensitive band that cannot be generated by DisA. It can be concluded that DisA does not prevent RuvAB from binding to the HJ, although the simultaneous binding of DisA and RuvAB could not be confirmed using this assay. It is likely that DisA produces a conformational change on RuvAB or displaces it from the centre of the HJ, abolishing its helicase activity, given that RuvAB can still bind HJ DNA in the presence of DisA. Alternatively, RuvAB forms very unstable complexes with HJs. This possibility will be addressed in the coming sections.

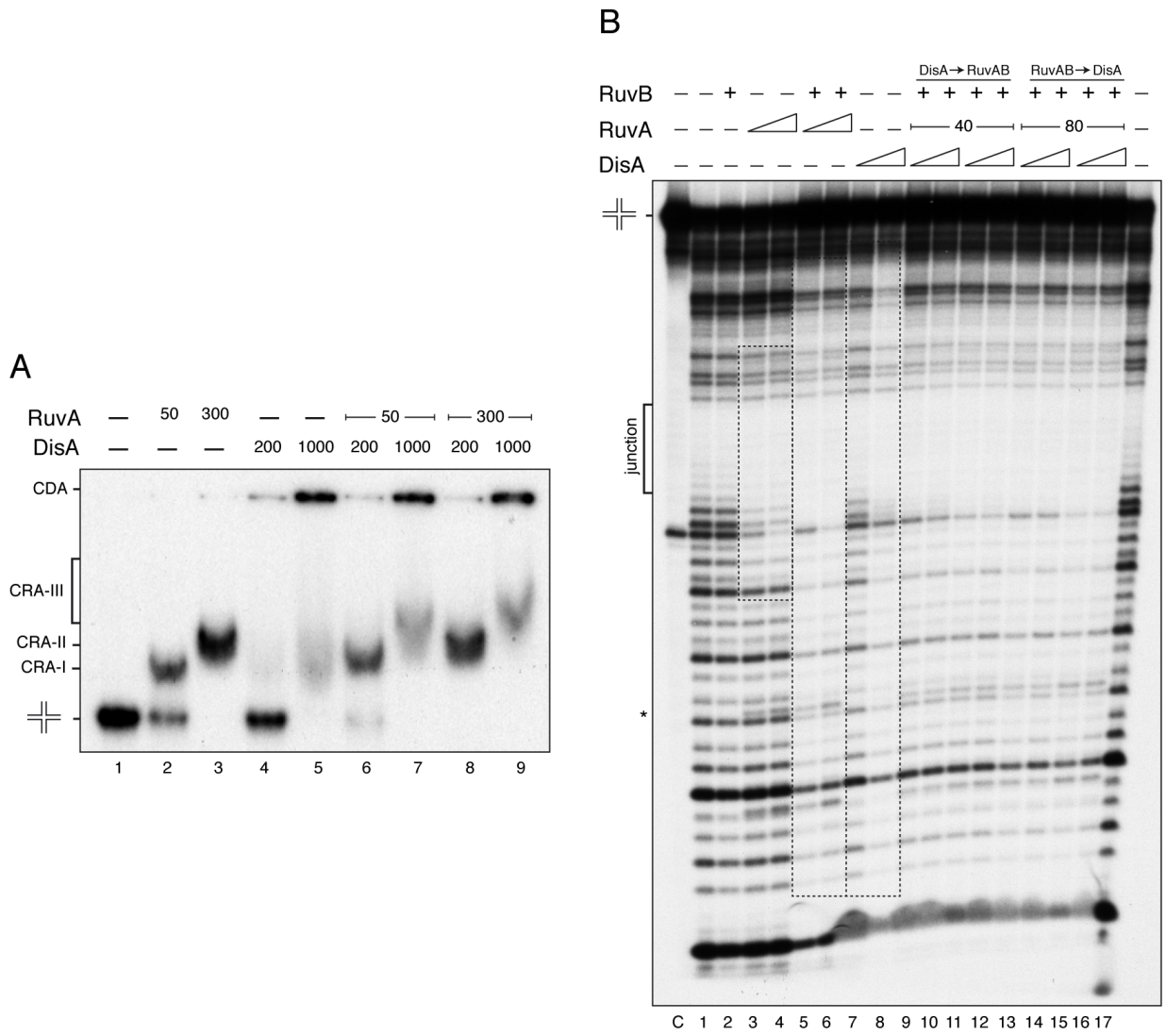

Figure 37. RuvAB-HJ complexes in the presence of DisA.
(A) EMSA to detect the binding of RuvA and/or DisA to HJ. The [γ-^{32}P]-labelled J3-4 HJ (0.1 nM) was incubated with the indicated amounts of DisA (*lanes 4-9*) and/or RuvA (*lanes 2 and 3, 6-9*) for 15 min at 37°C in buffer A without ATP. Then, reaction mixtures were loaded into 6% native PAGE and visualized by autoradiography. 'CRA-I' and 'CRA-II', complexes formed by RuvA-HJ; 'CDA', by DisA and 'CRA-III' by RuvA and DisA. (B) DNase I Footprinting analyses of the sequences protected on a fixed HJ due to interaction with RuvB (*lanes 2*), RuvA (*lanes 3 and 4*), RuvAB (*lanes 5 and 6*), DisA (*lanes 7 and 8*) and different combinations of the three proteins (*lanes 9-16*). The order of protein addition is indicated on top. In *lanes 1 and 17*, reaction in the absence of proteins. C, no DNase I was added. The footprint region generated by each protein is marked with a rectangle. The asterisk indicates a hypersensitive band that appears in presence of RuvA. The position of the DNA crossover is indicated in the figure as 'junction'.

1.9.13. DisA and RecG can bind HJ simultaneously

Previously (Figure 15), it was shown that *disA* is epistatic with *recG*, suggesting that they could act in the same DNA repair pathway. To investigate whether DisA could play a role with RecG in the restart of stalled replication forks, the ability of both proteins to bind HJ together

was analysed by EMSA and DNase I footprinting. In presence of 5 mM ATPγS and 10 mM Mg^{+2}, RecG forms a discrete complex with HJ DNA that is evident even at lower amounts of protein (Figure 38A, *lanes 5-7*). Once DisA was added to the reaction, RecG complexes nearly disappeared, and the formation of a large complex was detected in the wells (Figure 38A, *lanes 8-16*). When DisA was added before RecG, the formation of RecG-HJ complexes was completely inhibited (Figure 38A, *lanes 11-13*). These results suggest that either DisA is displacing RecG from the HJ or both proteins are binding together. To gain more insights into this observation, DNase I footprinting assays were performed.

Interestingly, RecG did not produce a distinguishable footprint in the HJ (Figure 38B, *lanes 2-4*). This could be explained by many reasons: (*i)* RecG is bound to another strand(s) other than the one analysed (strand 4); and (*ii)* RecG forms a very unstable complex with HJs and therefore could not be detected using this technique. Surprisingly, when DisA and RecG were added together to the reaction (Figure 38B, *lanes 8-10*), a different pattern was observed when compared to the footprint of DisA alone (Figure 38B, *lanes 5-7*). This result suggests that RecG is actually bound to the strand 4 of the HJ and is somehow displacing or relocating DisA, mainly from the 3'-end. These results provide *in vitro* evidence that DisA and RecG can bind HJ simultaneously.

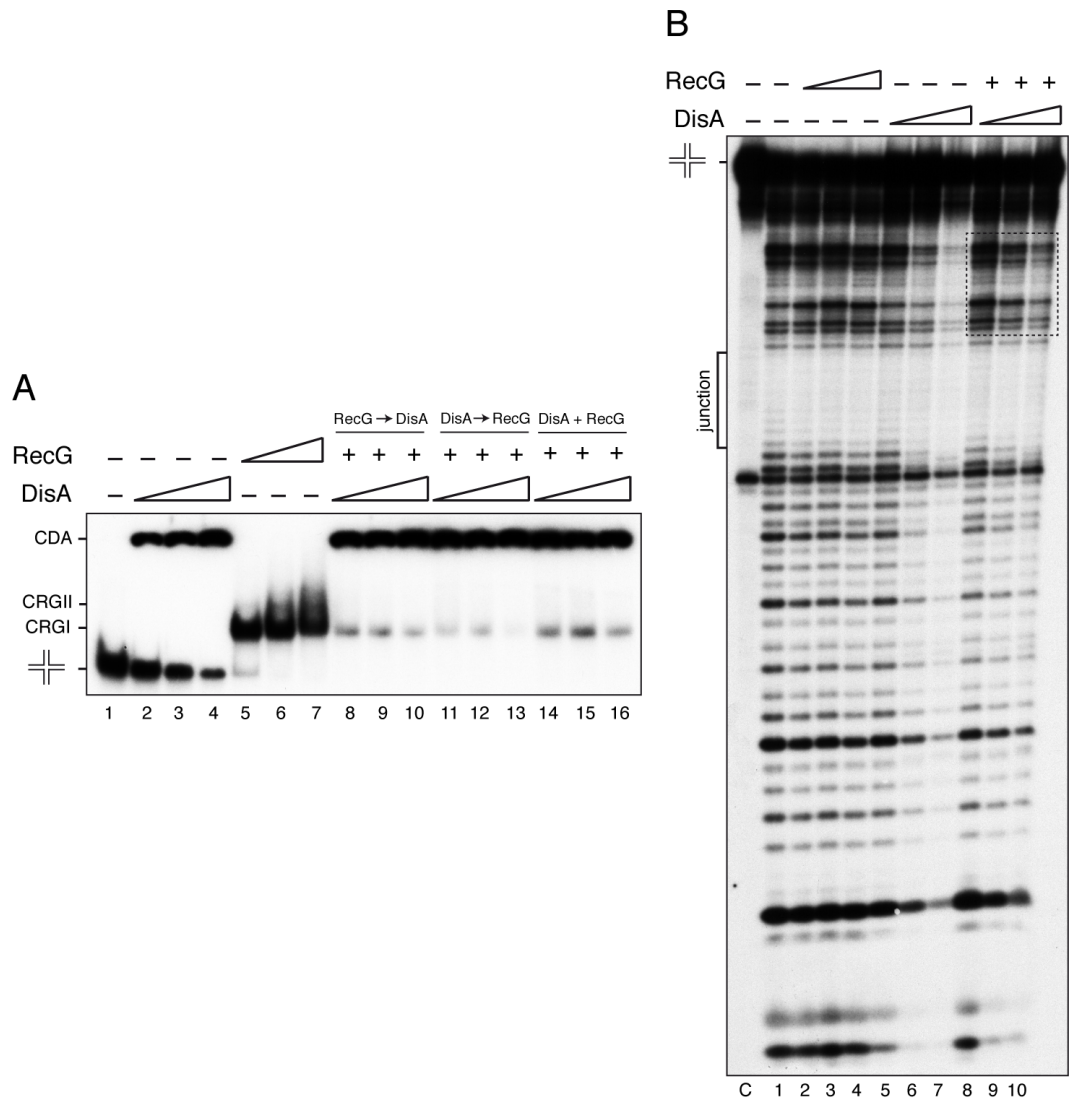

Figure 38. DisA and RecG can bind HJ together.
(A) EMSA analysis of RecG and/or DisA binding to HJ. The [γ-^{32}P]-labelled J3-4 HJ DNA (0.1 nM) was incubated with increasing concentrations of DisA (100, 200 and 400 nM, *lanes 2-4*) and/or RecG (7.5, 15 and 30 nM, *lanes 5-7;* 30 nM, *lanes 8-16*) for 15 min at 37°C in buffer A containing 5 mM ATPγS and 10 mM Mg^{+2}. Then, reaction mixtures were separated in 6% native PAGE and visualized by autoradiography. 'CRGI' and 'CRGII', complexes formed by RecG-HJ, 'CDA' and by DisA-HJ. (B) DNase I Footprinting analyses of the sequences protected on a fixed HJ due to interaction with increasing concentrations of RecG (15, 30 and 60 nM, *lanes 2-4*), DisA (250, 500 and 1000 nM, *lanes 5-7*) or 60 nM RecG with increasing amounts of DisA (250, 500 and 1000 nM, *lanes 8-10*). The order of protein addition is indicated at the top. C, no DNase I was added. The region protected by DisA in presence of RecG is marked with a rectangle. The position of the DNA crossover is indicated in the figure as 'junction'.

1.9.14. RecG-HJ and RuvAB-HJ complex stability

To test whether RecG or RuvAB could form stable complexes with HJ DNA, band-shift analysis of the dissociation of these proteins from HJ was performed, in the presence of 5 mM ATPγS and 10 mM Mg^{+2}. Binding reactions were performed at saturating protein concentrations, where 100% of the protein should be bound to DNA. A 50-fold excess of

unlabelled DNA was added as binding competitor at the end of the reaction and samples were collected at different time points. It has been previously observed for RuvAB-HJ binding assays that a fixation step is necessary to avoid disruption of the complex during EMSA (Bradley et al, 2011; Canas et al, 2014). Therefore, glutaraldehyde (0.1 % final concentration) was used to 'freeze' the complexes that had already been formed, and was added to each tube immediately before samples were loaded into a native PAGE. The half-life, calculated from at least three independent experiments, was less than 1 min for RecG-HJ and more than 30 min for RuvAB-HJ (Figure 39). This result is in strong agreement with the previously reported for RecG-HJ complex stability, which was less than 3 min in the presence of 5 mM Mg^{+2} (Canas et al, 2014).

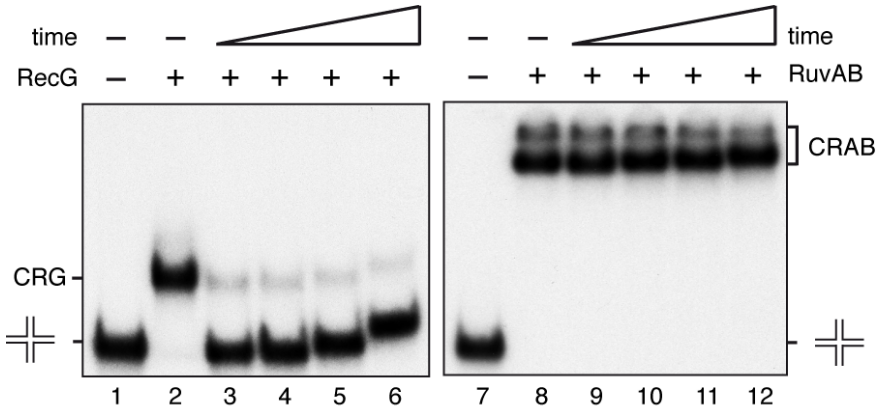

Figure 39. Stability of RecG and RuvAB complexes with HJ.
Reactions were performed at 37°C in buffer A containing 5 mM ATPγS and 10 mM Mg^{+2}, and analysed by EMSA. [γ^{32}-P]-labelled J3-4 HJ (0.1 nM) was incubated with RecG (7.5 nM) or RuvAB (30 nM) for 15 min (CRG, *lane 2* and CRAB, *lane 8*). Then, 50-fold excess of non-radiolabeled DNA was added to the reaction mixture and samples were collected after 1, 2, 10 and 20 min for RecG (*lanes 3-6*) and after 1, 10, 20 and 30 min for RuvAB (*lanes 9-12*). 0.1% glutaraldehyde (final concentration) was added after all reactions with RuvAB, immediately before they were loaded into the gel. In *lanes 1 and 7*, free HJ DNA.

Therefore, it can be concluded that the inhibition produced by DisA on the helicase activity of RuvAB (Figure 36) is unlikely due to a short half-life of the RuvAB-HJ complex. However, the existence of a "cage effect" in EMSA gels could lead to misinterpretations and this must be also considered (Fried & Liu, 1994). On the other hand, neither the "cage effect" produced by EMSA nor the use of glutaraldehyde was sufficient to stabilize RecG-HJ complexes (Figure 39). This result indicate that RecG, which has very high affinity for HJs, forms a much more unstable complex with HJ than DisA. This result suggests that DisA could be competing for the DNA substrate or displacing RecG from its regular position, preventing its translocation activity. Whereas, RuvAB forms highly stable complexes and binds HJ in the presence of DisA.

One possibility is that DisA produce a conformational change on RuvAB, affecting its helicase activity. Further experiments need to be performed to test this hypothesis.

1.9.15. DisA inhibits HJ resolution

RecU (functional counterpart of $RuvC_{Eco}$) specifically binds and cleaves mobile 4-way junctions (Ayora et al, 2004). The *recU* null mutation produces 1-3% anucleate cells, which have reduced viability (21% propidium-iodide-stained cells) and that are impaired in DNA repair (Figure 15) (Carrasco et al, 2004; Pedersen & Setlow, 2000; Sanchez et al, 2005). Moreover, it was observed that RecU and DisA could participate in the same DNA repair pathway (epistasis) (Figure 15). To study the effect of DisA in the resolution of HJs promoted by RecU, DNA binding and resolution assays were performed. RecU, which forms a dimer in solution, formed a discrete complex with HJ DNA, as detected by EMSA (Figure 40A, *lanes 5-7*). This is in agreement to previous observations (Ayora et al, 2004). In the presence of increasing concentrations of DisA (250, 500 and 1000 nM), the complex formed by RecU (0.1 nM) disappears in a protein concentration-dependent manner, becoming all DNA trapped into the wells (Figure 40A, *lanes 8-13*). The same effect was observed either when RecU or DisA was pre-incubated with the DNA. This result suggests that both proteins can bind the HJ together or that DisA is displacing RecU from the DNA.

The effect of DisA on RecU was also investigated by resolution assays. Reactions were performed at 37°C for 30 min in buffer A containing 10 mM $MgCl_2$ and 1 mM ATPγS. DisA alone was used as a negative control, which confirmed that purified DisA did not show endonuclease activity. When incubated with RecU, DisA significantly inhibited HJ cleavage, which was even more evident when DisA was pre-incubated 5 min with HJ DNA prior RecU addition (Figure 40B, *lanes 4-9*).

The simultaneous binding of DisA and RecU to the HJ, suggested in the EMSA, was further investigated using DNase I footprinting. RecU alone showed a clear footprint over the HJ, generating a hypersensitive band in the cross over region (Figure 40C, *lanes 2 and 3*). The addition of DisA generated an extended protection and did not prevent the appearance of the hypersensitive band produced by RecU. This indicates that both proteins can bind HJ DNA together. Altogether, these results support the idea that DisA displaces or produces a conformational change in RecU, inhibiting its endonuclease activity over HJs.

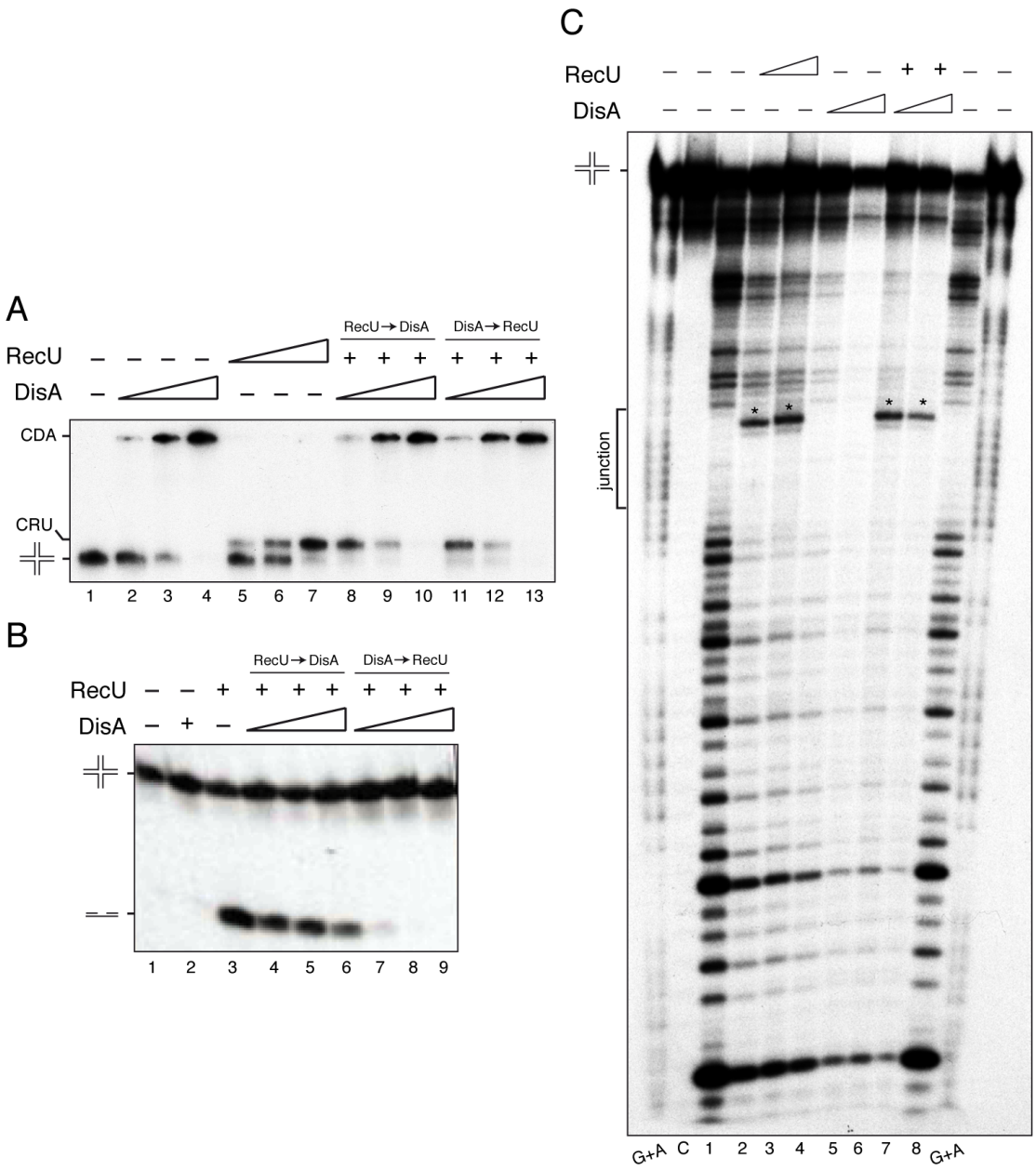

Figure 40. DisA bind to HJs in the presence of RecU and inhibits its resolvase activity.
(A) EMSA reactions were performed with [γ^{32}-P]-labelled HJ incubated with increasing concentrations of DisA (250, 500 and 1000 nM, *lanes 2-4* and *8-13*) and/or RecU (25, 50 and 100 pM, *lanes 5-7*; 100 pM, *lanes 8-13*) for 15 min at 37°C in buffer A containing 1 mM Mg^{+2}. CRU: complex formed by RecU-HJ. CDA: complex formed by DisA-HJ and/or DisA-RecU-HJ (B) HJ cleavage reaction in the absence (*lanes 1 and 3*) or presence of DisA (1000 nM, *lane 2*; 500, 1000 and 2000 nM, *lanes 4-6 and 7-9*). The RecU concentration used in this assay was 200 nM (as moles of monomers). (C) DNase I footprinting. Reactions were performed under the same conditions described for the EMSA (part A), except the concentration of RecU (50 and 100 nM, *lanes 2 and 3*; 100 nM, *lanes 6 and 7*) and DisA (500 and 1000 nM, lanes 4-7). G+A: Maxam-Gilbert sequencing ladder. In *lanes 1 and 8*, DNase I only. C: no proteins were added. The asterisk indicates a hypersensitive band generated after RecU binding (*lanes 2, 3, 6 and 7*). The position of the DNA crossover is indicated in the figure as 'junction'.

1.9.16. DisA directly inhibits RecA-mediated DNA strand exchange

An alternative of the DNA damage avoidance sub-pathway is an error-free DDT in which the stalled nascent strand invades and pairs the newly synthesized undamaged strand of the sister chromosome and utilises it, by a transient "template switching", as a template for replication across the DNA lesion. Although this process is not yet completely understood at the molecular level, it resembles recombinational repair. This is a process that requires the presence of an intact homologous DNA, which occurs during vegetative growth, when replication is active and the homologous sister chromosome is present, and RecA-mediated DNA pairing and strand exchange reactions take place. RecA is also essential for induction of the DNA damage-induced SOS response, DSB repair and activation of SOS mutagenesis (promoted by translesion DNA synthesis). RecA, in the dATP or ATP bound form [denoted as (d)ATP], slowly nucleates onto ssDNA and this reaction is followed by filament extension in the 5' to 3' direction (a fast process known as nucleoprotein filament formation). RecA does not require (d)ATP hydrolysis for binding, but requires it for disassembly, which also occurs in the 5' to 3' direction from the ssDNA. Then, RecA recruits a homologous duplex DNA to produce heteroduplex DNA. The active form of the RecA nucleoprotein filament catalyses the pairing and exchange of complementary DNA strands between homologous DNA regions. Thus, (d)ATP hydrolysis is required for dissociation of RecA from the heteroduplex product of DNA strand exchange.

In vivo, the ssDNA is coated by the single-strand DNA-binding protein, SsbA, which acts as a ssDNA protector, inhibiting the formation of secondary structures. SsbA also recruits another mediator, the RecO protein, to the ssDNA. *In vitro*, RecA nucleoprotein filament formation is partially inhibited or blocked if the ssDNA is coated by SsbA in presence of dATP or ATP, respectively. In presence of ATP, SsbA and RecO are necessary to modulate the assembly of RecA onto ssDNA. The RecO protein promotes the nucleation of RecA onto ssDNA and facilitates annealing of the complementary DNA strands (Cox, 2007; Galletto & Kowalczykowski, 2007; Manfredi et al, 2010).

To study whether DisA can modulate single-strand gap repair and/or template switching, RecA activities, such as ssDNA-dependent (d)ATPase and strand exchange activities, were tested in the presence of DisA. RecA showed higher hydrolysis rate in the presence of dATP rather than ATP as the nucleotide cofactor (Figure 41), which is in strong agreement with published results (Carrasco et al, 2008). The rate of RecA nucleation onto naked ssDNA and subsequent filament formation was biphasic, with a lag-phase of 6.5 ± 0.2 min and a hydrolysis

rate of 12.5 ± 0.2 min^{-1}, in presence of dATP (Figure 41A). DisA, which converts dATP into c-di-(d)AMP with very low efficiency, as previously demonstrated (Figure 27), did not display dATP hydrolysis under the experimental conditions used. Moreover, the addition of DisA did not impair RecA dATPase activity, as the rate of dATP hydrolysis continued to be at 12.5 ± 0.2 min^{-1}, with a slightly longer nucleation time (7.8 ± 1 min), if compared to the absence of DisA (Figure 41A). This could be attributed to the competition for ssDNA binding between DisA and RecA, delaying RecA nucleation but not significantly affecting filament growth.

To test whether DisA modulates the dATPase activity of RecA in the presence of a DNA heteroduplex, homologous circular ssDNA and linear dsDNA were used simultaneously. A similar lag-phase (6.8 ± 0.2 min) and rate of dATP hydrolysis was obtained in the presence of the heteroduplex substrate (12 ± 0.5 min^{-1}) compared to the presence of ssDNA alone. Likewise, the presence of DisA did not significantly impair RecA nucleation (8 ± 1 min) and filamentation (12 ± 0.5 min^{-1}) activities when assessed by means of (d)ATP hydrolysis (Figure 41A).

DisA specifically converts ATP into c-di-AMP, as previously demonstrated (Figure 27). Therefore, as expected, the rate of RecA ATP hydrolysis was strongly inhibited when DisA was included to the reaction (2.5 ± 0.1 min^{-1}), when compared to RecA and ssDNA alone (6.4 ± 0.3 min^{-1}) (Figure 41B). This result suggests that DisA depletes the ATP pool by converting it irreversibly to a nucleotide cofactor (c-di-AMP) that cannot be utilized by RecA.

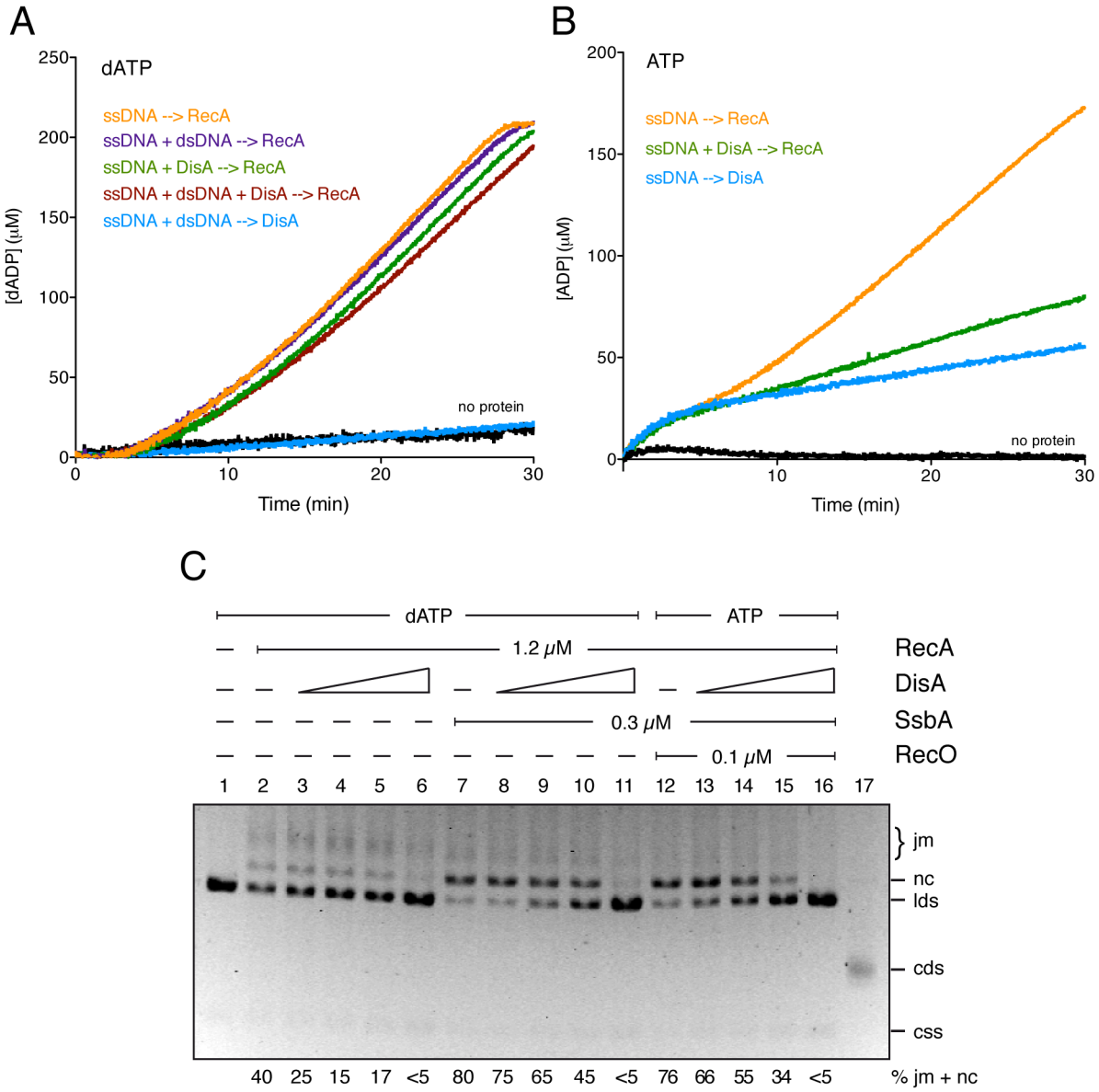

Figure 41. RecA-mediated (d)ATPase and strand exchange activities in the presence of DisA. (A-B) Circular 3.197-nt ssDNA (10 μM) was incubated with RecA (0.8 μM) in buffer G containing 5 mM dATP (A) or ATP (B) at 37°C. The rate of (d)ATP hydrolysis was measured for 30 min in the presence of DisA (0.2 μM) and/or dsDNA (20 μM). The DNA was pre-incubated with/out DisA for 5 min prior RecA or DisA addition, as indicated in the figure. (C) Strand exchange reactions between circular ssDNA (*css*, 10 μM) and homologous linear dsDNA (*lds*, 20 μM) mediated by RecA were performed in buffer G containing 5 mM dATP or ATP, at 37°C for 60 min, in the presence or absence of increasing concentrations of DisA (25-200 nM). When indicated, SsbA and/or RecO were pre-incubated with the DNA for 5 min prior RecA addition. The amount of recombination intermediates (*jm, joint molecules*) and products (*nc, nicked circular*) are indicated as percentages. The results shown are representative of the reactions repeated three or more times that gave similar outcomes.

It was investigated whether DisA affects RecA-mediated strand exchange activity. Here, a filament of RecA formed on ssDNA searches and pairs a homologous sequence within a second DNA molecule and catalyses the exchange of complementary base pairs to form a new heteroduplex. RecA initiates DNA recombination by pairing the linear dsDNA (*lds*) with the

complementary circular ssDNA (*css*), leading to the formation of a joint molecule (*jm*) between the free end of *lds* and the *css*, followed by extensive DNA strand exchange to generate the nicked circular duplex (*nc*) and the linear ssDNA (*lss*) products. In the presence of dATP, RecA (1 RecA monomer/12-nt), even in the absence of mediators, promotes strand exchange, although more efficiently when SsbA is pre-incubated with the ssDNA (Figure 41C, *lanes 2* and *7*). Surprisingly, the addition of DisA strongly inhibited the strand exchange reaction, in a concentration-dependent manner, and reaching total inhibition at 200 nM DisA (1 DisA monomer/50-nt) (Figure 41C, *lanes 3-6* and *8-11*). In the presence of ATP, the addition of recombinase mediators (SsbA and RecO) is necessary to activate the reaction promoted by RecA. When DisA was added to the strand exchange reaction performed in presence of RecA, SsbA, RecO and ATP, the same inhibitory effect was observed as in the reaction performed with dATP and RecA (Figure 41C, *lanes 12-16*). Because DisA hydrolyses and depletes the *in vitro* ATP pool, it cannot be ruled out that this is the cause of the inhibitory effect observed. However, in the case of the strand exchange reaction performed in presence of dATP, it is likely that DisA directly inhibits final product formation.

To further characterize how DisA affects RecA-mediated DNA strand exchange, time course reactions were performed (Figure 42). In the presence of dATP and SsbA, RecA generates joint molecules in the first 10 min of reaction with *css* and its homologous *lds* substrate, while *nc* DNA products start to accumulate at 30 min, reaching nearly 60% formation at 60 min (Figure 42A, *lanes 2-7*). When DisA, at a concentration that affects about 80% the strand exchange reaction (150 nM), is added 5 min prior RecA addition, recombination is extremely inhibited, rendering less than 20% of joint molecules and nicked circular products after 60 min (Figure 42A, *lanes 8-13*). When DisA is added 15 min after RecA starts the reaction, the formation of final *nc* products is also effected, while an accumulation of *jm* intermediates was observed (Figure 42B, *lanes 8-12*). It is likely that DisA blocks the extension of the *jm* generated by RecA preventing the formation of final recombination products.

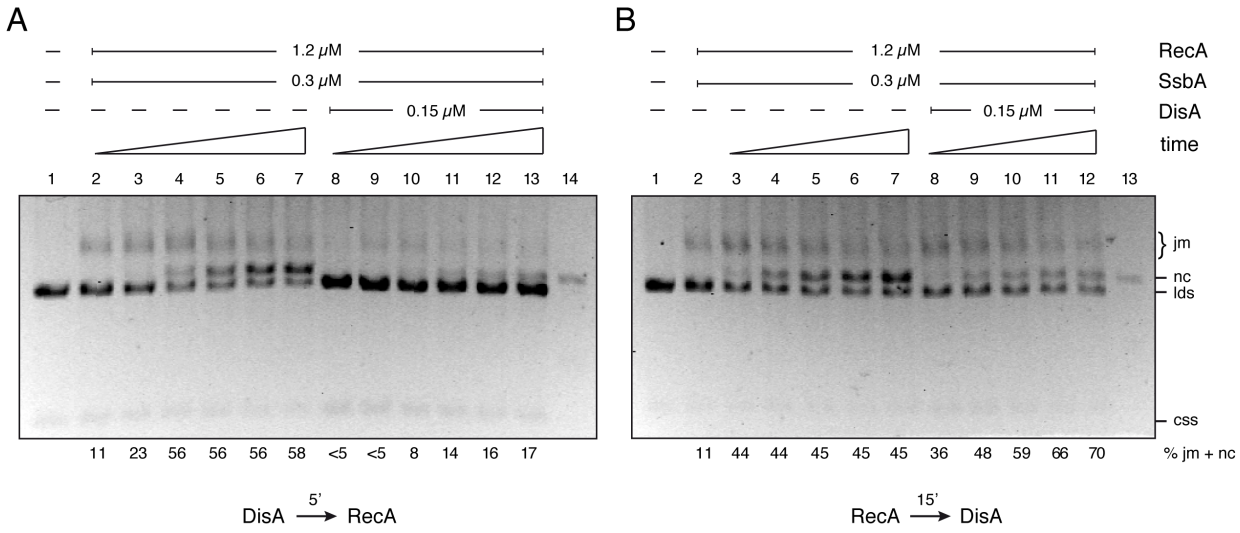

Figure 42. DisA negatively affects recombination.
Strand exchange reactions were performed as described in **Figure 41**C, in presence of RecA and SsbA, and dATP as the nucleotide cofactor. (A) DisA was added 5 min prior RecA addition; (B) RecA was pre-incubated 15 min prior DisA addition. Time points are 10, 20, 30, 40, 50 and 60 min (A, lanes *2-7* and *8-13*), and 10, 20, 30, 45 and 60 min (B, lanes *3-7* and *8-12*).

Taken together, these results show that DisA directly inhibits DNA strand exchange mediated by RecA. One hypothesis could be that DisA is affecting the dATPase activity of RecA, which is essential for RecA-ssDNA nucleoprotein filament formation and subsequent strand exchange. However, this hypothesis has been discarded since DisA did not affect RecA dATP hydrolysis (Figure 41A). Alternatively, DisA could be binding with strong affinity to the D-loops formed during strand invasion, inhibiting its extension and, therefore, preventing recombination. Additional experiments will be performed to confirm this hypothesis.

1.10. Biochemical study of the RadA/Sms protein

1.10.1. Purification of *B. subtilis* RadA/Sms

It was observed that DisA could bind a variety of DNA substrates with similar efficiency (Table 8), but that only binding to HJ inhibited the synthesis of c-di-AMP (Figure 35). In an attempt to understand this mechanism, it was speculated if another protein was required for the interaction of DisA with HJ. RadA/Sms seemed to be a good candidate for this interaction since it shares operon with DisA and has DNA repair functions (see 'Introduction'). To test this hypothesis, *B. subtilis* RadA/Sms protein was purified. Purification of RadA/Sms was very laborious, since its overexpression resulted in a very insoluble protein that once solubilized easily precipitated at salt concentrations lower than 0.7 M (NaCl). Therefore, to purify

RadA/Sms, denaturing conditions were used (4 M urea) combined with high salt buffers (1 M NaCl) and a refolding step in presence of CHAPS (0.5 %) to improve solubilisation (see more details in 'Materials and methods', page 31). Purified RadA/Sms was visualized by 12.5% SDS-PAGE and provided a single band of ~55 kDa (Figure 43), which is consistent with the calculated atomic mass of RadA/Sms (49.48 kDa). The identity of the purified protein was further confirmed by MALDI-TOF/TOF mass spectrometry of the peptide of the purified protein as being RadA/Sms from *B. subtilis*.

RadA/Sms has only been poorly characterized before, the first biochemical studies being recently performed in *E. coli* (Cooper et al, 2015) and *M. smegmatis* (Zhang & He, 2013). Thus, at the beginning of this work the activity of this protein was totally unknown. To test if the purified protein was still functional, the first attempt was to investigate if it possessed ATPase activity, considering that RadA/Sms contains walker A and B motifs, characteristic of AAA+ ATPases. The purified RadA/Sms protein (160 nM) showed some ATPase activity as measured by a coupled spectrophotometric enzyme assay (data not shown). The rate of ATP hydrolysis was very low, but it is likely that this is due to the low amount of protein used, that is limited by the low protein concentration. This result suggests that the purified RadA/Sms protein is functional, presenting a basal ATPase activity.

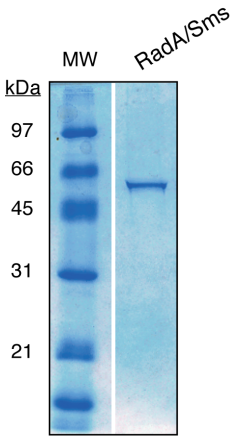

Figure 43. Purified *B. subtilis* RadA/Sms protein. The purified protein was loaded into a 12.5% SDS-PAGE and stained with comassie blue.

1.10.2. RadA/Sms is a DNA binding protein

Genetic analyses have implicated $RadA_{Eco}$ with late recombination functions due to its synergistic effects in combination with $RecG_{Eco}$ and $RuvABC_{Eco}$. The $recG_{Eco}$ or $ruvAB_{Eco}$ mutation renders cells marginally sensitive to DNA damaging agents, but they are very sensitive in the $radA_{Eco}$ context (Beam et al, 2002). Conversely, *B. subtilis*, *recG* and *ruvAB* are extremely sensitive to DNA damaging agents and *radA* or *disA* is epistatic with *recG* and non-epistatic with *ruvAB* (Figure 15). To characterize the role of RadA/Sms in DNA repair, binding

to DNA, in particular to those DNA structures that are produced as intermediates during late stages of HR, was investigated. For the first time, it is shown that RadA/Sms can bind HJ, dsDNA and ssDNA (Figure 44A), in a concentration-dependent manner. The apparent binding constants were about the same for HJ and ssDNA (~40 nM), and about 2.5-fold lower affinity for dsDNA (~100 nM). Since RadA/Sms had ATPase activity, binding to HJ DNA in the presence of ATP (1 mM) was investigated. The presence of ATP only moderately affected RadA/Sms binding to HJs, being approximately 4-fold reduced when compared to the absence of the nucleotide (K_{Dapp} = 150 nM) (Figure 44B). These results indicate that RadA/Sms is a DNA binding protein, with stronger affinity for ssDNA and HJ in the absence of ATP.

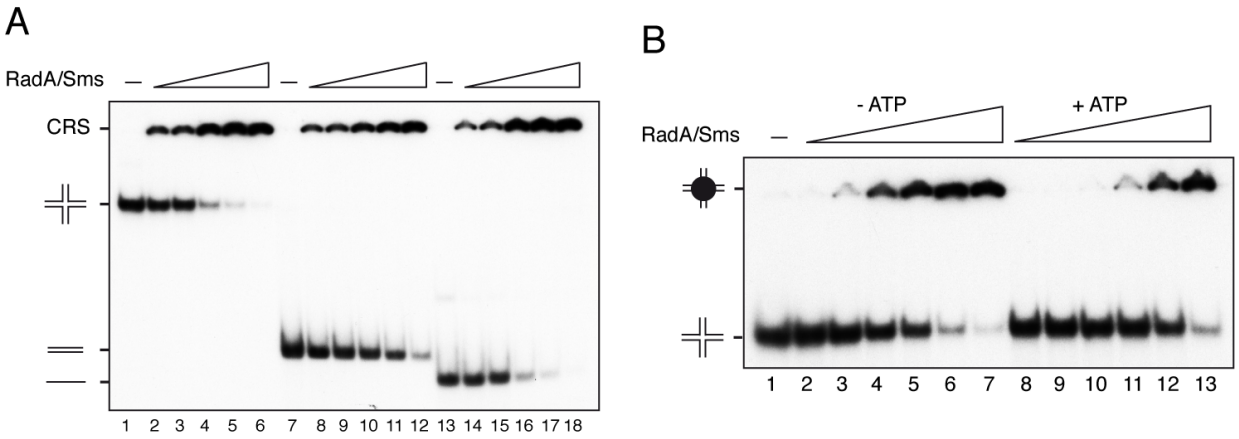

Figure 44. Purified RadA/Sms can bind DNA.
(A) EMSA to investigate the binding affinity of RadA/Sms to HJ (*lanes 1-6*), dsDNA (*lanes 7-12*) or ssDNA (*lanes 13-18*). The [γ-^{32}P]-labelled DNA (0.05 nM) was incubated with increasing concentrations of RadA/Sms (12.5, 25, 50, 100 and 200 nM) for 15 min at 37°C in buffer A containing 1 mM Mg^{+2}. CRS: complex formed by RadA/Sms-DNA. (B) HJ DNA binding affinity of RadA/Sms (6.25, 12.5, 25, 50, 100, 200 nM) in the presence (*lanes 2-7*) or absence of 1 mM ATP (*lanes 8-13*).

1.10.3. RadA/Sms bound to HJ DNA strongly inhibits DisA-mediated c-di-AMP synthesis

The binding of DisA to HJ DNA specifically inhibited its DAC activity [Figure 35 and (Witte et al, 2008)]. In *M. smegmatis*, it was suggested that RadA can also affect c-di-AMP synthesis *in vitro* (Zhang & He, 2013). To verify whether the presence of *B. subtilis* RadA/Sms could modulate the enzymatic activity of DisA, DAC assays were performed and analysed by TLC. Reactions were performed at 37°C in buffer A containing 100 µM ATP (containing 0.05 µM [α-^{32}P]-ATP) and 10 mM Mg^{+2}. The catalytic activity of DisA (50 nM) was only slightly affected by RadA/Sms addition (Figure 45, *lanes 5-7 vs. lane 2*). Surprisingly, c-di-AMP synthesis was strongly inhibited by concomitant addition of RadA/Sms and HJ DNA, reaching levels even lower than the obtained by HJ addition alone (Figure 45, *lanes 8 and 9 vs. lane 3*

and 4). These results support the idea that RadA/Sms negatively modulate DisA DAC activity, and this regulation being even more pronounced via binding to HJs.

There are few alternatives that could explain the mechanism of this regulation: (i) RadA/Sms improves the affinity of DisA for HJs; (ii) both proteins interact physically, which titrates DisA; (iii) RadA/Sms produces a conformational change in DisA. The simultaneous binding of DisA and RadA/Sms to HJ DNA could not be determined because both proteins form large complexes with the DNA, which are retained in the gel wells, providing no additional information. Moreover, increasing concentrations of RadA/Sms did not improve the affinity of DisA for HJs (data not shown). Cross-linking experiments did not provide new information because DisA forms octamers and RadA/Sms also seemed to form large complexes that did not enter the gel (data not shown).

Previously, by yeast two-hybrid assay it was shown that *B. subtilis* DisA interact with RadA/Sms (Zhang & He, 2013). Therefore, it is reasonable to suggest that RadA/Sms upon interaction with DisA bound to HJ DNA inhibits c-di-AMP synthesis. This hypothesis still needs to be further investigated.

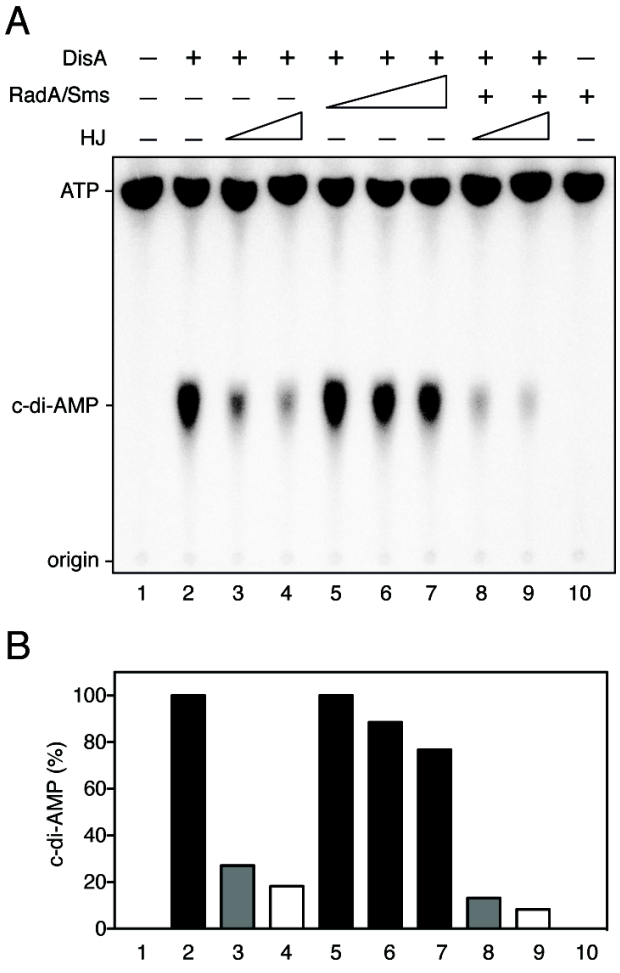

Figure 45. The DAC activity of DisA is strongly inhibited by RadA/Sms combined with HJs. (A) DisA (50 nM) was incubated with 100 μM ATP (containing 0.05 μM [α-^{32}P]-ATP) in buffer A containing 10 mM Mg^{+2} for 40 min at 37°C, in presence or absence of increasing concentrations of RadA/Sms (50, 100 and 200 nM, *lanes 5-7*; 200 nM, *lanes 8-10*) and/or HJ (125 and 250 nM, *lanes 3, 4, 8 and 9*). In *lane 10*, RadA/Sms only. The reaction products were separated by TLC and quantified using Quantity One. The quantification values of relative c-di-AMP amounts are shown in (B). The synthesis of c-di-AMP by 50 nM DisA in 40 min was considered as 100%.

Discussion

5. Discussion

1.11. Effect of the *disA* mutation in the DDR of exponentially growing *B. subtilis* cells

The viability assays performed with the Δ*disA* mutant provided evidence that DisA contributes especially to the response to DNA alkylation damage induced by MMS. Survival to other types of DNA damaging agents, such as H_2O_2, MMC and Nal, had no significant effect on Δ*disA*. This indicates that MMS causes a different spectrum of DNA damage and suggests that resistance to alkylation damage requires some activities that are distinct from those involved in H_2O_2, MMC and Nal resistance. MMS methylates purine bases causing replication fork stalling and needs to be actively repaired or bypassed to allow replication fork progression. There are two pathways responsible for removal of alkyl damage, BER and HR pathways. An alternative route is to reinitiate replication passing the lesion site and leaving a ssDNA gap that will be later repaired via SSG repair or template switching through recombination (Osborn et al, 2002). In the absence of these recombinational DNA repair systems, cells can ultimately activate TLS, a DDT pathway, to quickly restart replication and perhaps survive if the mutation is not lethal (Wit et al, 2015). Indeed, in *B. subtilis* the two dispensable Y-family DNA polymerases, PolY1 (YqjH) and PolY2 (YqjW) have been shown to be involved in lesion bypass (Duigou et al, 2004). The mutation frequencies of strains deficient in PolY1, PolY2 (which are homologous to E. coli PolIV [DinB] and PolV [UmuDC], respectively) or DisA were similar, or slightly lower (<2-fold), compared to the rates obtained with the wild type strain during exponentially growing cells (Million-Weaver et al, 2015; Walsh et al, 2014). In contrast, PolY1/PolY2-dependent-translesion synthesis operates in sporulating *B. subtilis* cells and contributes in processing spontaneous and artificially induced genetic damage, which is apparently required for an efficient sporulation process (Rivas-Castillo et al, 2010). Interestingly, spores lacking DisA have an increased mutation frequency compared to wt spores (Bejerano-Sagie et al, 2006; Campos et al, 2014). It is likely that in absence of homologous recombination, due to the absence of an undamaged template strand or chromosome, *B. subtilis* spore undergoes TLS in the Δ*disA* context with higher efficiency than during exponential growth.

In budding yeast, MMS strongly affects the rate of replication fork progression (Tercero & Diffley, 2001) and genes that responded specifically to MMS have been identified. These genes were related to the maintenance of replication fork stability or processivity during S-phase in *Saccharomyces cerevisiae* (Chang et al, 2002). Checkpoint proteins are required to maintain genome integrity in the presence of MMS. The processivity of replication forks through damaged-DNA is compromised in the absence of these checkpoints (Tercero & Diffley, 2001).

Therefore, with the information available and the results presented in this work, it is tempting to think that DisA could act as a replication fork protector in the presence of alkylating damage. Exposure to DNA damaging agents often result in differential gene expression (Fornace et al, 1988). To test whether exposure to MMS could modulate the levels of DisA expression, protein immunoblots were performed with whole cell extracts of cultures exposed to MMS treatment. In exponentially growing wt cells, the basal DisA protein level was estimated to be ~1.3 μM (~120 octamers per cell). After MMS treatment, no difference in DisA expression levels was observed. This is consistent with the lack of correlation found in *S. cerevisiae* of genes that are transcriptionally induced by MMS and those that are required for MMS resistance (Chang et al, 2002). It seems that a wide range of DDRs is independent of transcriptional regulation, the enzymes necessary for DNA repair being already at sufficient levels within the cell (Birrell et al, 2002). Moreover, similar levels of DisA expression were obtained throughout *B. subtilis* exponential growth (data not shown). Similar results were obtained with the DacA protein, which is a CdaA homologous and the only DAC enzyme of *S. aureus*. In this bacterium, constant DacA levels were detected during exponential growth, whereas a 3-fold increase in DacA expression levels was only observed as the cells entered stationary phase. This increase in DacA production correlated with an increase in c-di-AMP levels (Corrigan et al, 2015). An increase in c-di-AMP levels was also observed upon entry into sporulation (Oppenheimer-Shaanan et al, 2011), where an increase in DisA expression was detected (Bejerano-Sagie et al, 2006).

1.12. Variation in the intracellular levels of c-di-AMP modulates the DDR in exponentially growing cells

It is important to consider that the absence of DisA also implies a change in the intracellular c-di-AMP pool. Exponentially growing Δ*disA* cells showed a decrease of about 26% in c-di-AMP production compared to vegetative wt cells. A basal level of c-di-AMP is essential for the bacteria to survive and it seems that in the absence of DisA, the second vegetative DAC enzyme, CdaA, is responsible for maintaining the intracellular c-di-AMP pool. CdaA (formerly known as YbbP) is a membrane-bound protein involved in β-lactam antibiotics resistance in growing *B. subtilis* cells (Luo & Helmann, 2012a). In this work, it was found that CdaA participates in the response to oxidative damage, while the lack of DisA did not significantly impair survival to H_2O_2. The expression of high levels of c-di-AMP by overexpressing a hyperactive form of CdaS, however, was not sufficient to rescue resistance to H_2O_2 in Δ*cdaA*

cells. Therefore, it seems that the lack of CdaA *per se* or the lack of the c-di-AMP produced specifically by CdaA strongly affects the response to oxidative stress, perhaps because its absence imbalance membrane homeostasis. Alternatively, CdaA and DisA can form distinct c-di-AMP pools during vegetative growth, in a spatially ordered manner (DisA nearby the chromosome and CdaA close to the membrane). In this way, c-di-AMP molecules should be always close to its potential targets, affecting different pathways when produced at higher or lower amounts, or absent (Mehne et al, 2013).

Variation in the intracellular level of second messengers has been described in a variety of organisms to modulate different functions, including the DDR. In human cells, for example, cAMP promotes NER (Jarrett et al, 2014) and elevated levels of cAMP attenuate the DNA-damage induced accumulation of the tumor suppressor protein p53 (Safa et al, 2011). Cyclic dinucleotides also constitute an important group of signalling molecules, initially considered to be exclusive to bacteria species. Recently, it was found that c-di-GMP is also produced by dictyostelid social amoebas, although in this eukaryote c-di-GMP does not act as a second messenger, but is secreted to locally induce stalk cell differentiation (Chen & Schaap, 2012). Even more surprising was the recent discovery that human cells synthesize a hybrid cyclic dinucleotide (c-GMP-AMP or cGAMP) in response to the presence of cytosolic DNA (Sun et al, 2013; Wu et al, 2013). In bacteria, c-di-GMP, and the more recently described c-di-AMP, trigger a spectrum of pathways related to metabolism, virulence, biofilm formation, cell growth, morphogenesis, cell wall homeostasis, etc. (reviewed in Corrigan & Grundling, 2013). Interestingly, low c-di-GMP levels induce biofilm formation under DNA damage stress in *Pseudomonas aeruginosa* (Gotoh et al, 2008). In this bacterium, DNA damaging agents induce biofilm formation via the RecA-dependent SOS response (Gotoh et al, 2010). The involvement of c-di-AMP with DNA repair, however, has only been recently shown, with the discovery of DisA (Oppenheimer-Shaanan et al, 2011).

When DisA complexes pause at sites of DNA lesions, c-di-AMP synthesis ceases, leading to a temporary block in sporulation. External addition of c-di-AMP rescued sporulation progression, supporting the role of c-di-AMP in the DNA-damage checkpoint (Oppenheimer-Shaanan et al, 2011). However, the molecular targets of c-di-AMP, described to date, are all related to cellular metabolism, the exact c-di-AMP signalling cascade for DDR being still unknown.

As expected, the spore-specific DAC enzyme, CdaS, did not contribute to the DDR in vegetative cells. Surprisingly, however, the strain overexpressing GdpP phosphodiesterase

showed moderate sensitivity to MMS, in a similar extent to the phenotype observed with the strain lacking DisA. Both strains have comparable levels of c-di-AMP (~2.7 μM), which suggests an impaired response to alkylating DNA damage in cells that accumulate lower amounts of c-di-AMP. It was expected that cells lacking CdaA would be as sensitive or more sensitive to MMS as Δ*disA*, considering that CdaA is probably the major contributor to the intracellular c-di-AMP pool. Unexpectedly, however, Δ*cdaA* cells were as resistant to MMS as the wt strain. It seems that the c-di-AMP synthesized by CdaA forms a very specific pool that perhaps is not accessible to the entire cell, therefore not reaching the targets involved in the response to alkylation damage. Nevertheless, further experiments are needed to confirm this hypothesis. On the other hand, increased concentrations of c-di-AMP found in the Δ*gdpP* strain enhanced resistance to MMS. In a previous report, it was shown that spores lacking GdpP were more resistant to Nal than wt spores (Rao et al, 2009). Likewise, overexpression of hyperactive CdaS variants rescued to a certain extent resistance to MMS in vegetative cells lacking DAC enzymes. Therefore, it seems that higher c-di-AMP levels confer resistance to DNA insults.

To gain insights into the role played by DisA and/or c-di-AMP in the response to alkylation, a strain that contains a single amino acid substitution in the active site of DisA was used. This mutation in DisA prevents c-di-AMP synthesis, as suggested by an *in vitro* assay performed with the purified DisA D77N variant protein (Witte et al, 2008). Surprisingly, the *disA77* strain was as sensitive to MMS as the Δ*disA* strain. This result strongly supports the role of c-di-AMP produced by DisA in the response to MMS. It is important to notice, however, that a single amino acid substitution, that in this case abolished DisA DAC activity, could be enough to disturb, for example, the native protein folding. Therefore, further experiments need to be performed to exclude this hypothesis. In fact, the *disA77-gfp* strain was unable to form foci on the nucleoid (Oppenheimer-Shaanan et al, 2011), suggesting that this protein structurally differs from the native DisA protein. Furthermore, the external addition of c-di-AMP to Δ*disA* cells supplemented its defect in survival to MMS. This result strongly supports the role of c-di-AMP in the DDR to alkylation.

Interestingly, a cross-talk between c-di-AMP and (p)ppGpp, two signalling nucleotides, was proposed in *B. subtilis* by Rao et al (2009) and further characterized in *S. aureus* in a recent report (Corrigan et al, 2015). This provides additional evidence that variation in the levels of c-di-AMP modulate multiple pathways, as for instance the stringent response (Figure 46). Likewise, in this work, it is proposed that DisA and c-di-AMP act at the intersection between DDR and stress homeostasis in exponentially growing *B. subtilis* cells.

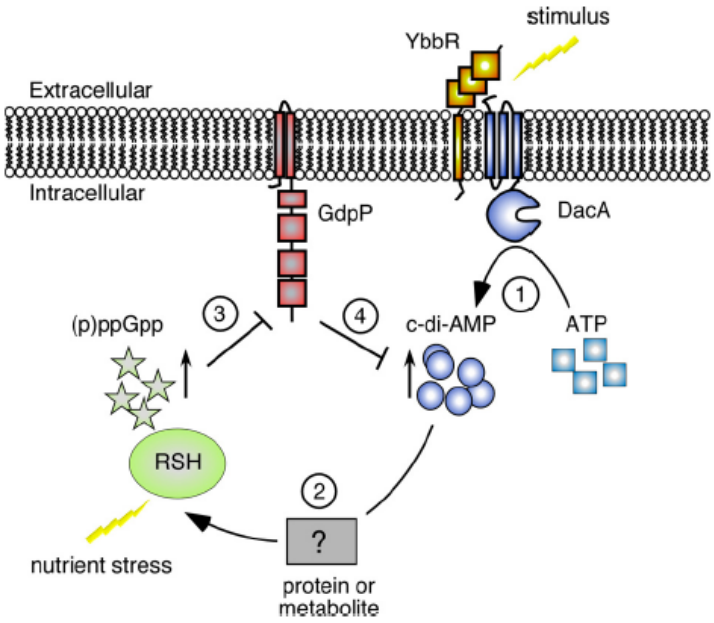

Figure 46. Cross-talk between c-di-AMP and (p)ppGpp in *S. aureus*.
An environmental signal is potentially recognized by sensor domains located in YbbR (also known as CdaR), which stimulate DacA activity to increase c-di-AMP synthesis. High c-di-AMP levels (*step 1*) leads to an increase in intracellular (p)ppGpp levels (*step 2*) and activation of a subset of stringent response genes. Under nutrient starvation the intracellular (p)ppGpp concentration increases, which inhibits the phosphodiesterase activity of GdpP (*step 3*), leading in turn to an increase in c-di-AMP levels (*step 4*). *Figure extracted from (Corrigan et al, 2015)*.

1.13. Could RadA/Sms and DisA work together?

The conservation of the *radA-disA* cluster in bacteria that possess DisA and their involvement in DNA repair individually, make it tempting to think that both proteins might act together. A connection between RadA/Sms and DisA has previously been suggested by Zhang & He (2013), who proposed that they interact both *in vitro* and *in vivo*. In this work it was demonstrated that *radA* and *disA* are epistatic, since deletion of the *radA-disA* cluster rendered cells as sensitive to MMS, MMC and Nal, as the most sensitive single mutant strain (Δ*radA*). The lack of RadA/Sms produced a strong decrease in viability to all DNA damaging agents tested in this work, unlike the lack of DisA, which only displayed a mild sensitivity in response to MMS. It must be remembered that the defect in DNA repair observed in the Δ*radA* strain could represent a sum of two events (lack of *radA* and lack of *disA*), as the promoter that controls the expression of *disA* is located within the *radA* gene. Interestingly, however, the Δ*radA* Δ*disA* double mutant displayed a distinct phenotype to Δ*radA* when submitted to H_2O_2 chronic assay. This result indicates two things: *(i)* that the Δ*radA* mutant is a genuine single mutant; and *(ii)* that in the absence of DisA, the Δ*radA* defect in repairing oxidative damage is somehow suppressed. One hypothesis can be formulated from the latter: if RadA/Sms has a role

in the stabilization of recombination intermediates, such as HJs, at its absence lethal intermediates would accumulate leading to unrepaired DSBs, which are induced by exposure to H_2O_2. However, if DisA is not present, an alternative route might take place, avoiding the accumulation of those intermediates.

RadA/Sms could not replace DisA's functions in DNA repair, since overexpressing RadA/Sms only partially suppressed the Δ*disA* defect to alkylation damage. The RadA/Sms overexpression fully recovered the Δ*radA* phenotype, however, giving additional support to the idea that Δ*radA* is a genuine single mutant. It seems that both proteins could act in the same pathway to modulate repair of alkylation damage, but it is also likely that RadA/Sms have additional roles in DNA repair, that are independent of DisA. This is consistent with observations in *E. coli*, *S. pneumoniae* and *R. etli*, where DisA is absent and RadA/Sms is involved in recombinational DNA repair, more specifically, related to late functions in recombination, such as HJ processing (Beam et al, 2002; Burghout et al, 2007; Castellanos & Romero, 2009; Chen et al, 2015; Cooper et al, 2015; Lovett, 2006; Martinezsalazar et al, 2009). In *B. subtilis*, where DisA is produced, the lack of RadA/Sms has a negative effect in chromosomal transformation (Carrasco et al, 2002; Krüger et al, 1997), suggesting a role for RadA/Sms in recombination in the presence of DisA too. It seems that the RadA/Sms protein has several DNA repair functions apparently related to recombination, but that are not necessarily DisA-dependent, while on the other hand, the functions exerted by DisA are potentially modulated by RadA/Sms.

The exact mechanism of action of RadA/Sms and DisA is still unknown, but it seems to occur at a later stage to the activation of the SOS response, since the absence of RadA/Sms had no effect in the DNA damage-dependent accumulation of RecA.

1.14. C-di-AMP synthesis is inhibited upon binding of DisA to stacked X-junctions

DisA binds different DNA substrates with less than 2-fold difference in affinity. The stability of DisA-HJ and DisA-dsDNA complexes were both long-living at different metal ions concentrations. However, the current model of DisA's role as a DNA-damage checkpoint protein came from *in vitro* experiments showing that a decrease in c-di-AMP production is observed when DisA is incubated with branched DNA, such as HJs (Witte et al, 2008). Experiments performed in this work with a newly purified DisA confirmed these results. Furthermore, in this work it was demonstrated that modulation of DisA's DAC activity occurs

exclusively when DisA binds a highly folded X-junction (10 mM Mg^{2+}), while binding to a more unstable stacked HJ (1 mM Mg^{2+}) did not produce an effect. This could be attributed to a better affinity of DisA to a more folded junction, but this possibility had been discarded since DisA bound both HJs with similar affinities. Binding to open form HJs (absence of Mg^{2+}), however, was slightly worse, suggesting that DisA recognizes stacked X-structures *in vivo*.

This was quite unexpected, since unfolded HJs are believed to be the real recombination intermediate. However, there are also a large number of proteins that show high affinity for the stacked X-structure (Khuu et al, 2006). Enzymes that recognize stacked X-junctions are mostly dimeric, while proteins that bind to the open form HJ are quite often tetrameric. HJ resolvases, for example, are dimeric proteins that recognize the stacked X-structure initially, but then distort it to adopt an unfolded open form (Fogg et al, 2001). The RuvAB translocase complex also induces a square-planar structure in the DNA junction, this conformation being more accessible for branch migration and cleavage (Parsons et al, 1995). It is attractive to think that the inhibitory effect produced by DisA over RuvAB and RecG helicase, and RecU resolution activities, could be explained by this mechanism. If DisA is binding to the stacked X-junction and preventing it from opening into a square-planar structure, branch migration and resolution of the 4-way junction would be inhibited.

1.15. DisA modulates recombinational DNA repair

The correlation of DisA with recombinational functions arose from three premises: *(i)* in the current model of DisA's role as a DNA-damage checkpoint protein (See Figure 7), binding to branched recombination intermediates specifically leads to an allosteric inhibition of DisA c-di-AMP synthesis activity (Witte et al, 2008), *(ii)* the expression of *disA* is regulated by the extracytoplasmic function sigma factor σ^M, which is the same transcription factor that controls the expression of the HJ resolvase protein RecU, essential in late steps of recombination (Eiamphungporn & Helmann, 2008); and *(iii)* in the Δ*recU* context, *i.e.* in the presence of branched recombination intermediates, DisA-YFP or RadA/Sms-YFP lost their dynamicity.

During recombinational repair, branched DNA intermediates are produced, such as HJs, which are very toxic if not processed back into duplex DNA. Therefore, the absence of both recombination translocases, RecG and RuvAB, is synthetically lethal in *B. subtilis* and *Neisseria gonorrhoeae*, although a different mechanism may occur in other species, since disrupting *recG* has only a mild effect in *E. coli* and a synergistic effect with *ruvAB*, while in *Helicobacter pylori* does not impair viability at all (reviewed in Ayora et al, 2011). The

construction of *B. subtilis* strains lacking each of the main HJ processing enzymes (RecG, RuvAB and RecU) individually and in combination with the *disA* mutation gave new insights into the role of DisA in recombination. In summary, *disA* is epistatic with *recG* and *recU*, and a synergistic phenotype was observed with *ruvAB,* in the presence of a DNA damaging agent that generates stalled replication forks. Interestingly, the same outcome was observed when the *radA* mutation was moved into these mutant strains instead of *disA*. These results provide more indications that DisA and RadA/Sms could be working in the same recombination pathway as RecG and RecU. In *E. coli*, the absence of both RadA/Sms and RecG produced a strong synergistic phenotype in the presence of DNA damaging agents that generate collapsed replication forks or DSBs, which proposed that lethal recombination intermediates accumulates in this double mutant (Cooper et al, 2015). It is likely that *B. subtilis* RadA/Sms has two activities: to protect recombination intermediates accumulated in the presence of stalled forks in the $radA^+$ and $disA^+$ context and to stabilize recombination intermediates generated in the presence of collapsed forks in the $radA^+$ context; whereas *E. coli* RadA/Sms only has the last activity.

DisA strongly inhibited the HJ-dependent helicase activity of RecG and RuvAB, as well as the HJ resolution activity of RecU. Different hypothesis could be formulated to explain the mechanism behind this effect. Does DisA prevent RecG, RuvAB and RecU from binding to the HJ DNA and from distorting it to a square-planar conformer that allows them to perform its activities? This is quite unexpected since the apparent binding constant to HJ of RecU, RuvAB and RecG is much lower than DisA's. Indeed, EMSA and DNaseI footprinting assays showed that RuvAB, RecG or RecU could still bind HJ in the presence of DisA, even when DisA was first pre-incubated with the DNA. Furthermore, it seems that DisA is not removed from the HJ as the other proteins bind, indicating that the inhibitory effect on HJ processing functions is not due to a substrate competition. Other hypotheses are that: DisA induces a protein or substrate conformational change; DisA displaces the protein from its target sites or DisA acts as a barrier for translocation and resolution. Further experiments need to be performed to test these hypotheses. A similar inhibitory mechanism was observed with the TRF2 human protein over WRN helicase activity (Nora et al, 2010). TRF2 seems to "lock down" the HJ into a stacked conformation that is unfavourable for WRN to branch migrate. The presence of RadA/Sms also produced a strong inhibitory effect on RecG helicase activity (data not shown). These results suggest that DisA and RadA/Sms could play a role in modulating recombinational DNA repair.

In exponentially growing cells, DisA also constituted a dynamic protein, but in contrast to sporulation in which DisA moves as single foci, vegetative DisA formed diverse foci that mostly co-localized with the nucleoid. The difference between single and multiple foci formation observed previously and now could be due simply to a higher image resolution obtained nowadays. However, more experiments should be performed to confirm this hypothesis.

To study whether DisA is involved in DSB recognition during vegetative growth, as proposed to occurring in sporulation, the strain expressing DisA-YFP protein from its native promoter was used and DSBs were induced using Nal and MMC. Neither of these drugs induced DisA-YFP foci to cease its dynamic movement. Then, the DisA-YFP fusion was moved into the Δ*recN* background, in order to study whether the lack of one of the first DSB responders impaired DisA-YFP foci formation and/or dynamic behaviour. The lack of RecN in combination or not with DSB induction, did not affect DisA-YFP foci dynamics, which maintained about the same velocity in the different conditions. An interesting observation is that the DisA-YFP foci velocities presented a huge deviation, ranging from 0.2 to 1.4 μm/s. This is consistent with a highly dynamic protein that moves randomly throughout the cell. Surprisingly, the DisA movement did not cease significantly in the presence of DNA damaging agents. The presence of an accumulation of branched intermediates, however, clearly stalled DisA's movement forming static patched structures. This result corroborates the *in vitro* assays that indicate that DisA recognizes HJ DNA, indicating that *in vivo* this may occur. A similar panorama was observed using RadA/Sms-YFP, although in a slightly lower frequency. Again, this suggests that both proteins could be working together. Co-localization experiments will be performed to further confirm if RadA/Sms and DisA could act over the same substrates.

The RecA protein, among other functions, is essential to promote HR. During DNA replication, ssDNA gaps can be originated when the replication fork encounters a blockage (alkylation damage, for example). These naked ssDNA regions are rapidly recognized by RecA, which induces LexA cleavage leading to the activation of the SOS response. With the help of specific modulators, RecA is loaded onto ssDNA, and promotes homology search and strand invasion of the sister chromosome in order to repair the damaged site and restore replication. Interestingly, DisA strongly inhibited DNA strand exchange reactions mediated by RecA. Moreover, in this work it was demonstrated that the effect produce by DisA was not due to an inhibition of RecA's nucleation or filamentation onto ssDNA. It is likely that DisA inhibits RecA's activity via binding to the branched D-loop structure formed during strand invasion,

preventing the formation of the final recombined product. Therefore, it seems that DisA modulates recombinational DNA repair by blocking HJ processing functions and DNA strand exchange reactions. A model was constructed to summarize the role played by DisA and c-di-AMP in the DDR of exponentially growing *B. subtilis* cells (Figure 47).

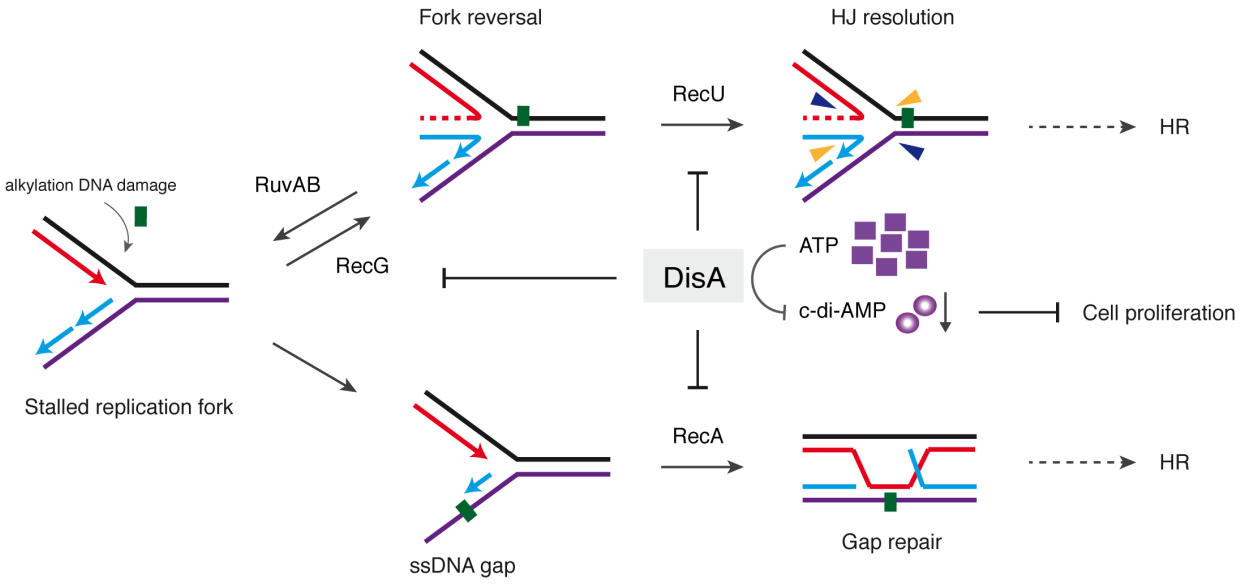

Figure 47. Model of the role of DisA and c-di-AMP in the DDR of vegetative *B. subtilis* cells. Alkylation DNA damage can stall replication fork progression that can be rescued via different pathways. If the damage is blocking the leading strand synthesis, RecG can promote fork reversal generating a HJ that is specifically recognized and cleavaged by RecU, and replication is finally reinitiated following HR. Alternatively, RuvAB induces fork regressing and unwinding to restart replication. If the lesion is disrupting the lagging strand synthesis, ssDNA gaps are generated which can be recognized by RecA that promotes homologous DNA pairing and strand exchange reactions. The gap repair system will finally restore the lesion site via recombination. DisA modulates the DDR by inhibiting recombinational activities promoted by RecU, RecG, RuvAB and RecA, and by decreasing the intracellular c-di-AMP pool.

In exponentially growing cells, a different role could be played by DisA. With the results obtained during this work, it is postulated that DisA acts as a DNA repair modulator and perhaps a replication fork protector. DisA seems to redirect the DDR towards the specific BER pathway or to a DDT pathway, avoiding a more complex, risky and time-consuming recombinational DNA repair. C-di-AMP also seems to contribute to this mechanism. As DisA binds stacked branched DNA structures, the levels of c-di-AMP decrease, guaranteeing cell proliferation. Furthermore, the results obtained in this work suggest that *B. subtilis* RadA/Sms could be working in partnership with DisA to modulate the DDR of dividing cells.

For the first time it was demonstrated that the RadA/Sms protein can bind DNA and with slightly more affinity for HJ and ssDNA rather than for dsDNA. Some ATPase activity was

also intuited from the purified RadA/Sms protein, which is consistent with its walker motifs. Perhaps the most interesting results came from the DAC assays, which showed that RadA/Sms bound to HJ DNA strongly inhibited DisA c-di-AMP synthesis. This data provides more evidence that RadA/Sms and DisA are not just casually expressed by neighbour genes, but seem to interact functionally. Additional *in vitro* experiments are needed to better characterize the quite unknown RadA/Sms protein and to further investigate the hypothesis presented in this work.

Conclusions

6. Conclusions

I. DisA participates in the DDR of exponentially growing *B. subtilis* cells, especially in the response to DNA alkylation damage induced by MMS. Other DNA damaging agents, such as H_2O_2, MMC and Nal, which produce DSBs, had no significant effect on Δ*disA*. Whereas the membrane protein CdaA, which is the second *B. subtilis* vegetative DAC enzyme, contributes to elicit repair of oxidative damage generated by H_2O_2.

II. Cells lacking both *disA* and *radA* are as sensitive to MMS as the most sensitive single parent (epistasis). Both genes have also an epistatic relationship with RecU and RecG, while a synergistic phenotype is observed in combination with RuvAB.

III. DisA contributes to the intracellular c-di-AMP pool of *B. subtilis* during vegetative growth, which varies in a narrow range between ~2.7 and ~4.3 μM. The DisA protein levels are constant during vegetative growth and are estimated to be ~1.3 μM (about 120 octamers per cell).

IV. Variation in the intracellular levels of c-di-AMP modulates the DDR to alkylation. Decreased levels impair cell proliferation while increased levels improve resistance to MMS.

V. DisA-YFP forms multiple foci in exponentially growing *B. subtilis* cells, which are highly dynamic and co-localize with the nucleoid, even in the absence of DNA damaging agents or in the absence of RecN. In the presence of branched recombination intermediates, however, several DisA-YFP foci abolished their movement, generating static patched regions. RadA-YFP also formed dynamic foci, but that not necessarily co-localized with the nucleoid.

VI. Purified DisA shows concentration-dependent DAC activity with preference for ATP over dATP to produce c-di-AMP, where pppApA is an intermediate product of this reaction.

VII. DisA shows little preference for binding among different DNA structures, although higher affinity is found for branched DNA, such as HJs, forks and D-loops. No sequence-specificity is required for DisA-HJ complex formation. Highly stacked HJs specifically reduce DisA c-di-AMP synthesis. RadA/Sms-bound to stacked HJs strongly inhibits DisA DAC activity.

VIII. RadA/Sms is a DNA binding protein with slightly preference for ssDNA and HJ rather than dsDNA.

IX. DisA modulates recombination, by directly inhibiting HJ processing functions, such as RuvAB and RecG helicase activities, or RecU HJ-dependent endonuclease activity, as wells as preventing RecA-mediated strand exchange reactions. While DisA reduces recombinatonal DNA repair, alternative pathways are favoured to repair or tolerate DNA alkylation damages, such as BER and TLS, respectively.

X. RadA/Sms seems to works in concert with DisA to rescue stalled replication forks during *B. subtilis* exponential growth. Although, RadA/Sms might have additional functions, since cells deficient in *radA* are sensitive to several DNA damaging agents, including those that produce only DSBs.

Resumen en Castellano

7. Resumen en Castellano

1.16. Introducción

Las células están constantemente sometidas a daños en el ADN que pueden dar lugar a horquillas de replicación paradas o colapsadas. Existe una gran variedad de rutas de reparación que responden a diferentes tipos de daños endógenos y exógenos en el ADN. Para coordinar estos procesos existe una regulación compleja llamada, en conjunto, respuesta a daños en el ADN (DDR). Se ha descrito DisA inicialmente como una proteína de control de daños que garantiza la integridad genómica de las esporas de *B. subtilis*. Sin embargo, se detectaron niveles basales de DisA en extractos de células vegetativas y se observaron focos altamente dinámicos en células vegetativas que expresan DisA-YFP bajo su promotor nativo. Puesto que DisA también está presente en algunas bacterias que no esporulan, se ha propuesto un papel más general para DisA que no se limita a esporulación.

El objetivo general de este trabajo fue estudiar el papel de DisA en la respuesta a daños en el ADN de células de *B. subtilis* en crecimiento exponencial. Los objetivos específicos propuestos fueron:

I. Caracterizar genéticamente la contribución de DisA, RadA/Sms y variaciones en los niveles de c-di-AMP en la respuesta a daños en el ADN de *B. subtilis* en crecimiento vegetativo;
II. Investigar la participación de DisA en las funciones de recombinación homóloga;
III. Estudiar *in vivo* la localización y dinámica de DisA-YFP y RadA/Sms-YFP en células vegetativas con o sin inducción de daño en el ADN;
IV. Caracterizar bioquímicamente la proteína DisA y estudiar su participación en el procesamiento de HJs y en las reacciones de intercambio de cadenas;
V. Estudiar el papel de RadA/Sms junto con DisA.

1.17. Conclusiones

1. DisA participa en la respuesta a daños en el ADN en células de *B. subtilis* en crecimiento exponencial, particularmente en la respuesta a daños inducidos por agentes alquilantes como MMS. Otros agentes que dañan el ADN, como H_2O_2, MMC y Nal, que generan DSBs, no producen efectos significativos en Δ*disA*. Por otro lado, la proteína de membrana CdaA, que es la segunda enzima DAC vegetativa de *B. subtilis*, contribuye a la reparación de daños oxidativos causados por H_2O_2.

2. Las células que carecen de *disA* y *radA* son tan sensibles a MMS como la cepa parental más sensible (epistasis). Ambos genes también tienen efecto epistático con *recU* y *recG*, mientras que un fenotipo sinérgico se observa en combinación con *ruvAB*.

3. DisA contribuye al 'pool' intracelular de c-di-AMP de *B. subtilis* en fase de crecimiento vegetativo, el cual apenas varia entre ~2.7 y ~4.3 μM. Los niveles de la proteína DisA son constantes durante la fase vegetativa y estimados en ~1.3 μM (aprox. 120 octámeros por célula).

4. La variación de los niveles intracelulares de c-di-AMP modula la respuesta a daños en el ADN producidos por agentes alquilantes. La disminución de los niveles de c-di-AMP limita el crecimiento celular mientras que el aumento de estos niveles mejora la resistencia a MMS.

5. DisA-YFP genera múltiples focos en células de *B. subtilis* en crecimiento exponencial, los cuales son muy dinámicos y co-localizan con el nucleoide, incluso en ausencia de agentes que dañan el ADN o en ausencia de RecN. Sin embargo, en presencia de intermedios de recombinación ramificados, muchos focos de DisA-YFP dejan de moverse, generando regiones de focos estáticos. RadA-YFP también genera focos dinámicos, pero que no siempre co-localizan con el nucleoide.

6. La proteína DisA purificada presenta actividad DAC con preferencia por ATP sobre dATP para producir c-di-AMP. pppApA es un producto intermedio de esta reacción.

7. DisA se une con poca preferencia a diferentes estructuras de ADN, aunque presenta mayor afinidad por ADN ramificados, como HJs, horquillas y D-loops. Para la formación del complejo DisA-HJ no se requiere una secuencia específica. La conformación apilada de las HJs reduce específicamente la síntesis de c-di-AMP mediada por DisA. RadA/Sms unida a estas HJs inhibe fuertemente la actividad DAC de DisA.

8. RadA/Sms es una proteína de unión a ADN con ligera preferencia por ssDNA y HJ comparado a dsDNA.

9. DisA modula la recombinación inhibiendo directamente las funciones de procesamiento de HJs, como la actividad helicasa de RuvAB y RecG, o la actividad endonucleasa dependiente de HJ de RecU, así como impidiendo las reacciones de intercambio de cadenas mediadas por RecA. Mientras DisA reduce la reparación del ADN por recombinación, se favorecen vías alternativas de reparación o vías para tolerar los daños de alquilaciones en el ADN, como BER y TLS, respectivamente.

10. Es probable que RadA/Sms actúe en conjunto con DisA para rescatar horquillas de replicación paradas durante el crecimiento vegetativo de *B. subtilis.* Sin embargo, RadA/Sms puede desempeñar otras funciones, ya que células deficientes en *radA* son sensibles a varios agentes que dañan el ADN, incluyendo aquellos que producen sólo DSBs.

References

8. References

Alonso JC, Cardenas PP, Sanchez H, Hejna J, Suzuki Y, Takeyasu K (2013) Early steps of double-strand break repair in Bacillus subtilis. *DNA Repair (Amst)* **12:** 162-176

Atkinson J, McGlynn P (2009) Replication fork reversal and the maintenance of genome stability. *Nucleic Acids Res* **37:** 3475-3492

Au N, Kuester-Schoeck E, Mandava V, Bothwell LE, Canny SP, Chachu K, Colavito SA, Fuller SN, Groban ES, Hensley LA, O'Brien TC, Shah A, Tierney JT, Tomm LL, O'Gara TM, Goranov AI, Grossman AD, Lovett CM (2005) Genetic composition of the Bacillus subtilis SOS system. *J Bacteriol* **187:** 7655-7666

Ayora S, Carrasco B, Cardenas PP, Cesar CE, Canas C, Yadav T, Marchisone C, Alonso JC (2011) Double-strand break repair in bacteria: a view from Bacillus subtilis. *FEMS Microbiol Rev*

Ayora S, Carrasco B, Doncel-Perez E, Lurz R, Alonso JC (2004) Bacillus subtilis RecU protein cleaves Holliday junctions and anneals single-stranded DNA. *Proc Natl Acad Sci U S A* **101:** 452-457

Bai Y, Yang J, Zarrella TM, Zhang Y, Metzger DW, Bai G (2014) Cyclic di-AMP impairs potassium uptake mediated by a cyclic di-AMP binding protein in Streptococcus pneumoniae. *J Bacteriol* **196:** 614-623

Bai Y, Yang J, Zhou X, Ding X, Eisele LE, Bai G (2012) Mycobacterium tuberculosis Rv3586 (DacA) is a diadenylate cyclase that converts ATP or ADP into c-di-AMP. *PLoS One* **7:** e35206

Barker JR, Koestler BJ, Carpenter VK, Burdette DL, Waters CM, Vance RE, Valdivia RH (2013) STING-dependent recognition of cyclic di-AMP mediates type I interferon responses during Chlamydia trachomatis infection. *MBio* **4:** e00018-00013

Barzilai A, Yamamoto K (2004) DNA damage responses to oxidative stress. *DNA Repair (Amst)* **3:** 1109-1115

Beam CE, Saveson CJ, Lovett ST (2002) Role for radA/sms in Recombination Intermediate Processing in Escherichia coli. *Journal of Bacteriology* **184:** 6836-6844

Bejerano-Sagie M, Oppenheimer-Shaanan Y, Berlatzky I, Rouvinski A, Meyerovich M, Ben-Yehuda S (2006) A Checkpoint Protein That Scans the Chromosome for Damage at the Start of Sporulation in Bacillus subtilis. *Cell* **125:** 679-690

Belikov S, Wieslander L (1995) Express protocol for generating G+A sequencing ladders. *Nucleic Acids Research* **23:** 310

Ben-Yehuda S (2002) RacA, a Bacterial Protein That Anchors Chromosomes to the Cell Poles. *Science* **299:** 532-536

Beranek DT (1990) Distribution of methyl and ethyl adducts following alkylation with monofunctional alkylating agents. *Mutat Res* **231:** 11-30

Bianco PR (2015) I came to a fork in the DNA and there was RecG. *Progress in biophysics and molecular biology*

Birrell GW, Brown JA, Wu HI, Giaever G, Chu AM, Davis RW, Brown JM (2002) Transcriptional response of Saccharomyces cerevisiae to DNA-damaging agents does not identify the genes that protect against these agents. *Proc Natl Acad Sci U S A* **99:** 8778-8783

Bott KF, Wilson GA (1968) Metabolic and nutritional factors influencing the development of competence for transfection of Bacillus subtilis. *Bacteriol Rev* **32:** 370-378

Bradley AS, Baharoglu Z, Niewiarowski A, Michel B, Tsaneva IR (2011) Formation of a stable RuvA protein double tetramer is required for efficient branch migration in vitro and for replication fork reversal in vivo. *J Biol Chem* **286:** 22372-22383

Burghout P, Bootsma HJ, Kloosterman TG, Bijlsma JJ, de Jongh CE, Kuipers OP, Hermans PW (2007) Search for genes essential for pneumococcal transformation: the RADA DNA repair protein plays a role in genomic recombination of donor DNA. *J Bacteriol* **189:** 6540-6550

Burhenne H, Kaever V (2013) Quantification of cyclic dinucleotides by reversed-phase LC-MS/MS. *Methods Mol Biol* **1016:** 27-37

Campeotto I, Zhang Y, Mladenov MG, Freemont PS, Grundling A (2015) Complex Structure and Biochemical Characterization of the Staphylococcus aureus Cyclic Diadenylate Monophosphate (c-di-AMP)-binding Protein PstA, the Founding Member of a New Signal Transduction Protein Family. *J Biol Chem* **290:** 2888-2901

Campos SS, Ibarra-Rodriguez JR, Barajas-Ornelas RC, Ramirez-Guadiana FH, Obregon-Herrera A, Setlow P, Pedraza-Reyes M (2014) Interaction of apurinic/apyrimidinic endonucleases Nfo and ExoA with the DNA integrity scanning protein DisA in the processing of oxidative DNA damage during Bacillus subtilis spore outgrowth. *J Bacteriol* **196:** 568-578

Canas C, Suzuki Y, Marchisone C, Carrasco B, Freire-Beneitez V, Takeyasu K, Alonso JC, Ayora S (2014) Interaction of branch migration translocases with the Holliday junction-resolving enzyme and their implications in Holliday junction resolution. *J Biol Chem* **289:** 17634-17646

Cardenas PP, Carrasco B, Defeu Soufo C, Cesar CE, Herr K, Kaufenstein M, Graumann PL, Alonso JC (2012) RecX facilitates homologous recombination by modulating RecA activities. *PLoS Genet* **8:** e1003126

Cardenas PP, Carrasco B, Sanchez H, Deikus G, Bechhofer DH, Alonso JC (2009) Bacillus subtilis polynucleotide phosphorylase 3'-to-5' DNase activity is involved in DNA repair. *Nucleic Acids Research* **37:** 4157-4169

Cardenas PP, Carzaniga T, Zangrossi S, Briani F, Garcia-Tirado E, Deho G, Alonso JC (2011) Polynucleotide phosphorylase exonuclease and polymerase activities on single-stranded DNA ends are modulated by RecN, SsbA and RecA proteins. *Nucleic Acids Res* **39:** 9250-9261

Cardenas PP, Gandara C, Alonso JC (2014) DNA double strand break end-processing and RecA induce RecN expression levels in Bacillus subtilis. *DNA Repair (Amst)* **14:** 1-8

Carrasco B, Cozar MC, Lurz R, Alonso JC, Ayora S (2004) Genetic recombination in Bacillus subtilis 168: contribution of Holliday junction processing functions in chromosome segregation. *Journal of Bacteriology* **186:** 5557-5566

Carrasco B, Fernandez S, Asai K, Ogasawara N, Alonso JC (2002) Effect of the recU suppressors sms and subA on DNA repair and homologous recombination in Bacillus subtilis. *Mol Genet Genomics* **266:** 899-906

Carrasco B, Manfredi C, Ayora S, Alonso JC (2008) Bacillus subtilis SsbA and dATP regulate RecA nucleation onto single-stranded DNA. *DNA Repair (Amst)* **7:** 990-996

Castellanos M, Romero D (2009) The extent of migration of the Holliday junction is a crucial factor for gene conversion in Rhizobium etli. *J Bacteriol* **191:** 4987-4995

Ceglowski P, Luder G, Alonso JC (1990) Genetic analysis of *recE* activities in *Bacillus subtilis*. *Mol Gen Genet* **222:** 441-445

Chang M, Bellaoui M, Boone C, Brown GW (2002) A genome-wide screen for methyl methanesulfonate-sensitive mutants reveals genes required for S phase progression in the presence of DNA damage. *Proc Natl Acad Sci U S A* **99:** 16934-16939

Chen SH, Byrne RT, Wood EA, Cox MM (2015) Escherichia coli radD (yejH) gene: a novel function involved in radiation resistance and double-strand break repair. *Mol Microbiol* **95:** 754-768

Chen ZH, Schaap P (2012) The prokaryote messenger c-di-GMP triggers stalk cell differentiation in Dictyostelium. *Nature* **488:** 680-683

Choi PH, Sureka K, Woodward JJ, Tong L (2015) Molecular basis for the recognition of cyclic-di-AMP by PstA, a P -like signal transduction protein. *MicrobiologyOpen*

Cleaver JE (1969) Xeroderma pigmentosum: a human disease in which an initial stage of DNA repair is defective. *Proc Natl Acad Sci U S A* **63:** 428-435

Cooper DL, Boyle DC, Lovett ST (2015) Genetic analysis of Escherichia coli RadA: functional motifs and genetic interactions. *Mol Microbiol* **95:** 769-779

Corrigan RM, Abbott JC, Burhenne H, Kaever V, Grundling A (2011) c-di-AMP is a new second messenger in Staphylococcus aureus with a role in controlling cell size and envelope stress. *PLoS Pathog* **7:** e1002217

Corrigan RM, Bowman L, Willis AR, Kaever V, Grundling A (2015) Cross-talk between Two Nucleotide-signaling Pathways in Staphylococcus aureus. *J Biol Chem* **290:** 5826-5839

Corrigan RM, Campeotto I, Jeganathan T, Roelofs KG, Lee VT, Grundling A (2013) Systematic identification of conserved bacterial c-di-AMP receptor proteins. *Proc Natl Acad Sci U S A* **110:** 9084-9089

Corrigan RM, Grundling A (2013) Cyclic di-AMP: another second messenger enters the fray. *Nature reviews Microbiology* **11:** 513-524

Cox MM (2007) Motoring along with the bacterial RecA protein. *Nature reviews Molecular cell biology* **8:** 127-138

Cox MM, Goodman MF, Kreuzer KN, Sherratt DJ, Sandler SJ, Marians KJ (2000) The importance of repairing stalled replication forks. *Nature* **404:** 37-41

Crumplin GC, Smith JT (1976) Nalidixic acid and bacterial chromosome replication. *Nature* **260:** 643-645

De Silva IU, McHugh PJ, Clingen PH, Hartley JA (2000) Defining the roles of nucleotide excision repair and recombination in the repair of DNA interstrand cross-links in mammalian cells. *Mol Cell Biol* **20:** 7980-7990

Dey B, Dey RJ, Cheung LS, Pokkali S, Guo H, Lee JH, Bishai WR (2015) A bacterial cyclic dinucleotide activates the cytosolic surveillance pathway and mediates innate resistance to tuberculosis. *Nature medicine*

Diver WP, Sargentini NJ, Smith KC (1982) A mutation (radA100) in Escherichia coli that selectively sensitizes cells grown in rich medium to x- or u.v.-radiation, or methyl methanesulphonate. *International journal of radiation biology and related studies in physics, chemistry, and medicine* **42:** 339-346

Duckett DR, Murchie AI, Bhattacharyya A, Clegg RM, Diekmann S, von Kitzing E, Lilley DM (1993) The structure of DNA junctions and their interaction with enzymes. *European journal of biochemistry / FEBS* **211:** 285-295

Duckett DR, Murchie AI, Diekmann S, von Kitzing E, Kemper B, Lilley DM (1988) The structure of the Holliday junction, and its resolution. *Cell* **55:** 79-89

Duckett DR, Murchie AI, Lilley DM (1990) The role of metal ions in the conformation of the four-way DNA junction. *EMBO J* **9:** 583-590

Duigou S, Ehrlich SD, Noirot P, Noirot-Gros MF (2004) Distinctive genetic features exhibited by the Y-family DNA polymerases in Bacillus subtilis. *Mol Microbiol* **54:** 439-451

Eiamphungporn W, Helmann JD (2008) The Bacillus subtilis σM regulon and its contribution to cell envelope stress responses. *Molecular Microbiology* **67:** 830-848

Elsholz AK, Hempel K, Michalik S, Gronau K, Becher D, Hecker M, Gerth U (2011) Activity control of the ClpC adaptor McsB in Bacillus subtilis. *J Bacteriol* **193:** 3887-3893

Elsholz AK, Michalik S, Zuhlke D, Hecker M, Gerth U (2010) CtsR, the Gram-positive master regulator of protein quality control, feels the heat. *EMBO J* **29:** 3621-3629

Elsholz AK, Turgay K, Michalik S, Hessling B, Gronau K, Oertel D, Mader U, Bernhardt J, Becher D, Hecker M, Gerth U (2012) Global impact of protein arginine phosphorylation on the physiology of Bacillus subtilis. *Proc Natl Acad Sci U S A* **109:** 7451-7456

Fogg JM, Kvaratskhelia M, White MF, Lilley DM (2001) Distortion of DNA junctions imposed by the binding of resolving enzymes: a fluorescence study. *J Mol Biol* **313:** 751-764

Fornace AJ, Jr., Alamo I, Jr., Hollander MC (1988) DNA damage-inducible transcripts in mammalian cells. *Proc Natl Acad Sci U S A* **85:** 8800-8804

Fried MG, Liu G (1994) Molecular sequestration stabilizes CAP-DNA complexes during polyacrylamide gel electrophoresis. *Nucleic Acids Res* **22:** 5054-5059

Friedberg EC, Lehmann AR, Fuchs RP (2005a) Trading places: how do DNA polymerases switch during translesion DNA synthesis? *Mol Cell* **18:** 499-505

Friedberg EC, Walker GC, Siede W, Wood RD (2005b) *DNA repair and mutagenesis*, Washington DC: American Society for Microbiology Press.

Fuhrmann J, Schmidt A, Spiess S, Lehner A, Turgay K, Mechtler K, Charpentier E, Clausen T (2009) McsB is a protein arginine kinase that phosphorylates and inhibits the heat-shock regulator CtsR. *Science* **324:** 1323-1327

Galas DJ, Schmitz A (1978) DNAse footprinting: a simple method for the detection of protein-DNA binding specificity. *Nucleic Acids Res* **5:** 3157-3170

Galletto R, Kowalczykowski SC (2007) RecA. *Current biology : CB* **17:** R395-397

Giri N, Bhowmik P, Bhattacharya B, Mitra M, Das Gupta SK (2009) The mycobacteriophage D29 gene 65 encodes an early-expressed protein that functions as a structure-specific nuclease. *J Bacteriol* **191:** 959-967

Goranov AI, Kuester-Schoeck E, Wang JD, Grossman AD (2006) Characterization of the global transcriptional responses to different types of DNA damage and disruption of replication in Bacillus subtilis. *J Bacteriol* **188:** 5595-5605

Gotoh H, Kasaraneni N, Devineni N, Dallo SF, Weitao T (2010) SOS involvement in stress-inducible biofilm formation. *Biofouling* **26:** 603-611

Gotoh H, Zhang Y, Dallo SF, Hong S, Kasaraneni N, Weitao T (2008) Pseudomonas aeruginosa, under DNA replication inhibition, tends to form biofilms via Arr. *Res Microbiol* **159:** 294-302

Gundlach J, Dickmanns A, Schroder-Tittmann K, Neumann P, Kaesler J, Kampf J, Herzberg C, Hammer E, Schwede F, Kaever V, Tittmann K, Stulke J, Ficner R (2015) Identification, Characterization, and Structure Analysis of the Cyclic di-AMP-binding PII-like Signal Transduction Protein DarA. *J Biol Chem* **290:** 3069-3080

Gupta S, Yeeles JT, Marians KJ (2014) Regression of replication forks stalled by leading-strand template damage: I. Both RecG and RuvAB catalyze regression, but RuvC cleaves the holliday junctions formed by RecG preferentially. *J Biol Chem* **289:** 28376-28387

Haldenby S, White MF, Allers T (2009) RecA family proteins in archaea: RadA and its cousins. *Biochemical Society transactions* **37:** 102-107

Hanahan D (1983) Studies on transformation of Escherichia coli with plasmids. *Journal of Molecular Biology* **166:** 557-580

Helmann JD, Wu MF, Kobel PA, Gamo FJ, Wilson M, Morshedi MM, Navre M, Paddon C (2001) Global transcriptional response of Bacillus subtilis to heat shock. *J Bacteriol* **183:** 7318-7328

Henle ES, Linn S (1997) Formation, prevention, and repair of DNA damage by iron/hydrogen peroxide. *J Biol Chem* **272:** 19095-19098

Hiom K, West SC (1995) Branch migration during homologous recombination: assembly of a RuvAB-Holliday junction complex in vitro. *Cell* **80:** 787-793

Hobbs MD, Sakai A, Cox MM (2007) SSB protein limits RecOR binding onto single-stranded DNA. *J Biol Chem* **282:** 11058-11067

Hoeijmakers JH (2001) Genome maintenance mechanisms for preventing cancer. *Nature* **411:** 366-374

Holliday R (1964) A mechanism for gene conversion in fungi. *Genet Res* **5:** 32-304

Ireton K, Grossman AD (1994) DNA-related conditions controlling the initiation of sporulation in Bacillus subtilis. *Cellular & molecular biology research* **40:** 193-198

Iwasaki H, Takahagi M, Nakata A, Shinagawa H (1992) Escherichia coli RuvA and RuvB proteins specifically interact with Holliday junctions and promote branch migration. *Genes Dev* **6:** 2214-2220

Jarrett SG, Wolf Horrell EM, Christian PA, Vanover JC, Boulanger MC, Zou Y, D'Orazio JA (2014) PKA-mediated phosphorylation of ATR promotes recruitment of XPA to UV-induced DNA damage. *Mol Cell* **54:** 999-1011

Jervis AJ, Thackray PD, Houston CW, Horsburgh MJ, Moir A (2007) SigM-Responsive Genes of Bacillus subtilis and Their Promoters. *Journal of Bacteriology* **189:** 4534-4538

Kamegaya T, Kuroda K, Hayakawa Y (2011) Identification of a Streptococcus pyogenes SF370 gene involved in production of c-di-AMP. *Nagoya J Med Sci* **73:** 49-57

Khuu PA, Voth AR, Hays FA, Ho PS (2006) The stacked-X DNA Holliday junction and protein recognition. *Journal of molecular recognition : JMR* **19:** 234-242

Kidane D, Sanchez H, Alonso JC, Graumann PL (2004) Visualization of DNA double-strand break repair in live bacteria reveals dynamic recruitment of Bacillus subtilis RecF, RecO and RecN proteins to distinct sites on the nucleoids. *Molecular Microbiology* **52:** 1627-1639

Kruger E, Hecker M (1998) The first gene of the Bacillus subtilis clpC operon, ctsR, encodes a negative regulator of its own operon and other class III heat shock genes. *J Bacteriol* **180:** 6681-6688

Kruger E, Msadek T, Hecker M (1996) Alternate promoters direct stress-induced transcription of the Bacillus subtilis clpC operon. *Mol Microbiol* **20:** 713-723

Krüger E, Msadek T, Ohlmeier S, Hecker M (1997) The *Bacillus subtilis* clpC operon encodes DNA repair and competence proteins. *Microbiology* **143:** 1309-1316

Krwawicz J, Arczewska KD, Speina E, Maciejewska A, Grzesiuk E (2007) Bacterial DNA repair genes and their eukaryotic homologues: 1. Mutations in genes involved in base excision

repair (BER) and DNA-end processors and their implication in mutagenesis and human disease. *Acta biochimica Polonica* **54:** 413-434

Lee YJ, Park SJ, Ciccone SL, Kim CR, Lee SH (2006) An in vivo analysis of MMC-induced DNA damage and its repair. *Carcinogenesis* **27:** 446-453

Lenhart JS, Schroeder JW, Walsh BW, Simmons LA (2012) DNA Repair and Genome Maintenance in Bacillus subtilis. *Microbiol Mol Biol Rev* **76:** 530-564

Lovett ST (2006) Replication arrest-stimulated recombination: Dependence on the RecA paralog, RadA/Sms and translesion polymerase, DinB. *DNA Repair (Amst)* **5:** 1421-1427

Lundin C, North M, Erixon K, Walters K, Jenssen D, Goldman AS, Helleday T (2005) Methyl methanesulfonate (MMS) produces heat-labile DNA damage but no detectable in vivo DNA double-strand breaks. *Nucleic Acids Res* **33:** 3799-3811

Luo Y, Helmann JD (2012a) Analysis of the role of Bacillus subtilis sigma(M) in beta-lactam resistance reveals an essential role for c-di-AMP in peptidoglycan homeostasis. *Molecular Microbiology* **83:** 623-639

Luo Y, Helmann JD (2012b) A sigmaD-dependent antisense transcript modulates expression of the cyclic-di-AMP hydrolase GdpP in Bacillus subtilis. *Microbiology* **158:** 2732-2741

Manfredi C (2009) Estudio de los mediadores de RecA en la Recombinación Homóloga. PhD Thesis, Departamento de Biologia Molecular, Universidad Autónoma de Madrid, Madrid

Manfredi C, Suzuki Y, Yadav T, Takeyasu K, Alonso JC (2010) RecO-mediated DNA homology search and annealing is facilitated by SsbA. *Nucleic Acids Res* **38:** 6920-6929

Martinezsalazar J, Zunigacastillo J, Romero D (2009) Differential roles of proteins involved in migration of Holliday junctions on recombination and tolerance to DNA damaging agents in Rhizobium etli. *Gene* **432:** 26-32

McGlynn P, Lloyd RG (2001) Rescue of stalled replication forks by RecG: simultaneous translocation on the leading and lagging strand templates supports an active DNA unwinding model of fork reversal and Holliday junction formation. *Proc Natl Acad Sci U S A* **98:** 8227-8234

McKinney SA, Declais AC, Lilley DM, Ha T (2003) Structural dynamics of individual Holliday junctions. *Nature structural biology* **10:** 93-97

Mehne FM, Gunka K, Eilers H, Herzberg C, Kaever V, Stulke J (2013) Cyclic di-AMP homeostasis in bacillus subtilis: both lack and high level accumulation of the nucleotide are detrimental for cell growth. *J Biol Chem* **288:** 2004-2017

Mehne FM, Schroder-Tittmann K, Eijlander RT, Herzberg C, Hewitt L, Kaever V, Lewis RJ, Kuipers OP, Tittmann K, Stulke J (2014) Control of the Diadenylate Cyclase CdaS in Bacillus subtilis: An Autoinhibitory Domain Limits c-di-AMP Production. *J Biol Chem*

Million-Weaver S, Samadpour AN, Moreno-Habel DA, Nugent P, Brittnacher MJ, Weiss E, Hayden HS, Miller SI, Liachko I, Merrikh H (2015) An underlying mechanism for the increased mutagenesis of lagging-strand genes in Bacillus subtilis. *Proc Natl Acad Sci U S A* **112:** E1096-1105

Morrical SW, Lee J, Cox MM (1986) Continuous association of Escherichia coli single-stranded DNA binding protein with stable complexes of recA protein and single-stranded DNA. *Biochemistry* **25:** 1482-1494

Muller M, Hopfner KP, Witte G (2015) c-di-AMP recognition by Staphylococcus aureus PstA. *FEBS letters* **589:** 45-51

Nagai T, Ibata K, Park ES, Kubota M, Mikoshiba K, Miyawaki A (2002) A variant of yellow fluorescent protein with fast and efficient maturation for cell-biological applications. *Nature biotechnology* **20:** 87-90

Neelsen KJ, Lopes M (2015) Replication fork reversal in eukaryotes: from dead end to dynamic response. *Nature reviews Molecular cell biology*

Nelson JW, Sudarsan N, Furukawa K, Weinberg Z, Wang JX, Breaker RR (2013) Riboswitches in eubacteria sense the second messenger c-di-AMP. *Nature chemical biology* **9:** 834-839

Neuwald AF, Berg DE, Stauffer GV (1992) Mutational analysis of the *Escherichia coli serB* promoter region reveals transcriptional linkage to a downstream gene. *Gene* **120:** 1-9

Nicolas P, Mader U, Dervyn E, Rochat T, Leduc A, Pigeonneau N, Bidnenko E, Marchadier E, Hoebeke M, Aymerich S, Becher D, Bisicchia P, Botella E, Delumeau O, Doherty G, Denham EL, Fogg MJ, Fromion V, Goelzer A, Hansen A, Hartig E, Harwood CR, Homuth G, Jarmer H, Jules M, Klipp E, Le Chat L, Lecointe F, Lewis P, Liebermeister W, March A, Mars RA, Nannapaneni P, Noone D, Pohl S, Rinn B, Rugheimer F, Sappa PK, Samson F, Schaffer M, Schwikowski B, Steil L, Stulke J, Wiegert T, Devine KM, Wilkinson AJ, van Dijl JM, Hecker M, Volker U, Bessieres P, Noirot P (2012) Condition-dependent transcriptome reveals high-level regulatory architecture in Bacillus subtilis. *Science* **335:** 1103-1106

Nora GJ, Buncher NA, Opresko PL (2010) Telomeric protein TRF2 protects Holliday junctions with telomeric arms from displacement by the Werner syndrome helicase. *Nucleic Acids Res* **38:** 3984-3998

Oppenheimer-Shaanan Y, Wexselblatt E, Katzhendler J, Yavin E, Ben-Yehuda S (2011) c-di-AMP reports DNA integrity during sporulation in Bacillus subtilis. *EMBO Rep* **12:** 594-601

Osborn AJ, Elledge SJ, Zou L (2002) Checking on the fork: the DNA-replication stress-response pathway. *Trends in cell biology* **12:** 509-516

Parsons CA, Stasiak A, Bennett RJ, West SC (1995) Structure of a multisubunit complex that promotes DNA branch migration. *Nature* **374:** 375-378

Parsons CA, Tsaneva I, Lloyd RG, West SC (1992) Interaction of Escherichia coli RuvA and RuvB proteins with synthetic Holliday junctions. *Proc Natl Acad Sci U S A* **89:** 5452-5456

Parvatiyar K, Zhang Z, Teles RM, Ouyang S, Jiang Y, Iyer SS, Zaver SA, Schenk M, Zeng S, Zhong W, Liu ZJ, Modlin RL, Liu YJ, Cheng G (2012) The helicase DDX41 recognizes the bacterial secondary messengers cyclic di-GMP and cyclic di-AMP to activate a type I interferon immune response. *Nat Immunol* **13:** 1155-1161

Pedersen LB, Setlow P (2000) Penicillin-binding protein-related factor A is required for proper chromosome segregation in Bacillus subtilis. *J Bacteriol* **182:** 1650-1658

Pommier Y, Leo E, Zhang H, Marchand C (2010) DNA topoisomerases and their poisoning by anticancer and antibacterial drugs. *Chemistry & biology* **17:** 421-433

Rallu F, Gruss A, Ehrlich SD, Maguin E (2000) Acid- and multistress-resistant mutants of Lactococcus lactis : identification of intracellular stress signals. *Mol Microbiol* **35:** 517-528

Rao F, See RY, Zhang D, Toh DC, Ji Q, Liang ZX (2009) YybT Is a Signaling Protein That Contains a Cyclic Dinucleotide Phosphodiesterase Domain and a GGDEF Domain with ATPase Activity. *Journal of Biological Chemistry* **285:** 473-482

Rivas-Castillo AM, Yasbin RE, Robleto E, Nicholson WL, Pedraza-Reyes M (2010) Role of the Y-family DNA polymerases YqjH and YqjW in protecting sporulating Bacillus subtilis cells from DNA damage. *Curr Microbiol* **60:** 263-267

Roelofs KG, Wang J, Sintim HO, Lee VT (2011) Differential radial capillary action of ligand assay for high-throughput detection of protein-metabolite interactions. *Proc Natl Acad Sci U S A* **108:** 15528-15533

Romling U (2008) Great Times for Small Molecules: c-di-AMP, a Second Messenger Candidate in Bacteria and Archaea. *Science Signaling* **1:** pe39-pe39

Rosenberg J, Dickmanns A, Neumann P, Gunka K, Arens J, Kaever V, Stulke J, Ficner R, Commichau FM (2015) Structural and Biochemical Analysis of the Essential Diadenylate Cyclase CdaA from Listeria monocytogenes. *J Biol Chem* **290:** 6596-6606

Safa M, Kazemi A, Zaker F, Razmkhah F (2011) Cyclic AMP-induced p53 destabilization is independent of EPAC in pre-B acute lymphoblastic leukemia cells in vitro. *Journal of receptor and signal transduction research* **31:** 256-263

Sanchez H, Carrasco B, Cozar MC, Alonso JC (2007a) Bacillus subtilis RecG branch migration translocase is required for DNA repair and chromosomal segregation. *Molecular Microbiology* **65:** 920-935

Sanchez H, Cozar MC, Martinez-Jimenez MI (2007b) Targeting the Bacillus subtilis genome: an efficient and clean method for gene disruption. *Journal of microbiological methods* **70:** 389-394

Sanchez H, Kidane D, Reed P, Curtis FA, Cozar MC, Graumann PL, Sharples GJ, Alonso JC (2005) The RuvAB branch migration translocase and RecU Holliday junction resolvase are required for double-stranded DNA break repair in Bacillus subtilis. *Genetics* **171:** 873-883

Sedgwick B (2004) Repairing DNA-methylation damage. *Nature reviews Molecular cell biology* **5:** 148-157

Simmons LA, Goranov AI, Kobayashi H, Davies BW, Yuan DS, Grossman AD, Walker GC (2009) Comparison of responses to double-strand breaks between Escherichia coli and Bacillus subtilis reveals different requirements for SOS induction. *J Bacteriol* **191:** 1152-1161

Slade D, Lindner AB, Paul G, Radman M (2009) Recombination and replication in DNA repair of heavily irradiated Deinococcus radiodurans. *Cell* **136:** 1044-1055

Smith WM, Pham TH, Lei L, Dou J, Soomro AH, Beatson SA, Dykes GA, Turner MS (2012) Heat resistance and salt hypersensitivity in Lactococcus lactis due to spontaneous mutation of llmg_1816 (gdpP) induced by high-temperature growth. *Applied and environmental microbiology* **78:** 7753-7759

Song Y, Sargentini NJ (1996) Escherichia coli DNA repair genes radA and sms are the same gene. *J Bacteriol* **178:** 5045-5048

Sun L, Wu J, Du F, Chen X, Chen ZJ (2013) Cyclic GMP-AMP synthase is a cytosolic DNA sensor that activates the type I interferon pathway. *Science* **339:** 786-791

Sureka K, Choi PH, Precit M, Delince M, Pensinger DA, Huynh TN, Jurado AR, Goo YA, Sadilek M, Iavarone AT, Sauer JD, Tong L, Woodward JJ (2014) The cyclic dinucleotide c-di-AMP is an allosteric regulator of metabolic enzyme function. *Cell* **158:** 1389-1401

Tercero JA, Diffley JF (2001) Regulation of DNA replication fork progression through damaged DNA by the Mec1/Rad53 checkpoint. *Nature* **412:** 553-557

Tippin B, Pham P, Goodman MF (2004) Error-prone replication for better or worse. *Trends in microbiology* **12:** 288-295

Walker JM (2002) *The Protein Protocols Handbook: Second Edition*, Second edition edn. Totowa, New Jersey: Humana Press Inc.

Walsh BW, Bolz SA, Wessel SR, Schroeder JW, Keck JL, Simmons LA (2014) RecD2 helicase limits replication fork stress in Bacillus subtilis. *J Bacteriol* **196:** 1359-1368

Wit N, Buoninfante OA, van den Berk PC, Jansen JG, Hogenbirk MA, de Wind N, Jacobs H (2015) Roles of PCNA ubiquitination and TLS polymerases kappa and eta in the bypass of methyl methanesulfonate-induced DNA damage. *Nucleic Acids Res* **43:** 282-294

Witte CE, Whiteley AT, Burke TP, Sauer JD, Portnoy DA, Woodward JJ (2013) Cyclic di-AMP is critical for Listeria monocytogenes growth, cell wall homeostasis, and establishment of infection. *MBio* **4:** e00282-00213

Witte G, Hartung S, Büttner K, Hopfner K-P (2008) Structural Biochemistry of a Bacterial Checkpoint Protein Reveals Diadenylate Cyclase Activity Regulated by DNA Recombination Intermediates. *Molecular Cell* **30:** 167-178

Woodward JJ, Iavarone AT, Portnoy DA (2010) c-di-AMP Secreted by Intracellular Listeria monocytogenes Activates a Host Type I Interferon Response. *Science* **328:** 1703-1705

Wu J, Sun L, Chen X, Du F, Shi H, Chen C, Chen ZJ (2013) Cyclic GMP-AMP is an endogenous second messenger in innate immune signaling by cytosolic DNA. *Science* **339:** 826-830

Yadav T, Carrasco B, Myers AR, George NP, Keck JL, Alonso JC (2012) Genetic recombination in Bacillus subtilis: a division of labor between two single-strand DNA-binding proteins. *Nucleic Acids Research* **40:** 5546-5559

Yasbin RE, Cheo D, Bol D (1993) DNA Repair Systems. In *Bacillus subtilis and other gram-positive bacteria: Biochemistry, Physiology, and Molecular Genetics*, Sonenshein AL, Hoch JA, Losick R (eds), p 987. American Society for Microbiology

Yasbin RE, Young FE (1974) Transduction in Bacillus subtilis by bacteriophage SPP1. *J Virol* **14:** 1343-1348

Ye M, Zhang JJ, Fang X, Lawlis GB, Troxell B, Zhou Y, Gomelsky M, Lou Y, Yang XF (2014) DhhP, a cyclic di-AMP phosphodiesterase of Borrelia burgdorferi, is essential for cell growth and virulence. *Infect Immun* **82:** 1840-1849

Yu J, Ha T, Schulten K (2004) Conformational model of the Holliday junction transition deduced from molecular dynamics simulations. *Nucleic Acids Res* **32:** 6683-6695

Zhang L, He ZG (2013) Radiation-sensitive gene A (RadA) targets DisA, DNA integrity scanning protein A, to negatively affect cyclic Di-AMP synthesis activity in Mycobacterium smegmatis. *J Biol Chem* **288:** 22426-22436

Zhang L, Li W, He ZG (2013) DarR, a TetR-like transcriptional factor, is a cyclic di-AMP-responsive repressor in Mycobacterium smegmatis. *J Biol Chem* **288:** 3085-3096

Appendix

9. Appendix – List of publications

This work resulted in the following publications:

- **Gandara C**, Alonso JC (2015) DisA and c-di-AMP act at the intersection between DNA-damage response and stress homeostasis in exponentially growing Bacillus subtilis cells. *DNA Repair (Amst)* **27:** 1-8.

- **Gandara C**, Altenburger S, de Lucena D, Graumann, PL, Alonso JC (2015) DisA and RadA/Sms in concert with Holliday junction processing functions contribute to elicit repair of alkyl groups during *Bacillus subtilis* vegetative growth. *In preparation*

- **Gandara C**, Carrasco B, Cañas C, Ayora S, Alonso JC (2015) DisA reduces homologous recombination to facilitate DNA repair of stalled replication forks. *In preparation*

- Cardenas PP, **Gandara C**, Alonso JC (2014) DNA double strand break end-processing and RecA induce RecN expression levels in Bacillus subtilis. *DNA Repair (Amst)* **14:** 1-8.